MODELLING THE IMPACT OF LAND USE LAND COVER CHANGES ON THE RUNOFF PROCESSES OF CHALAKUDY BASIN USING HEC-HMS MODEL

by

NCHUMBENI M ODYUO

(2018-18-002)

Department of Irrigation and Drainage Engineering

KELAPPAJI COLLEGE OF AGRICULTURAL ENGINEERING AND TECHNOLOGY

TAVANUR--679573, MALAPPURAM

KERALA, INDIA

2020

MODELLING THE IMPACT OF LAND USE LAND COVER CHANGES ON THE RUNOFF PROCESSES OF CHALAKUDY BASIN USING HEC-HMS MODEL

by

NCHUMBENI M ODYUO

(2018-18-002)

THESIS

Submitted in partial fulfilment of the

requirement for the degree of

MASTER OF TECHNOLOGY

IN

AGRICULTURAL ENGINEERING

(Soil and Water Engineering)

Faculty of Agricultural Engineering and Technology

Kerala Agricultural University

Department of Irrigation and Drainage Engineering

KELAPPAJI COLLEGE OF AGRICULTURAL ENGINEERING AND TECHNOLOGY

TAVANUR-- 679573, MALAPPURAM

KERALA, INDIA

2020

DECLARATION

I, hereby declare that this thesis entitled "**MODELLING THE IMPACT OF LAND USE LAND COVER CHANGES ON THE RUNOFF PROCESSES OF CHALAKUDY BASIN USING HEC-HMS MODEL**" is a bonafide record of research work done by me during the course of research and the thesis has not previously formed the basis for the award to me of any degree, diploma, associateship, fellowship or other similar title, of any other University or Society.

Place: Tavanur **NCHUMBENI M ODYUO**

Date: **(2018-18-002)**

CERTIFICATE

Certified that this thesis entitled "**MODELLING THE IMPACT OF LAND USE LAND COVER CHANGES ON THE RUNOFF PROCESSES OF CHALAKUDY BASIN USING HEC-HMS MODEL**" is a record of research work done independently by **Ms. Nchumbeni M Odyuo (2018-18-002)** under my guidance and supervision and that it has not previously formed the basis for the award of any degree, diploma, fellowship or associateship to her.

Place: Tavanur

Date:

Dr. Rema K.P.
(Major Advisor, Advisory Committee)
Professor, Dept. of IDE,
KCAET, Tavanur.

CERTIFICATE

We, the undersigned members of the advisory committee of **Ms. Nchumbeni M Odyuo (2018-18-002),** a candidate for the degree of **Master of Technology in Agricultural Engineering with major in Soil and Water Engineering**, agree that the thesis entitled "**MODELLING THE IMPACT OF LAND USE LAND COVER CHANGES ON THE RUNOFF PROCESSES OF CHALAKUDY BASIN USING HEC-HMS MODEL**" may be submitted by **Ms. Nchumbeni M Odyuo (2018-18-002),** in partial fulfilment of the requirement for the degree.

Dr. Rema K.P
(Chairman, Advisory Committee)
Professor, Dept. of IDE
KCAET, Tavanur

Dr. Anu Varughese
(Member, Advisory Committee)
Asst. Professor, Dept. of IDE
KCAET, Tavanur.

Dr. Sasikala D
(Member, Advisory Committee)
Professor & Head, Dept. of IDE
KCAET, Tavanur

Er. Shivaji K.P.
(Member, Advisory Committee)
Asst. Professor, Dept. of Agrl.Engg,
RARS, Ambalavayal

EXTERNAL EXAMINER

ACKNOWLEDGEMENT

It is a pleasure to acknowledge the assistance from several individuals during the preparation of this project. No words are sufficient to express my gratitude to all the helping hands. Indeed I consider it as a pleasant duty, though equally difficult to acknowledge the motivating efforts of several people who have helped me in bringing this project to its delight.

First of all I would like to thank God for offering me His gentle grace and guidance throughout my project work. It had only been possible for me to carry out this work successfully because of his amazing grace and I am immensely thankful to Him for bestowing His blessings unceasingly all throughout my work.

I would also like to express my profound sense of gratitude and veneration to my guide **Dr. Rema K.P.,** Professor, Department of Irrigation and Drainage Engineering, KCAET, Tavanur, Chairman of my Advisory Committee for her untiring supervision, forbearance and firm belief in me, who has patiently corrected and edited the huge stack of materials I had written based on my research. She had constantly encouraged and motivated me to do things which I didn't feel I was capable of and always have had more faith in my ability than I did. It was indeed a privilege to work under her supervision.

I place my special thanks to **Dr. Sathian K.K.** Professor and Dean, KCAET, Tavanur, for rendering his advice and guidance during this study. I would also like to thank **Dr. Sasikala D.,** Professor and Head, Department of Irrigation and Drainage Engineering, KCAET, Tavanur, member of my advisory committee for the timely help, advice and valuable suggestions during the research work. I would like to express my heartfelt thanks to **Er. Shivaji K.P.,** Assistant Professor, Department of Agricultural Engineering, RARS, Ambalavayal, member of my advisory committee for his encouragement and support throughout my research.

My special thanks and gratitude goes to **Dr. Anu Varughese,** Assistant Professor, Department of Irrigation and Drainage Engineering, KCAET, Tavanur and

a member of my advisory committee for her constant guidance and encouragement, untiring help and insightful consults throughout the period of the study.

I would like to express my gratitude to **Dr. Kurien E.K.,** Professor and Head, ARS, Chalakudy, for providing me the meteorological data which was prerequisite for the successful completion of my work.

I am also grateful and thankful at the same time to all faculty members of the department and the staff members of KCAET for their support and encouragement. It also gives me immense pleasure in expressing out my sincere gratitude to all my friends at KCAET who had constantly encouraged and helped me by all possible means during the course of my project work.

I extend my sincere thanks and gratitude to my parents for their sacrifices, unceasing prayers and encouragement all throughout this work. It would have remained only a dream for the successful completion of this work and not a reality without their support.

Special thanks to **Kerala Agricultural University** for giving me an opportunity and providing me a platform to study in this institute. It was indeed a wonderful and handful of experience to study in KCAET.

Last but not least, I express my sincere gratitude to all those who have supported and helped me through their encouraging words and deeds and are directly or indirectly connected to my successful completion of work.

Nchumbeni M Odyuo

Dedicated to

My parents

CONTENTS

LIST OF TABLES

LIST OF FIGURES

SYMBOLS AND ABBREVIATIONS

^{o}	:	Degree
^{O}C	:	Degree Celsius
‘	:	Minute
%	:	Percentage
+	:	Plus
3D	:	Three Dimensional
AMC	:	Antecedent Moisture Condition
ARS	:	Agricultural Research Station
ASTER	:	Advanced Space borne Thermal Emission and Reflection Radiometer
AWLR	:	Automatic Water Level Recorder
CN	:	Curve Number
CWC	:	Central Water Commission
DEM	:	Digital Elevation Model
ERDAS	:	Earth Resources Data Analysis System
ET	:	Evapo transpiration
et al.,	:	and others
etc	:	et cetera
FAO	:	Food and Agriculture Organization
GCMs	:	General Circulation Models
GDP	:	Gross Domestic Product
GIS	:	Geographic Information System
GUI	:	Graphical User Interface
ha	:	Hectare
HEC-GeoHMS	:	Geospatial Hydrologic Modeling Extension
HEC-HMS	:	Hydrologic Engineering Centre- Hydrologic Modelling System
hr	:	Hour
HSG	:	Hydrological Soil Group

i.e.	:	that is
IRS P5	:	Indian Remote Sensing Satellite-P5
ILWIS	:	Integrated Land and Water Information System
IMD	:	Indian Meteorological Department
ISMR	:	Indian Summer Monsoon Rainfall
km^2	:	kilometre square
km/h	:	kilometre per hour
LiDAR	:	Light Detection and Ranging
LISS III	:	Linear Imaging Self-Scanning System-III
LULC	:	Landuse Land Cover
MARE	:	Mean Absolute Relative Error
m	:	meter
mm	:	millimeter
m^3/s	:	meter cube per second
min.	:	minutes
NASA	:	National Aeronautics and Space Administration
NRCS	:	National Remote Sensing Centre
NSE	:	Nash-Sutcliffe Efficiency
PBIAS	:	Percent bias
PCS	:	Projected Co-Ordinate System
Pct	:	Percentage
PEPF	:	Percent Error Peak Flow
PEV	:	Percent Error in Volume
R^2	:	Correlation Coefficient
RCP	:	Representative Concentration Pathway
REP	:	Relative Error in Peak
REV	:	Relative Error in Volume
RH	:	Relative Humidity
RMSE	:	Root Mean Square Error
RS	:	Remote Sensing
SCS-UH	:	Soil Conservation Services- Unit Hydrograph
SMA	:	Soil Moisture Accounting

SOI	:	Survey Of India
SPOT	:	Satellite Pour I'Observation de la Terre (French) meaning 'Satellite to observe Earth'
SRTM	:	Shuttle Radar Topography Mission
SSC	:	Stennis Space Center
SWAT- CUP	:	Soil and Water Assessment Tool-Calibration and Uncertainty Procedures
SUFI-2	:	Sequential Uncertainty Fitting-2
T_c	:	Time of Concentration
TM	:	Thematic Mapper
TNAU	:	Tamil Nadu Agricultural University
USGS	:	United States Geological Survey
QGIS	:	Quantum Geographic Information System
WMS	:	Web Map Service

Introduction

CHAPTER I
INTRODUCTION

Flood is one of the most hazardous ecological perils that threaten the lives of human beings and their properties. It is one of the primary worldwide hazard making gigantic harms to agribusiness, fisheries, lodging and buildings etc., that vigorously influence social and monetary exercises. Flood usually happens after occurrence of intensive precipitation as a result of fast aggregation of rainfall and the overflow from upstream section to downstream section. Investigations of worldwide hazard proves flood as one of the primary risks that have influenced the lives of individuals around the world with huge mortality rate. Flood represents about 40% of the death from commonly occurring hazards and in the recent decade it has caused a death of around 100,000 individuals and has influenced the life of 1.4 billion individuals worldwide (Ezemonye and Emeribe, 2011). Recognizing the chances of flood occurrence in certain areas with the point of managing the affected area optimally is very important. Overseeing and decreasing the flood risk, plays a fundamental job in keeping up the physical and social condition of various societies and their development of economy. Likewise, dealing with this hazard is urgent for diminishing harm and dealing with the impact of environmental change due to land use changes.

India is the most flood affected country with 4.84 million people exposed to floods, followed by its South Asian neighbour, Bangladesh, with 3.48 million people. Around 0.84 per cent of India's estimated GDP is affected by floods on an average each year (Winsemius *et al*., 2013). India has experienced serious floods over the most recent two decades attributing to very high precipitation events and among the affected states, Kerala has also taken its place since 2018. The years 2019 & 2020 also experienced high intensity short duration rainfalls in Kerala leading to floods. Even though, the state of Kerala has numerous dams and reservoirs, the job of dams in moderating the flood couldn't be satisfied which was later on questioned and criticized on logical, social and political grounds. During August 2018, Kerala state experienced one of the most serious outrageous precipitations on record. Very high intensity storms of more than 100 years return period was reported in Kerala. This brought about flooding and avalanche across most areas of the state, making serious harm to

both the constructed and natural biological systems. Kerala received high ISMR (Indian summer monsoon rainfall) from 1st June to 19th of August 2018 (2346.6 mm), which is generally 42% above the usual precipitation for the same period. During the initial 19 days of August 2018, Kerala got 164% above average precipitation, out of which the major share was from two extreme precipitation occasions during 8–10 and 14–19 of August 2018 (Sudheer *et al.* 2019). The Chalakudy river basin located in Kerala is considered to be one of the worst affected basins in Kerala. Aside from receiving heavy rainfall by the basin in the year 2018, another major reason behind the occurrence of flood was the changes in the land use/land cover of the basin in the last few decades.

At present land is considered to be one of the rare assets because of population development and industrialization. Due to the advancement in lifestyle of the people and setting up of various industries there is a quick change in LULC and in urban regions specifically. The sporadic development in urban spread has caused an incredible effect on the land. The terms land use land cover is regularly utilized conversely, yet each term has its own interesting significance. Land cover is the physical material at the outside of the earth. Land use is the portrayal of how individuals use the land for their developmental activities. Land-use and land-cover changes may have four significant direct impacts on the hydrological cycle and water quality: they can cause changes in waterway, floods, dry seasons and groundwater systems; they can even influence water quality. LULC of the earth is changing drastically as a result of human exercises and cataclysmic events like floods and drought. Changes of LULC design particularly in developed zones have prompted an extension of impenetrable land which has altogether influenced the surface overflow in the urban domain.

Expanded pace of urbanization alongside other human intercession factors have been referred to as significant difficulties encountered by streams, which in turn changes the overall basin ecology and ends up in characteristic ruins like floods and dry seasons. Deforestation and change of waterlogged wetlands into developed zones directly influence the qualities of the basin, common water stream systems and the conspicuous result is flood. Most definitely the spatio-temporal changes in land use have direct impact on its hydrological domain. Flooding is unpredictable and this

hazard is frequently being experienced. To diminish the flood peril, a basic job is to keep up the balance between natural environment, physical and social condition of various social orders and their financial improvement. Dealing with flood hazard is essential for lessening harm and adjusting the impacts of environmental change to land use change. Therefore, the evaluation to decrease the flood dangers ought not to be overlooked.

LULC changes examination gives data to organizers and helps the users on what ought to be done to have sensible and adjusted improvement that will be economical and eco-accommodating. Comprehending the spatial and transient changes in LULC map is a demonstrative technique which helps us in understanding several issues continuing in a watershed. Remotely detected information and GIS have been distinguished as amazing and viable techniques in recognizing urban development. In watershed modelling, Remote sensing and GIS are seen as important techniques for giving data input information and for assessing model parameters. Remote sensing data is typically the most exact and cutting-edge information accessible for studying the LULC changes. Particularly with quickly developing towns and urban communities in India it is the only promising option to catch up with the urban development spread and map the information on a temporal scale.

Estimation of runoff in a watershed based on rainfall distribution is an important analysis in hydrology. From the past few years remote sensing technology and GIS have also been applied to assess and model flood risk at a widespread level globally. A model for simulating the runoff needs to be developed for the study area and calibration of the model can be done based on historical time series data. Hydrological models incorporate a lot of parameters which are evaluated and optimized during the calibration of the model. The calibrated model afterwards could create a new set of data for different future scenarios and can later on be validated for a different set of years. Manual calibration of the model is attempted by visual assessment, trial and error procedure which can get monotonous, tedious and may also need individual experiences and trial data particularly when it comes to dealing with countless parameters. Use of hydrological models along with remote sensing and GIS can help us in getting rid of dealing with various complicated equations and time consuming calculations. The user must be qualified and well aware of all the

calculations and numerical functions going on behind various activities in the software. Absence of adequate information by the user could prompt a deceptive and wrong answer. Another advantage of using remote sensing and GIS in hydrological modelling is that one can join different layers of geographic data and make a new integrated dataset. Additionally the user must also know about the combination of different layers. While overlaying, all the layers need to be projected into the same co-ordination system and scale in ArcGIS.

Rainfall-runoff models are frequently utilized as an instrument for a wide scope of assignments, for example, modelling of flood occasions, checking of water levels during various water conditions or the forecasting of flood and to simulate runoff. However, such sort of model regularly relies upon the reason the model is being used for, accessibility of data and convenience. In general hydrologic model is classified into two *viz.*, stochastic and deterministic. A stochastic model gives partial randomness however the deterministic model doesn't give any randomness. Further, hydrologic model is ordered into three significant classifications i.e. the lumped model, semi-distributed model and distributed model. Utilization of remote sensing and GIS in addition to semi distributed hydrologic model gives additional opportunities to determine spatially distributed time series of input variables. Many a times the measurement of all the parameters influencing the runoff of a watershed is not possible, therefore, picking an appropriate model requiring minimum input data, simple structure and giving an accurate result is essential. One such hydrologic model meeting all these criteria is Hydrologic Engineering Center-Hydrologic Modelling System (HEC-HMS) model.

The procedure for hydrologic modelling of a watershed can be represented by three stages:

Stage I: Incorporates data collection, model information arrangement, and parameter assessment which are the procedures expected to run a model.

Stage II: The model testing stage which includes sensitivity analysis, approval and if necessary further review is to be done too. This is the stage where the model is assessed to evaluate whether it can sensibly represent the watershed behaviour for the motivation behind the study.

Stage III: Incorporates a definitive utilization of the model as a choice help apparatus for the management and administrative purposes.

The HEC-HMS model created by the US Army Corps of Engineers Hydrologic Engineering Center (HEC) is a co-ordinated demonstrating instrument for all hydrologic procedures of a dendritic watershed. It comprises of various forms of precipitation loss, direct runoff and flood routing. HEC-HMS has become exceptionally well known and has been used in numerous hydrological examinations on account of its capacity to simulate runoff both for short and long duration of rainfall and utilization of regular techniques. Hydrographs created by HEC-HMS are utilized for investigating urban seepage, water accessibility, future urbanization impact, flood forecasting, flood harm decrease, flood plain guideline, and frameworks activity. HEC-HMS can assist in setting up the hydrologic model framework and simulate rainfall-runoff processes of a watershed. A GIS extension tool i.e., the HEC-GeoHMS tool has been created which helps in creating basin models and meteorological models for further use in HEC-HMS model. The HEC-HMS model is used to simulate rainfall-runoff of a networked watershed system by incorporating sub-basins, reaches, junctions, reservoirs, diversions, sources, and sinks.

The recorded figures and results from the recent floods revealed that most of the flood affected areas are hilly and lacks hydrological statistics which explains an assessment of the area that is vulnerable to flood risk. One of the major river basins that was severely affected by the August 2018 floods in Kerala state was the Chalakudy basin .The basin has been the victim of many floods since the last few years and lot of damages to the basin has occurred including the loss of plantation, livestock, residential areas, and infrastructures such as building, roads, bridges and so on. Chalakudy basin has encountered numerous critical situations such as repeated flood occurrences and dry seasons that has become an overwhelming element of this stream which is considered as the life saver of the area. The changes in the LULC of Chalakudy basin has undergone negative changes disturbing the overall basin ecology which is presently being experienced in the form of repeated flood and dry season circumstances. The recorded outcomes from the recent floods uncovered that the greater part of the flood affected basins are missing hydrological studies which clarifies an appraisal of the hazard vulnerability.

Taking into account the above mentioned issues this study mainly focuses on investigating the impact of land use land cover (LULC) changes on the runoff processes of Chalakudy basin using the HEC-HMS model along with remote Sensing and GIS tools.

The specific objectives of the study are highlighted below:

1) Study of spatio-temporal LULC changes in the Chalakudy basin over a period of two decades.
2) Modelling the hydrology of the basin using HEC-HMS and Arc-GIS tools.
3) Evaluation of model performance by sensitivity analysis.
4) Analyze the impact of land use land cover changes on the runoff for the study period by simulation runs.

Review of Literature

CHAPTER II

REVIEW OF LITERATURE

Runoff estimation from a watershed is significant for planning of water resources and management, for example flood control, mitigating drought, irrigation scheduling, water harvesting, and designing different engineering structures. Hydrological modelling is an essential tool for exact estimation of runoff from a watershed or basin. A significant issue in the hydrological modelling is the deficient field estimated information to depict the complex hydrologic cycle governing the conversion of rainfall to runoff. A few computer based hydrological models have been created for simulation of runoff in watersheds and studies related to water resources. The utilization of remote sensing and GIS along with hydrological models gives additional opportunity to obtain spatially distributed time series of input variables for calibrating and validating the model. A review of several previous research works related to the effect of land use land cover changes on the hydrological response of the watersheds and basins, modelling runoff of basins, model calibration, sensitivity analysis, and validation are presented below.

2.1 DELINEATION OF WATERSHED USING DEM:

Coskun *et al.,* (2010) made a study on a watershed situated in Eastern Black Sea region of Turkey to determine the hydroelectric water potential in a basin which is poorly rain gauged. Boundary of the basin, its area, mean, maximum and minimum height and slope data of the basin have been obtained from DEM using remote sensing (RS) and GIS techniques. IRS P5 satellite information with 2.5m spatial resolution has been utilized for DEM. The DEM was utilized to deliver the flow accumulation and flow segment maps of the basin. Subsequently, drainage network was derived with the examination of these maps. Utilizing the topographical data for study area, mean basin height and limited point observation of precipitation information, a regression model was obtained for the entire watershed. This regression model was validated on a sub-basin with satisfactory outcomes utilizing mean areal precipitation which was calculated isohyetal map created by kriging method inbuilt in ArcGIS 2.2.

DEM method proposed by Australian National University provides more accurate

DEM method proposed by Australian National University provides more accurate

Zamfir *et al.,* (2011) made a study introducing a few solutions for delineating a watershed automatically so as to discover the importance of his studies in the geographical reality. The area chosen for the study was Oltet watershed. Olteţ watershed was delineated automatically utilizing ArcGIS Desktop 9.3 and Quantum GIS 1.7.0 Wroclaw with an SRTM DEM of 90 m resolution. After utilizing GIS procedures, two maps of the Olteţ watershed was obtained showing the boundary. Overlapping the two maps acquired with ArcGIS and QGIS some contrasts were seen in the maps produced by the software involved in the study. They have likewise determined a circularity coefficient for the Oltet watershed and a value of 2.15 was obtained supporting its elongated form.

Li (2014) used stream network information to model the Jackpine watershed in Ontario, Canada, utilizing Arc Hydro Tools. The modelling results incorporate stream network and catchment delineation. The impacts of the DEM reconditioning process and the stream threshold value on the modelling precision were analyzed through three simulations. The precision was examined by overlaying the recreated and actual maps, just by looking at stream densities, network lengths and quantities of streams, catchment area, and number of catchments. Their study concluded that Arc Hydro tool was useful for performing watershed modelling with satisfactory execution. It also indicated that DEM reconditioning can improve the precision of watershed modelling. It was likewise concluded that lower stream threshold value cannot just lead to a progressively detailed stream network but in addition upgrade the precision of catchment delineation.

Sheak *et al.,* (2019) used DEM of 30 m resolution to delineate the catchment area of Kangsabati reservoir in ArcGIS 10.4. The watershed area acquired from this outline procedure is 3622 km^2 while it was 3625 km^2 as reported by the Department of water system, Government of West Bengal. This distinction in watershed area is because of errors from the estimation utilizing conventional delineation. The diverse watershed parameters, for example: area, flow path, drainage pattern, watershed slope, rain gauge position and so on produced from delineated watershed shape file can be utilized in HEC-HMS to create watershed modelling for exploring the chance of flood event in the Kangsabati reservoir. Their study concluded that it may very well be helpful for additional investigation of sedimentation, improved LULC practices, and watershed management for the Kangsabati reservoir in future.

2.2 PREPARATION OF LAND USE LAND COVER MAP:

Long *et al.,* (2004) made a study to classify the vegetation, man-made structures, and different features from the Satellite Image of NASA Stennis Space Center (SSC), Mississippi, and USA by utilizing ERDAS Imagine 8.5. To classify the SSC picture, the multi spectral information was utilized for arranging terrestrial objects, vegetation and shadows of the trees. They used supervised and unsupervised classification. Unsupervised classification using ERDAS Imagine helped in distinguishing the terrestrial objects in the study image (SSC). The spectral pattern present inside the data for every pixel was utilized as the reason for classification into four classes (Grass, Trees, Man-Made and Unknown). The resulting map by the unsupervised classification method was utilized to make another map by supervised classification. Image stacking was used to completely classify the satellite image to separate classes like shadow, grass, man-made, and trees. Computer-guided (unsupervised) and user-guided (supervised) procedures will be portrayed on picture stacking to see every classification each in turn and stack them into a total classified image. The application of unsupervised and supervised classification in agriculture land was discussed by giving examples of measurement of field reflectance of two classes of giant salvinia [green giant salvinia (green foliage) and senesced giant salvinia (mixture of green and brown foliage)], and invasive aquatic weed in Texas.

Kaul *et al.,* (2012) for his study in Jalgoan District of Maharashtra state, used the satellite images of March and November 2007 for making the LULC (Land Use/Land Cover) map by supervised classification. For classification seven LULC classes were chosen. KAPPA analysis, accuracy assessment and classification error matrix analysis were done. Change detection between both the pictures for all the LULC classes was obtained. The highest land cover class of Jalgoan District in November was found to be agricultural area i.e. 49.43% and secondly the barren land of about 28.31% in March. Saline region shows critical distinction in the two seasons. The significant change (+ 9.02%) recognized, in the study was in agricultural zone from pre-monsoon to post-monsoon season. The accuracy obtained from supervised classification was 89% and 91.02% and Kappa statistics was 0.86 and 0.88 for March and November images respectively.

Rawat *et al.,* (2013) represents an integrated use of remote sensing and GIS for evaluation of LULC of a town situated in the lower region of the Uttarakhand state *viz*., the Ramnagar. Land sat satellite of two diverse time frames, i.e., Land sat Thematic Mapper (TM) of 1990 and 2010 were downloaded from USGS Earth Explorer and the obtained LULC changes were evaluated for 1990 to 2010. Supervised classification approach was done using maximum likelihood technique in ERDAS 9.3. The satellite image of the study area were classified into five distinct classes, viz. built-up, vegetation, agricultural land, water bodies and sand bar. Study uncovers that the Ramnagar town is growing most extreme towards the southern region along the National Highway-121. The study in addition features the significance of change detection techniques for studying the nature and area of progress in Ramnagar Town. Their results concluded that the vegetation and built-up area increased by 3.51% (9.39 km^2) and 3.55% (9.48 km^2) due to afforestation and expansion of Almora town during their study period. Agriculture and barren land was found to decrease by 1.52% (4.06 km^2) and 5.46% (14.59 km^2) respectively.

Butt *et al.,* (2015) applied maximum likelihood algorithm for supervised classification in ERDAS in order to distinguish LULC changes in Simly watershed, Pakistan utilizing multi spectral satellite information acquired from Land sat 5 and SPOT 5 for the years 1992 and 2012 separately. The watershed was classified into

five significant LULC classes viz. agriculture land, barren soil/rocks, urban, vegetation and water. The final LULC and overlaid maps produced in ArcGIS 10 demonstrated a critical change of vegetation and water bodies to agriculture where as barren soil/rock and urban spread shrank by 38.2% and 74.3% respectively.

Munthali *et al.,* (2019) studied the LULC changes that took place in the years 1991, 2001 and 2015 by applying remote sensing and GIS in Dedza district of Malawi, Africa. In their investigation, both the supervised and unsupervised classifications were performed on the images. The accuracy achieved for the classified image was 91.86%. The outcomes revealed that water bodies, wetlands, forest land, and agricultural land radically declined while builtup regions and barren land significantly expanded between 1991 and 2015. For water bodies, the annual rate change declined from 5.54% ha^{-1} to 1.74% ha^{-1} within the study period. In the same manner, the annual rates change of forest land, agricultural land and builtup area increased from 1.71% ha^{-1} to 1.94% ha^{-1}, 0.02% ha^{-1} to 0.11% ha^{-1} and 7.22% ha^{-1} to 9.80% ha^{-1} respectively. Post classification comparison of the classified images dependent on the transition matrix showed that roughly 61.48% and 2.70% of the total forest land and agricultural land in 1991 was changed over to barren land and built-up land in 2015. Therefore, their investigation, subsequently gives dependable LULC information which detected the degree and pace of land use changes that had happened in the Dedza region of Malawi for the period 1991-2015.

2.3 RUNOFF ESTIMATION BY USING CN METHOD:

Gangodagamage (2001) for his studies used hydrological model for the Bata River basin, which is one of the tributaries of Yamuna stream basin in India. Losses from infiltration, Unit hydrograph and flood routing were the fundamental model components used. ILWIS, ERDAS and AutoCAD map programming were utilized. Satellite based remote sensing and GIS systems were utilized to estimate the spatial variation of the hydrological parameters, which were utilized as a contribution to the model. Survey of India (SOI) toposheet maps, field information, IRS LISS III multi temporal satellite information for rabi and kharif seasons and IRS pan information were utilized. SCS curve number and unit hydrograph strategies were

utilized for the calculation of infiltration losses and synthesis of unit hydrographs individually. The total watershed was partitioned into 10 sub basins, where hydrographs were incorporated by directing the hydrographs along the stream reach. Muskingum hydrological routing technique was utilized for stream routing. Result shows average slope percentage and CN of the watershed to be 21.4 and 52.4 respectively while average slope and CN of sub basin to be varying from 8.9 to 44 and 41 to 78 respectively. Their study concluded the model to be capable of forecasting the runoff for a given input of precipitation and determining the hydrographs for the necessary time span.

Askar (2014) in his study estimated the depth of runoff utilizing the SCS-CN strategy with GIS. The examination was done in the Gomal river watershed which was around 540 km^2. Hydrologic soil group, streamflow, soil slope and land use maps were produced in GIS. The CN method was utilized to estimate the runoff depth for a chosen storm event in the basin. WMS 7.1 program was used to analyze the impact of slope on runoff depth and CN values. The maximum precipitation with various return periods was determined and the mean yearly precipitation depth for the year 1947 to 2005 of Mosul meteorological station was utilized to ascertain the runoff depth of the catchment zone. The consequences of the WMS 7.1 program demonstrated that the curve number for the study area was around 80. The average yearly runoff depth was equivalent to 311.14 mm.

Singhal *et al.,* (2018) made a study on Modikuntavagu watershed which is situated in the Khammam district for computing the runoff by SCS-CN strategy utilizing Geo-spatial information. Direct runoff has been determined dependent on precipitation, soil type, soil moisture, drainage density, geography, size and shape of the basin and land cover. The layers of soil, land use, and slope have been created in GIS. The polygon wise Curve Number (CN) has been assessed utilizing a blend of land use, soil, and antecedent soil moisture condition (AMC). The surface runoff depth has been determined dependent on CN value for the years from 2006 to 2015 and the average percentage of runoff to rainfall was found as 38.9%. The study shows statistically positive correlation (R^2=0.93) between rainfall and runoff depth. The runoff assessed by SCS-CN technique has been compared to rainfall obtained

dependent on nearby gauge catchment (Taliperu) and found that mean variation was 9.3%. The study uncovers that SCS-CN technique along with GIS and remote sensing can viably be utilized to gauge the runoff in an ungauged catchment with identical hydrological attributes.

Pathan *et al.,* (2019) utilized the method of SCS-CN for estimating runoff in Karjan reservoir basin. The daily precipitation information of five raingauge stations was gathered and utilized for daily runoff estimation utilizing the SCS CN method along with GIS. The linear regression model was utilized for checking the runoff resulted from SCS-CN method. It was discovered that the runoff estimated from SCS-CN method showed deviations from the observed runoff. Linear regression method was found to be closely similar to the observed runoff of the basin in contrast to the SCS-CN model. The value of coefficient of determination (R^2) for SCS-CN model found was 0.65 and the value of coefficient of determination (R^2) for linear regression model was 0.83.

Rajkumar *et al.,* (2019) assessed the runoff depth for Tiruchirappalli district situated in Tamil Nadu for which the base map, land use map and soil map were created in ArcGIS 10.5. After the intersection of these thematic maps with rainfall map, CN value was assigned and CN map was generated. By mathematical calculations, spatial distribution of runoff depth over the district was obtained. For estimation of surface runoff depth the spatial distribution map of curve number and rainfall were created in ArcGIS environment. They were intersected and then runoff depth was estimated using NRCS-CN formula in Ms excels to find out the spatially distributed runoff depth over the area. The runoff generated for precipitation event was distributed as low (0-0.57cm), very low (0.58cm-1.13cm) medium (1.14cm-2.13cm), high (2.14cm-3cm) and very high (3.01cm-6cm) by natural break classification system. It shows that the runoff values increases with an expansion in the amount of rainfall in the study area. The agricultural land had the highest runoff with 52.14% of runoff depth due to its higher coverage area in the district. The builtup had runoff next to agricultural land with 20.80% due to its low infiltration rate. Waste land had the least runoff creating limit (0.01%). Close to agriculture, the expanding region of built-up area gives more runoff and low infiltration depth in the study area.

Muthusi *et al.,* (2020) utilized the SCS-CN technique integrated with remote sensing and GIS to estimate urban runoff and to analyze the effect of LULC changes on surface runoff rates from 1989 to 2018 for Mavoko municipality which borders Nairobi city in Kenya. Precipitation data was from two precipitation stations i.e. Mua Hills precipitation station and the Jomo Kenyatta International Airport (JKIA) precipitation station. DEM was utilized to determine the drainage network. Previous LULC changes were mapped from 1989 to 2018 and combined with SCS-CN model to assess the depth and volume of runoff from the watershed. Built-up zones that are to a great extent impenetrable expanded from 24.6% in 1989 to 37.0% in 2018 while the more pervious land under grasslands open spaces and barren land diminished from 65.5% in 1989 to 44.5% in 2018. 69% of the yearly precipitation in 1989 was transformed to runoff while in 2018 76% of the yearly precipitation was transformed to runoff. The outcome was reliable for the LULC changes and results indicated that 68% of the area experienced increasing runoff while 23% had no change and 9% experienced reduction in runoff. Relation between potential maximum storage and the runoff volumes increased from 0.56 in 1989 to 0.59 in 2004 and 0.77 in 2018. The observed correlation between potential maximum storage and the runoff volume showed that the use of SCS-CN method integrated with remote sensing and GIS approach can be a valuable technique for runoff assessment.

2.4 APPLICATION OF HEC-HMS MODEL FOR RUNOFF SIMULATION:

Asadi *et al.,* (2012) simulated rainfall-runoff processes in Kabkian basin (846.5 km^2) and Delibajak sub basin (16.3 km^2) in Iran. The basins for the study were considered as lumped. The hydrologic model HEC-HMS was utilized along with the HEC-GeoHMS. The SCS curve number method was considered for the rainfall-runoff modelling and the model was calibrated and validated utilizing the historical data simultaneously. Co-efficient of agreement and determination coefficient for all the flood events were found to be above 0.9 and the percentage error in volume and peak flow were approximately within the acceptable range. There are three parameters (curve number, lag time and initial abstraction) of the model that were dependent upon the sensitivity analysis. In the kabkian and Delibajak basin the highest difference between the simulated peak hydrograph and the baseline peak hydrograph were

brought about by curve number and initial abstraction methods. The optimized hydrologic parameters, curve number and initial abstraction were compared. In the Kabkian basin, lag time, curve number and initial abstraction were 347 min, 62 and 34 mm respectively whereas in Delibajak sub basin these parameters were 92 min, 53 and 49 mm. This variation was because of contrasts in basin slope, land use in the basin, geologic formations and vegetation cover.

Halwatura *et al.,* (2013) made a study utilizing three unique ways to deal with calibration and validation of the HEC-HMS 3.4 model for Attanagalu Oya river catchment and create long term flow information for the Oya river and its tributaries. Twenty year daily precipitation information from five rainfall gauging stations dispersed within the Attanagalu Oya catchment, monthly evaporation data together with daily stream flow information at Dunamale from 2005 to 2010 were utilized for the study. GIS data layers providing information required for the stream flow simulation were prepared using ArcGIS 9.2 and finally loaded in the HECHMS 3.4 model for the calibration of Dunamale sub catchment. The daily stream flow information from 2005 to 2007 was used. The model was calibrated changing three distinct methods. The model parameters were changed and the model calibration was performed independently for the three chosen methods i.e. the Soil Conservation Service Curve Number loss method, the deficit constant loss method (the Snyder unit hydrograph and the Clark unit hydrograph method) so as to decide the most appropriate simulation method for the study area. The calibrated model was validated later on with another set of precipitation and flow data (2008–2010). The stream flow simulated using every method was tested statistically utilizing the coefficient of performance, the relative error and the residual methods. The results showed that the Snyder unit hydrograph technique simulates stream flow more dependably than the Clark unit hydrograph method.

Reshma *et al.,* (2013) made a study utilizing HEC-HMS hydrological model to simulate runoff process in Walnut Gulch watershed situated in Arizona, USA. To study infiltration, precipitation excess to runoff and flood routing, techniques like Green-Ampt, Clark's Unit hydrograph and Kinematic wave routing were selected. The model has been calibrated and validated for seven rainfall events. The calibration

was done for four rainfall events (July 20 2007, August 28 2008, August 23 2009 and July 29 2011) and validation for three rainfall events (August 4 2009. September 13 2009 and August 28 2010). From the outcome of the model it was perceived that HEC-HMS model has performed satisfactorily for runoff simulation of different rainfall events. From the simulated results of calibrated events they concluded that the volume of runoff has been simulated within the variation of 60% except for the event July 29, 2011 where the variation was 93%. For validation, the variation was found to be -27% except for the event August 28, 2010. Time to peak has been simulated within the variation of 33% for calibration period while for validation a variation of -3% was observed.

Roy *et al.,* (2013) used Hydrologic Modelling System for their study after which the calibration and validation of the model was done for Subarnarekha basin located in eastern India for forecasting its hydrologic response. The Nash-Sutcliffe efficiency, error percentage in volume, peak error percentage and net difference of observed and simulated time to peak were utilized for model efficiency analysis. The values were found to vary from (0.72 to 0.84), (4.39 to 19.47%), (1.9 to 19%) and (0 to 1 day) respectively, showing a good performance of the model for simulation of stream flow and quantification of the available water. The investigation likewise exhibits that the utilization of semi yearly parameter sets that accounts for changing hydrologic conditions improves model performance. The study also concludes that the model might be applied to different watersheds in the Subarnarekha stream basin and other hydro-meteorologically comparative watersheds.

Choudhari *et al.,* (2014) utilized HMS model for their study to simulate rainfall-runoff process in Balijore Nala watershed of Odisha, India. To calculate runoff volume, peak runoff rate, base stream flow and stream routing techniques, SCS curve number, SCS unit hydrograph, Exponential recession and Muskingum routing methods were chosen. Rainfall-runoff simulation was directed utilizing 24 irregular rainstorm occasions covering four years (2010–2013) information. Out of these, 12 events were chosen for calibrating the model and the remaining 12 for validating the model. The value of mean absolute relative error (MARE) obtained were 0.20 and 0.25 while root mean square error (RMSE) between the observed and simulated

information were 2.30 mm and 0.28 m^3/s for depth of runoff and peak discharge. After optimization of the parameters were done, the error decreased to 0.10, 0.12, 0.75 mm and 0.09 m^3/sec in succession. The simulated model with improved parameters was utilized for validating the model.

Reza Kabiri (2014) conducted a study to indicate the efficiency of SCS-CN loss model to assess runoff in Klang watershed. Daily data of 23 rainfall gauging stations were entered into the model to create hydrograph at the sub-basin. At first, the basin was partitioned into sub-basins utilizing HEC-GeoHMS to get the sub-basin geometric information and afterwards the hydrological model was created in HEC-HMS utilizing all the parameters acquired from the past events. Modified SCS-CN loss method was carried out by replacing the initial abstraction ratio to 0.05 so as to calculate the efficiency of calibration and validation of the hydrologic model. The flood hydrograph was calibrated best for peak discharge with the altered ratio of initial abstraction to maximum potential retention in SCS model. The results uncovered that initial abstraction ($\lambda = 0.05$) and $CN_{0.05}$ of daily precipitation by percent error in peak has given no significant difference in the result when compared with initial abstraction with a value of 0.2 and $CN_{0.2}$. In light of utilizing $CN_{0.05}$ for loss model rather than using initial abstraction value as 0.2 and $CN_{0.2,}$ the simulated flows were found to be underestimated when compared to observed discharges which were equivalent to 23.6% and 13.49% for the calibration and validation time frame.

Hilbert (2015) made a study to develop a relationship between rainfall-runoff utilizing hydrological model and GIS in Kuantan watershed and to analyze the use of HEC-HMS model in runoff forecasting and assessing the precision of altered SCS-CN in tropical areas. HEC-HMS model was utilized to simulate the occurrence of storm event that happens in the watershed dependent on a chosen event for which calibration and validation of the model was done. The technique utilized in the model was the SCS Unit Hydrograph for the transform method, SCS-CN for the loss method and lag time for flood routing method. Simulation was completed dependent on two chosen storm events which were first done on December 2006 and secondly on January 2012. The estimation of initial abstraction ratio utilized was 0.2 and 0.05 in which the results dependent on both values of the ratio were analysed. Values of the

simulated results over the actual values of runoff were used to estimate the Nash-Sutcliffe Efficiency (NSE).The NSE value for the model when calibrated ranged from 0.7 to 0.9. The use of two distinct equations to figure the lag time gave slight changes in the outcome as the utilization of Kirpich equation gives a superior result in contrast to the utilization of SCS curve number equation for the forecasting of peak discharge.

Pampaniya *et al.,* (2015) used HEC-HMS 5.0 hydrologic model for simulating runoff in the Hadaf stream watershed, Gujarat, India. Two elevation datasets (DEM) of the Hadaf Basin were used i.e., SRTM 90m DEM and ASTER DEM 30m which were further processed to generate HEC-HMS model input files by applying HEC-GeoHMS extension tool of ArcGIS 10. Land use maps for three different years i.e. 2008, 2012 and 2013 were prepared which was obtained by utilizing remote sensing satellite images. The catchment was divided into a number of sub catchments to consider variation in the geomorphologic parameters. SCS-CN loss method, SCS unit hydrograph, and Muskingum approaches were selected as loss, transformation and routing methods respectively for calibration of the model. Runoff simulation for calibration and validation of HEC-HMS model and evaluation of different unit hydrographs were made with two transformation methods i.e. SCS UH (approach-1) and the Clark UH (approach-2). It was found that the Clark method delivers better outcomes over SCS-UH transformation method in rainfall-runoff simulation in terms of both the peak runoff and runoff volume. The study concluded that the enhancement of the parameters altogether improved the model.

Rathod *et al.,* (2015) made an investigation to compute runoff for various precipitation events in three sub basins of Tapi river in India. Continuous lumped hydrological model was produced for the study area utilizing HEC-HMS 3.5. For calculating the losses Green-Ampt strategy was utilized. For better runoff estimation SCS unit hydrograph and Snyder Unit hydrograph techniques were compared and best appropriate strategy for the study region was picked up for the last simulation. To compute the reference evapotranspiration, FAO Penman-Monteith technique was utilized. Sensitivity analysis was done for various parameters of the model and the most sensitive parameters were enhanced and the parameters were utilized for calibrating and validating the model. The aim of their examination was to fit the peak

flow discharge and amplify the Nash-Sutcliffe efficiency. Conclusive results showed that Nash-Sutcliffe efficiency was more than 0.8 for the three sub basins. Correlation coefficient among observed and simulated discharge was more than 0.9 for the three sub basins. Their study concluded that HEC-HMS model can be utilized with sensible approximations for runoff estimations for Tapi river.

Ismael *et al.,* (2017) assessed the hydrological processes of Ruiru reservoir catchment to compute its runoff using HEC-HMS 4.1 hydrologic model (with Soil moisture Accounting Algorithm). WMS 10.1 (Watershed Modeling Surface) was utilized as an interface to delineate the watershed and produce some input parameters. The SMA parameters were computed in WMS utilizing land use and soil type information. Daily precipitation and monthly evapotranspiration for 5 years (2011-2015) were utilized for the meteorological information sources. The outcomes demonstrated an absolute volume of runoff 202,860,900 m^3 during the five years of the simulation. The peak discharge was seen as 79.6m^3/s and the average daily inflow during the five years was seen as 1.28m^3/s. The model assessment has demonstrated the efficiency of the model to be 0.74 and 0.72 separately for the calibration and validation showing the results of the simulation to be good.

Koneti *et al.,* (2018) made an investigation utilizing the HEC-HMS model and remote sensing-GIS procedures for detecting the spatial and qualitative changes in the precipitation overflow that had occurred because of the LULC changes from 1985–2014 in the Godavari river basin. This paper analyzed the LULC changes for the years 1985, 1995, 2005 and 2014 of Godavari basin. The findings uncover an expansion of developed land, an abatement of shrub land and an increase in water bodies for the period 1985-2014. The study had a general classification accuracy of 92% and a general Kappa co-efficient of 0.9. The HEC-HMS model was utilized to simulate the hydrology of the Godavari basin. The analysis done was essentially focused on the effect of LULC changes on the stream flow design. The surface runoff was simulated for the year 2014 to evaluate the progressions that have occurred because of changes in LULC. The observed and the simulated peak stream flow was seen as the same i.e., 56,780 m^3/s on 9 September 2014. Linear regression was utilized for validating the model to relate the observed and simulated stream flow information

at the gauging station of the Badrachalam outlet for the Godavari river basin and a relationship co-efficient of 0.83 was obtained. The hydrological modelling that was done utilizing the HEC-HMS model has drawn out significant effect of LULC on rainfall-runoff at the Pranhita sub-basin scale demonstrating the model's capacity to effectively reflect the entirety of the ecological and scene factors. The results of the investigation showed that the use of remote sensing, GIS and the hydrological model (HEC-HMS) can effectively depict the hydrological issues in a stream basin.

Paudel *et al.,* (2019) simulated the flow of Marshyangdi river basin situated in Nepal. Furthermore, the assessment and investigation of discharges for each subbasins of Marshyangdi basin was done in their study. The HEC-HMS model was utilized to calibrate (from 2003-2007) and validate (from 2008-2012) the Marshyangdi basin. The main output from the model was the discharge value at the outlet of the catchment. At last, the output was compared with the observed discharge at selected gauging station of the basin. The model performance was tested for the river basin during calibration and validation period, The Nash-Sutcliffe efficiency (NSE) and Coefficient of determination (R^2) was utilized to assess the performance of the model. The outcomes obtained were satisfactory and acceptable for simulation of runoff. The SCS curve number technique, SCS unit hydrograph strategy, constant monthly technique and Muskingum routing technique were utilized as the loss method, direct runoff transformation, base flow and routing methods respectively. Thus, their study identified HEC-HMS model to successfully model the upper Marshyangdi river basin for better assessment and hydrological response. Result shows both NSE and R^2 value to be 0.778 for calibration period and 0.842 for validation period which indicates the model has well simulated the daily stream flow at the outlet of the river basin.

Sarminingsih *et al.,* (2019) studied the relationship of rainfall-runoff in the Garang watershed utilizing HEC-HMS 4.2. For calibration, the observed data of discharge was utilized from AWLR Kreo. Based on optimization studies, the hydrological parameters for HEC-HMS were acquired i.e. CN composite 66.4, groundwater accounts 128.48 mm, Initial abstraction 25.7 mm and percentage impervious as 9.27%. The validity of the model was satisfactory based on the co-

relation values, RMSE and Nash-Sutcliffe efficiency. The results of this study concluded that the HEC-HMS model was good enough to be used for modelling rainfall-runoff in the Garang watershed. The increase of CN values and imperviousness and the decrease of groundwater content and initial abstraction values have increased the amount of runoff. This has caused an increase in flood discharge while decreasing low flow discharge which has an impact on decreasing water availability.

Tassew *et al.,* (2019) simulated the surface runoff utilizing the Hydrologic Modeling i.e. HEC-HMS for the Gilgel Abay Catchment (1609 km^2) located in Ethiopia. Delineation of the basin was done utilizing 30m×30m DEM of the Lake Tana Basin. The meteorological model was created inside the HEC-HMS model from precipitation information and the period and time step of the simulation run were defined by the control specifications. To take into account the losses, runoff estimation and flood routing, the SCS-CN, SCS-UH and Muskingum method were utilized. The rainfall-runoff simulation was done utilizing six extreme daily time series events. The calibration of the model was carried out with an optimization method and sensitivity analysis. The after effects of the sensitivity analysis indicated that the curve number was a very sensitive factor. Furthermore, the validation of the model results indicated a sensible contrast in peak flow (Relative error in peak, REP = 1.49%) and total volume (Relative error in volume, REV = 2.38%). The examination of the observed and simulated hydrographs, the model execution (Nash Sutcliffe Efficiency = 0.884) and their co-relation (R^2 = 0.925) indicated that the model fitted perfectly for hydrological simulations in the Gilgel Abay Catchment.

2.5 IMPACT OF LAND USE LAND COVER CHANGES ON THE WATERSHED CHARACTERISTICS

Sai Hin Lai *et al.,* (2008) made a study depicting the use of GIS and remote sensing for analyzing the effect of land use changes to the turbidity of runoff water in different watersheds. Information data sets consisting of hydrologic parameters, climate data, soil type, DEM, land use, and surface features were incorporated in GIS in a tabular, vector and grid format for their study. The land use

maps obtained from Landsat-5 TM imagery utilizing a mixture of various characterization strategies gave a precision of 95%. Results from the study had indicated that there exists a close relationship between the degree of open area and sedimentation loading rate. The sediment loading rates were seen as non-linear extending from 1.47 to 2.13 tons per millimetre of precipitation for every km^2 increment of open zones, depending upon their area with respect to variables such as accessibility of sediments, soil type, slope length, slope steepness and so on.

Letha *et al.,* (2011) analysed the discharge data of Vamanapuram basin situated in Kerala for a time period of 40 years and to check the changes in the pattern of stream flow because of the changes in the land use/land cover (LULC) during the study period. The trend analysis of the runoff data shows that the peak discharge has an increasing pattern over the time period and low stream flow values have a diminishing pattern. The rainfall runoff relationship determined for various periods uncovered that the runoff created from a similar precipitation amounts demonstrated an increasing pattern towards the end of the study period. The LULC examination demonstrated that there is a significant increment in the built up region and barren lands to the detriment of forest and other thick vegetations. Subsequently it was observed that the increasing pattern of peak flow and the diminishing pattern of low stream flow are the consequence of LULC. From the study it may very well be reasoned that as the LULC over a river basin changes, the runoff of the basin is likewise influenced or changed. Results show that the built up region expanded from 75 km^2 to 196.10 km^2 i.e. a total increment of 261%. Simultaneously, the forest area diminished from 290.15 km^2 to 93.78 km^2, i.e. a total decline of 67.67%. Henceforth their study suggested that urgent watershed management and control measures are to be adapted for checking the change of land use.

Mayaja *et al.,* (2017) made a study to assess the LULC changes that had occurred in Pampa basin during the recent three decades by utilizing the remote sensing based digital pictures for the period from 1985 to 2012. The outcome inferred by investigating the satellite pictures showed conceivable human intercession which was later examined. The changes in the land use of Pampa basin uncovered negative changes which were disturbing and causing the destructions currently being

experienced in the form of repeated flood and dry spells. The results concluded highest increment in urban territory by 31.4% and quick conversion of fertile land to wastelands by 8.5%, decrease in agricultural land by 3% and increase in deforested area by 4.5%. This led to a change in the production intensity leading to the critical requirement of a strategy to ensure the protection of stream and basin.

Prakash *et al.,* (2017) took up an investigation in Serilingampally Mandal of Ranga Reddy locale, a peri-urban territory of Hyderabad city, Telangana state for evaluating surface overflow by utilizing Land sat-MSS information and Resourcesat 2 LISS-IV information gathered in 1975 and 2016 separately through visual understanding methodology. At first, LULC was produced to analyze the development of urban settlements. The increment in surface runoff during the rainstorm seasons (June-October) 1975 and 2016 were computed utilizing the Soil Conservation Service (SCS) curve number method. Results demonstrated a sharp increment in built-up land during the period 1975-2016 with subsequent higher runoff. The results reflected an increase in built up area from 0.91% to 69.36%. In the year 2016 an increase in runoff by 27.5% was found as compared to 1975.

Lydia *et al.*, (2018) studied the LULC changes in Coimbatore Corporation (257 km^2) for the year 2005 and 2010. To analyze LULC changes, satellite pictures of Land sat 7 (2005) and Sentinel-2 (2010) were utilized. The change detection analysis has been performed for the years 2005 and 2010. ERDAS Imagine 2015 was used to prepare the LULC map and Arc GIS 10.0 was used to evaluate the LULC changes for the above periods. The after effects of the analysis have shown that Coimbatore Corporation has encountered quick changes in LULC especially the urban zone. In the past five years the urban area was found to increase by 19.6 km^2 which led to a decline of agricultural and vegetation area. The agricultural area was decreased by 60% while the urban and water body area was found to increase by 33.4% and 24% respectively. The LULC change recognition investigation revealed that the study area has expanded in contrast with 2001 and every single different class diminished. This study concluded that urbanization has affected the LULC changes of the Coimbatore Corporation zone.

Mousavi *et al.,* (2018) estimated LULC changes in the Marand basin utilizing remote sensing and GIS. The runoff coefficient was computed utilizing the LULC map prepared from the satellite pictures, slope map, hydrologic soil group, and precipitation intensity. Peak runoff for each sub-basin was also determined. Next, by using linear relationship function in the fuzzy logic model, the integration of two layers of peak runoffs and the elevation line layers ranging between 0 and 1 were transformed into fuzzy values. Later on, numerous overlaps of weights were applied to both the layers and their outcomes and classes of flood hazard map were created. The accuracy of the map was found to be 87.83%. Their study concluded that about 25.3% of the total LULC area is under high and very high risk category. Urban, rural and industry area occupies about 17.3 km^2 while garden and plantation area occupy 123.8 km^2 which is under high risk of flood vulnerability.

Venkatesh *et al.,* (2018) studied the effect of land use land cover change (LULC) on stream flow by utilizing SWAT model for Tungabhadra basin, situated in Karnataka, India. The land use maps of 1993, 2003 and 2018 were utilized for evaluating the stream changes caused by changes in LULC. Calibration and validation of the model for stream flow was done by utilizing the SUFI-2 algorithm in SWAT-CUP for the years 1983-1993 and 1994-2000 separately. Statistical parameters such as Coefficient of Determination (R^2) and Nash–Sutcliffe Efficiency (NSE) were utilized to survey the efficiency and performance of the SWAT model. It was discovered that the observed and simulated stream flow values were almost similar, which thus extends that the model outcomes were acceptable. The calibrated model was utilized for simulation of future land use scenario to evaluate the effect on stream flow. Based on LULC classification, the predominant classes were barren and cultivated land. Both the classes were decreased in 2018 when compared to 1993 which was accompanied by the increase in agriculture and urban area. For daily simulations the outcomes were acceptable (R^2 = 0.727, 0.729, 0.73 during calibration phase and R^2 = 0.753, 0.754, 0.75 during validation phase) for the years 1993, 2003 and 2018. Using monthly time steps the outcomes were additionally improved for runoff (R^2 = 0.8, 0.804, 0.8 during calibration phase and R^2 = 0.852, 0.854, 0.85 during validation phase) for the 3 years respectively.

Younis *et al.,* (2018) focuses on the effects of LULC change for a multi year time frame (2000–2010) on the stream discharge in a sub-watershed of Indus river utilizing the lumped model HEC-HMS. The input factors for model structure in HEC-HMS were determined using the DEM, LULC, soil and precipitation information which was gathered and pre-processed in HEC- GeoHMS. The model was calibrated for the year 2000 and validation was accomplished for the year 2010. For the calibration period the correlation coefficient was found to be 0.96 and Nash-Sutcliffe Efficiency (NSE) to be 0.87 while for the validation period the correlation coefficient was found to be 0.95 and NSE to be 0.91. The model outcome of LULC changes examination utilizing Landsat pictures for 10 years showed irrelevant changes in discharge showing that the effect of LULC changes seems to be negligible within the study period.

Jin *et al.,* (2019) for their study developed a modified SWAT (LU-SWAT) that incorporates yearly land use/ spread information to simulate LULC effects on hydrological processes under various climatic conditions. To approve this methodology, the modified model and two different models (one model dependent on the 2000 land use map, called SWAT 1 and the other model dependent on the 2009 land use map, called SWAT 2) were applied to the middle reaches of the Heihe River in northwest China. Results demonstrated that from 1990 to 2009 farmland, forest and urban zones all indicated expanding patterns while grassland and bare land regions indicated diminishing patterns. Predominant land use changes in the study area were from grassland to farmland and from bare land to forest. During this same period, surface runoff, groundwater runoff, and total water yield showed decreasing trends, while lateral flow and ET volume showed increasing trends under dry, wet, and normal conditions. Changes in the various hydrological parameters were most evident under dry and normal climatic conditions. From 1990 to 2000 farmland zones expanded by 10.65% while grassland regions diminished by 9.13% and from 2000 to 2009 farmland zones kept on expanding and grassland zones kept on diminishing however at much more slower rates of 3.45% and 0.90% respectively. Under dry, wet and normal conditions, surface runoff diminished by 75.93%, 23.61%, and 40.44, groundwater runoff diminished by 45.73%, 11.42%, and 49.55% and total water yield

diminished by 33.74%, 4.23%, and 18.47% respectively. Lateral flow increased by 99.93%, 30.22%, and 120.21% and ET volume increased by 35.11%, 13.10%, and 23.60% respectively. The results showed that the modified LU-SWAT created in this investigation performed better compared to the ordinary SWAT while anticipating the impacts of LULC change on the hydrological cycle of the basin. Comparative with the regular SWAT, the proposed LU-SWAT accomplished NSE estimations of 0.75 and 0.82, PBIAS estimations of 4.43% and 4.43% and RSR estimations of 0.50 and 0.42 in the calibration time frame. Similarly, NSE values of 0.72 and 0.80, PBIAS values of 7.97% and 7.97%, and RSR values of 0.53 and 0.45 in the validation time frame were obtained while simulating monthly and annual runoff in the middle reaches of the Heihe River respectively.

The area of all classified materials is significant in flood hazard, so that totally 25.3% of the entire LULC area is in high and very high risk categories. Constructed lands including urban, rural, industrial, and industrial-productive centres, with a sig-

nificant area of about 17.3 square kilometres, is at risk of flooding and vulnerability. Garden and plantation with a surface area of 123.8 square kilometres are at the risk
of flooding as one of the most important sources of indigenous income.
The area of all classified materials is significant in flood hazard, so that totally 25.3% of the entire LULC area is in high and very high risk categories. Constructed lands including urban, rural, industrial, and industrial-productive centres, with a sig-

nificant area of about 17.3 square kilometres, is at risk of flooding and vulnerability. Garden and plantation with a surface area of 123.8 square kilometres are at the risk of flooding as one of the most important sources of indigenous income.
The area of all classified materials is significant in flood hazard, so that totally 25.3% of the entire LULC area is in high and very high risk categories. Constructed lands including urban, rural, industrial, and industrial-productive centres, with a significant area of about 17.3 square kilometres, is at risk of flooding and vulnerability.

Garden and plantation with a surface area of 123.8 square kilometres are at the risk of flooding as one of the most important sources of indigenous income.
The area of all classified materials is significant in flood hazard, so that totally 25.3% of the entire LULC area is in high and very high risk categories. Constructed lands including urban, rural, industrial, and industrial-productive centres, with a significant area of about 17.3 square kilometres, is at risk of flooding and vulnerability.
Garden and plantation with a surface area of 123.8 square kilometres are at the risk

of flooding as one of the most important sources of indigenous income.
The area of all classified materials is significant in flood hazard, so that totally 25.3% of the entire LULC area is in high and very high risk categories. Constructed lands including urban, rural, industrial, and industrial-productive centres, with a significant area of about 17.3 square kilometres, is at risk of flooding and vulnerability. Garden and plantation with a surface area of 123.8 square kilometres are at the risk of flooding as one of the most important sources of indigenous income

The area of all classified materials is significant in flood hazard, so that totally 25.3% of the entire LULC area is in high and very high risk categories. Constructed lands including urban, rural, industrial, and industrial-productive centres, with a significant area of about 17.3 square kilometres, is at risk of flooding and vulnerability. Garden and plantation with a surface area of 123.8 square kilometres are at the risk of flooding as one of the most important sources of indigenous income
The area of all classified materials is significant in flood hazard, so that totally

25.3% of the entire LULC area is in high and very high risk categories. Constructed lands including urban, rural, industrial, and industrial-productive centres, with a significant area of about 17.3 square kilometres, is at risk of flooding and vulnerability. Garden and plantation with a surface area of 123.8 square kilometres are at the risk of flooding as one of the most important sources of indigenous incom

Quihui Chen *et al.*,(2019) through their study in the Jinsha river basin found out that the environmental change and LULC change are both important in affecting the rainfall-runoff relations. For this study, SWAT model was set up for the area and the strategy for scenario simulation was utilized to examine the runoff response to environmental change and LULC change. The climate factors exported from 7 General Circulation Models (GCMs) under RCP 4.5 and RCP 8.5 scenarios were corrected and imported to the SWAT model to predict runoff in 2017–2050. Results concluded that during the past 57 years both the average annual rainfall and temperature in the watershed increased and the increasing trend of runoff was also found to be much higher than expected. They also concluded that the change in LULC

had only a minor influence on the hydrological processes of the basin while the change in climate was seen to be the major factor influencing the runoff. Their study will help to tackle the challenge of probably increased flood risks by providing data for decision making inorder to implement prevention and mitigation measures.

Materials & Methods

CHAPTER 3

MATERIALS AND METHODS

A study on the impact of land use and land cover changes on the runoff processes in Chalakudy basin was done by modelling the hydrology of the basin using HEC-HMS model. The various software and tools used and the methodologies involved are detailed in this section under the following sub headings.

3.1 STUDY AREA

Chalakudy basin was taken for the present study to assess the impact of land use land cover changes on the basin over a period of two decades. This was one of the worst affected basins in the Kerala floods of 2018 and most of its basin area was severely affected. Chalakudy river is the fifth longest basin in Kerala which lies between 10^0 05' to 10^0 35' north latitude and 76^0 15' to 76^0 55' east longitude and passes through “Palakkad”, “Thrissur” and “Ernakulam” districts. The basin is bounded by “Chittur” and “Alathur Taluks of Palakkad district” and “Mukundapuram Taluk of Thrissur” district in the North, “Alwaye”, “Kunnathunad” and “Paravur Taluks of Eranakulam” district in the South, “Kodungallur Taluk of Thrissur” district in the West and “Tamil Nadu” in the East. Chalakudy river originates from the Anamalai hills of the Western Ghat mountain ranges and courses through the northern part of Periyar river. The basin gets a normal precipitation of around 3,300 mm. Chalakudy basin is partitioned into fifty seven sub watersheds and one hundred and forty mini watersheds. The shape of the basin is roughly triangular with its base along the east, having a length-width proportion of 3:1. It is formed by the meeting of four significant tributaries *viz* Sholayar, Parambikulam, Kuriarkutty and Karapara. The stream has a length of around 130 km and a catchment area of around 1,704 km^2. Out of the total catchment area, around 1404 km^2 is in Kerala state and the rest 300 km^2 lies in Tamil Nadu.

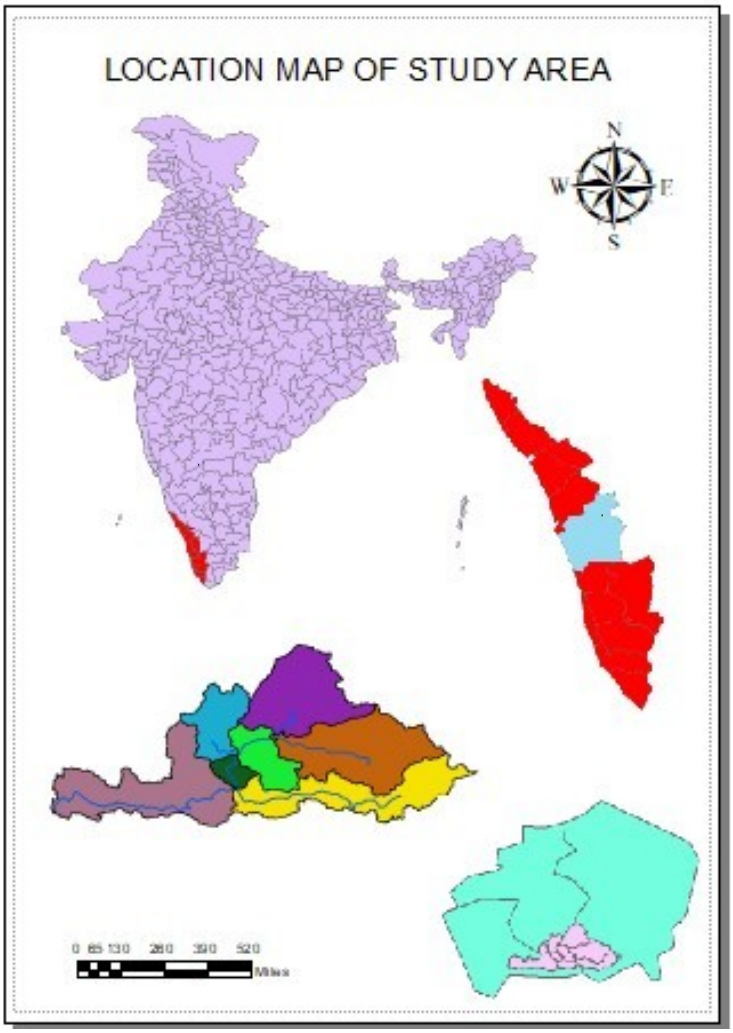

Fig. 3.1: Location map of the study area

3.2 METEOROLOGICAL AND PHYSIOGRAPHIC INFORMATION OF CHALAKUDY RIVER BASIN

3.2.1 Rainfall

The yearly average precipitation in the Chalakudy basin is about 3,300 mm, shifting from 3,700 mm in the uphill area to 2,900 mm in the downstream area (Maya, K. 2005). The precipitation in the basin area increases from west to east. About 68.2% of the total precipitation occurs starting from the month of June to August (South-West monsoon). A total of about 17.5 % of total precipitation occurs from September-November (North East monsoon) while 13% of precipitation is received from March to May and the remaining rainfall during the month of January to February. Daily

rainfall data from five stations along with other meteorological data like maximum and minimum temperature, relative humidity, sunshine hours, wind speed etc., have been collected from ARS, Chalakudy and IMD, Pune. Daily stream flow data at CWC gauging station, Arangali, located near the outlet of the basin has been collected from Cauvery & Southern Rivers Circle, CWC, Bengaluru, for the study period.

The average monthly rainfall values were calculated from the daily rainfall data collected from ARS Chalakudy and IMD, Pune for the years 1997-2017 and the results are shown in chapter 4. The raw rainfall and flow data collected are given in appendix I and II.

3.2.1.1 Location of the rainfall gauging stations

Table 3.1 GPS location of the rainfall gauging stations

Sl No.	Gauging station	Latitude	Longitude
1	Thunacadavu	$10^{o}44'$	$76^{o}78'$
2	Chalakudy	$10^{o}30'$	$76^{o}33'$
3	Peruvaripallam	$10^{o}44'$	$76^{o}76'$
4	Parambikulam	$10^{o}39'$	$76^{o}78'$
5	KSD	$10^{o}32'$	$76^{o}73'$

3.2.2 Climate

Chalakudy basin falls under a humid tropical climate with a summer season extending from March to May and the rainy season from June to September. Wet climatic condition prevails in the higher slope ranges. The relative humidity (RH) is found to be higher during the monsoon months. Highest wind speed is recorded during May (10.9 km/h) (Maya, K. 2005). The basin encounters practically uniform temperature consistently throughout the entire year. However, seasonal variation of temperature is found to be within the range of 25.77^{o}C to a maximum of 35.12^{o}C during the month of March. The information on climate parameters for a period of 20 years (1997-2017) was collected from ARS Chalakudy. The raw meteorological data collected are given in appendix III, IV, V and VI.

3.2.3 Soil

Soils of Chalakudy basin are mainly of six classifications. They are ‘lateritic soil’, ‘riverine alluvium’, ‘seaside alluvium’, ‘hydromorphic saline’, ‘earthy coloured hydromorphic’, and ‘timberland topsoil’. Out of this, the lateritic soils are the most prevalent soil found in the midland district. The earthy coloured hydromorphic soil is found in the valley base of undulating geology of the midland. A significant part of the upland is having timberland soil with the surface layer wealthy in organic matter. The riverine alluvium is present along the waterway channels and their tributaries. As the Chalakudy river basin covers both the Kerala and Tamil Nadu region, the soil data for Kerala region was collected from the Department of Soil Survey and Soil Conservation, Govt. of Kerala, Thiruvananthapuram and the soil data for the Tamil Nadu region was collected from the Dept. of Remote sensing & GIS, TNAU, Coimbatore.

3.2.4 Land use land cover (LULC)

LULC of Chalakudy basin comprises mainly of the classes like coffee and tea plantations, barren land, forest, oil palm, paddy, urban areas and water bodies. The upper locale consists of barren land, forest area and water bodies. The forest area is almost covered by 10% of forest plantation, 12% by degraded forest area while around 8% is covered by deciduous forest and 5% by semi evergreen forest (Maya, K. 2005). The upland area is covered by 40% agricultural land which is predominantly under a mixed plantation of both agricultural and horticultural crops. About 10% of upland region is covered by wasteland while rest of the area is covered by water bodies. The lower region of the basin is mainly occupied by paddy fields and urban settlements.

3.3 DIGITAL DATABASE USED:

3.3.1 DEM

It is the 3D portrayal of a terrain's surface, made from the information of the land surface elevation with respect to any reference datum. DEM is oftentimes used for the digital portrayal of geography and topography and is widely utilized in hydrologic and geologic examinations, hazard checking and monitoring, natural resources

investigation etc. For the present study, DEM of 30 m resolution downloaded from USGS earth explorer was used for delineating the basin and to decide basin characteristics such as elevation, slope, slope length, flow direction and drainage characteristics.

3.3.2 Satellite image

For preparing the LULC map, Landsat-7 satellite imagery of three different years i.e. 1997, 2007 and 2017 were downloaded from USGS earth explorer. Landsat-7 images were downloaded as it provides simultaneous acquisition of high resolution multispectral data of the earth surface. The images for the months of February and April were selected for 1997 and 2017 to make sure that the image is cloud free. The satellite image for 2007 was downloaded for the month of December as there was no clear image from the month of February to April.

3.4 DETAILS OF VARIOUS SOFTWARE AND EXTENSION TOOLS USED:

3.4.1 GIS (Geographical Information System)

GIS is used for capturing, storing, managing and presenting a wide range of spatial information. Because of its incredible capacity for spatial information investigation, GIS empowers hydrologists to coordinate different information from numerous sources with equivalent spatial reference into a reasonable framework.

The extension tool in ArcGIS i.e., HEC-GeoHMS is utilized to portray the physical surface by distinguishing sinks, figuring stream flow direction and flow accumulation and making stream networks. For the present study HEC-GeoHMS extension tool was used for delineating the basin using DEM. It was also used for generating the average precipitation of the basin by using the tool ‘Gage Theissen polygon’. The ‘Generate CN grid’ tool was used for generating the Curve Number by merging both the land use map and soil map polygons.

3.4.2 ERDAS Imagine

ERDAS Imagine developed by Intergraph, USA is an image processing software that permits the users to process geospatial, vector data and other imagery as well. It can likewise deal with hyper spectral imagery and LiDAR from different sensors and can

offer a 3D virtual module (VirtualGIS). The preparation of LULC map was done by using the ERDAS Imagine 2014 software available in the Geo spatial lab of KCAET, Tavanur and the method used was unsupervised classification.

3.4.3 HEC-GeoHMS (Geospatial Hydrologic Modelling Extension)

HEC-GeoHMS is an extension tool of ArcGIS and is explicitly intended to process geospatial information and make input documents for the HEC-HMS. Through the Graphical User Interface (GUI), which comprises a set of menus and tools, one can examine the data and delineate the sub-basin to produce the hydrologic inputs. The database generated using GIS comprises of soil map, DEM, land use data, precipitation and so forth. HEC-GeoHMS works on the DEM to determine basin outline and to set up various inputs for HEC-HMS. Fig. 3.2 depicts the significant procedures involved in beginning project and proceeding using the HEC-GeoHMS extension tool.

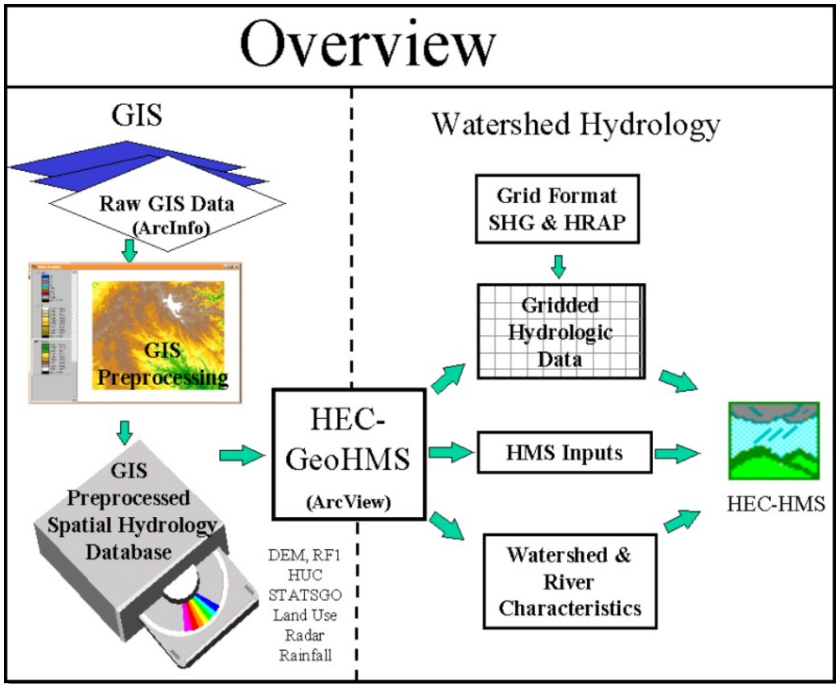

Fig. 3.2: Overview of working with GIS and hydrologic modeling
(Fleming, M. J., and Doan, J. D., 2013)

3.4.4 HEC-HMS Model

The Hydrologic Modeling System HEC-HMS was developed by the US Army Corps of Engineers, Hydrologic Engineering Centre. HEC is a software that enables analysis

of all hydrologic procedures in a watershed framework. The HEC-HMS model consists of two main models i.e., a basin model and a meteorological model. HEC-GeoHMS produces various files which can directly be utilized by the HEC-HMS model. These documents include the “meteorological model document”, “background shape files”, “basin model file” and the “recorded project”. For running the model, all the hydrologic parameters which are to be included in the model run should be assessed and entered manually into the HEC-HMS basin model. When all the model segments are finished, the user can go for a simulation run and finally calibrate the model and optimize the parameters involved in it.

3.5 PREPARATION OF SOIL MAP AND LULC MAP:

3.5.1 Soil map

Soil map of the basin was prepared by using ArcMap by first connecting the soil map folder from the catalogue tool box to the ArcMap and adding the soil map layer in tiff format. The map was then geo referenced by adding the X and Y Co-ordinates. In order to draw the polygons of the soil map the option ‘polygon’ from the drop down menu of feature type was selected and the polygon for each soil type was drawn one by one. The polygons were drawn based on the soil type and the soil characteristics. Once the polygons of different soil groups were drawn, the information based on the soil type such as the HSG (hydrological soil group), area, Pct A, Pct B, Pct C and Pct D etc., were added to the attribute table. Pct A, Pct B, Pct C and Pct D indicates the percentage of HSG A, B, C and D. Suppose, the soil type belongs to HSG A then the value of Pct A in the attribute table must be ‘100’ and the rest of the value i.e., Pct B, Pct C and Pct D must correspond to ‘0’. For calculating the area, the co-ordinate system selected was in projected co-ordinate system (PCS) with the units in square meters. As Chalakudy basin covers both Kerala and Tamil Nadu region, once the soil map for the Kerala region was prepared, it was merged with the soil map of Tamil Nadu region collected from TNAU, Remote sensing and GIS department. Finally, clipping of the soil map was done using the clipping tool provided under the “Geoprocessing” menu. The clipping of the soil map was done as per the basin boundary.

3.5.2 Land use Land cover map

ERDAS Imagine 2014 software available in the Geo Spatial lab of KCAET, Tavanur was used to prepare the land use land cover map. In this study, the land use classes taken were seven *viz* water body, vegetation, urban area, barren land, tea, paddy and oil palm. Before classifying the different classes within the study area, ground truthing and data collection was done. The raster tool in ERDAS Imagine was used to prepare the LULC map. The method used in this study was unsupervised classification and hence, no training data sets were needed. The classification of different pixels into a class was purely based on experience and information captured during the field survey of the basin. Cross checking of the basin area was also done using the 'Google Earth Pro' for identifying the different classes. After the classification of each pixel is completed, every class is ought to be inspected and a name assigned to it. Initially the number of classes was set to forty and the pixels belonging to the same class category were merged into a single class by using the menu 'recode'. Each merged class was renamed and iterations were done following the same procedure to produce seven LULC classes.

3.5.3 Correlation analysis of the average rainfall and average flow

As rainfall is the most important component in a watershed that has a direct influence on the runoff at the outlet, a correlation analysis between the average rainfall and the average flow was done for two different decades and the results were depicted in a graphical format. The first decade of correlation analysis was done from 1997-2007 followed by 2007-2017.

3.5.4 Delineation of the basin

Delineation of the basin was done by using the HEC-Geo HMS extension tool loaded in the ArcMap. In order to delineate the basin, the DEM was imported in the ArcMap and the HEC-GeoHMS extension tool was activated. The "Pre processing" menu in the HEC-GeoHMS tool was selected and all the pre processing steps were carried out to generate the stream lines, drainage lines and flow directions etc. After all such procedures were carried out, the outlet for the watershed was chosen at the

downstream section and the “Project Setup menu” was selected. From the dropdown menu, “Generate project” icon was clicked to complete the delineation procedure. Finally the delineated shape file was saved in a folder. Fig. 3.3 shows the basin delineation procedure in HEC-GeoHMS

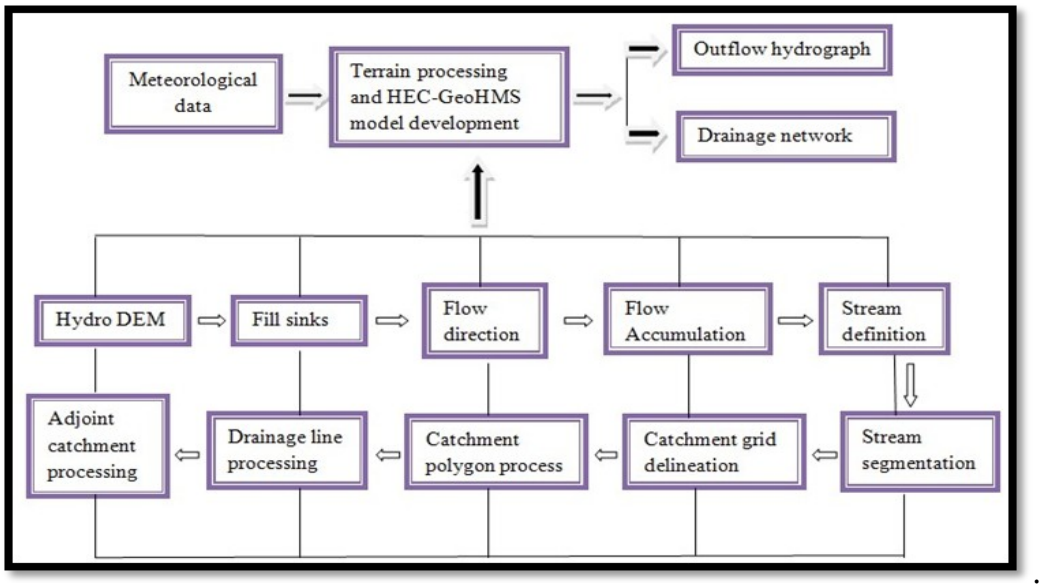

Fig. 3.3: Flow chart of the basin delineation procedure in HEC-GeoHMS

3.6 CREATING A PROJECT IN HEC-Geo-HMS

The steps highlighted below give the procedure involved in HEC-GeoHMS before beginning a project in HEC-HMS. The toolbar of HEC-GeoHMS is shown below in fig. 3.4

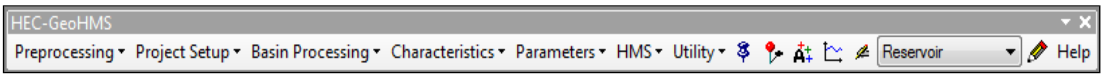

Fig. 3.4: HEC-GeoHMS toolbar loaded within ArcMap

3.6.1 Pre-processing:

The Pre-processing menu was mainly used to develop the initial stream and sub basin delineations. Once the terrain processing was completed, the data was extracted for the creation of hydrologic model using the “Project Setup” menu.

DEM reconditioning tool was mainly used to permit the stream cell height minimization. It also gives an alternative step to bring down the nearby cells along the

streamline. The “DEM Reconditioning” menu thus changes the elevation by lowering cells of grid along the line features. Another menu used for altering the terrain information was the “Build Walls” device. The ‘Build Walls’ ensure delineation of sub basin from the terrain data equivalent to the existing data sets.

The depressions in the DEM are generally considered to be an error and the “Fill sinks” tool was used for filling the pits in the DEM by elevating the depressed cells in the terrain. The ‘Flow Direction’ tool was mainly used for defining the direction of the steepest slope for each terrain cell while the “Flow Accumulation” tool was used for determining all the upstream cells which was draining to a particular cell.

The “Stream Definition” helped in ordering all the cells to have a flow accumulation more prominent than the user characterizing a threshold cells belonging to a stream network. ‘Stream Segmentation’ tool separates the grid of streams into fragments. Stream fragments are the part of a stream that interface two junctions, an outlet or a drainage divide.

‘Catchment Grid Delineation’ tool was used for creating a vector layer of each sub basin utilizing the previously computed catchment grid. The ‘Drainage Line Processing’ step was carried out for creating a vector stream layer. The “Adjoint Catchment Processing” tool was used for totalling the upstream sub basins at each stream intersection. Since, it is a necessary step it was performed in improving the execution for intelligently delineating the basin and in enhancing the information extraction while characterizing the HEC-GeoHMS project.

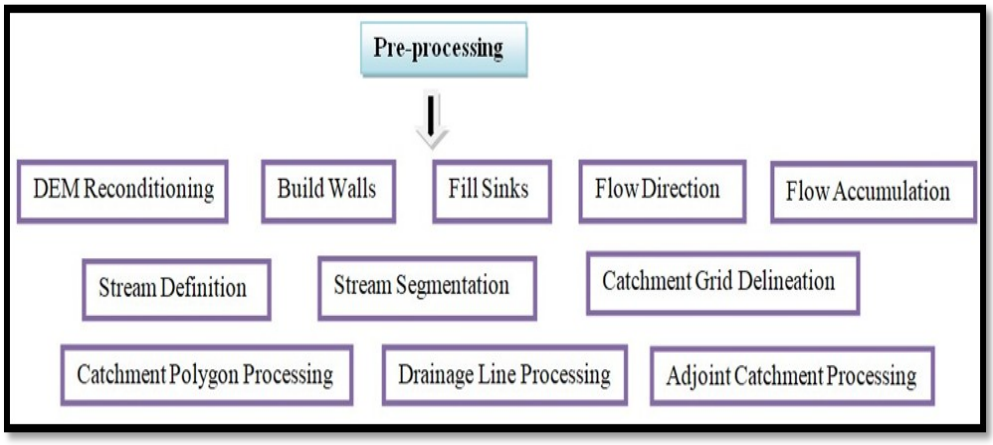

Fig. 3.5: Procedures involved in pre-processing menu

The above procedure concludes the use of the “Pre-processing” tool. The next step is to set up a project for the HEC-HMS model.

3.6.2 Project Setup:

This menu was utilized for creating the essential data for extracting information for setting up a project in HEC-HMS. Methodology for extracting the information includes determining an outlet control point at the downstream section. The delineated area which was finally generated portrays the boundary for the working of HEC-HMS project. The “Data Management” menu in the project set up tool enables the creation of an examination area, permits us to erase the tasks that are not needed and helps us in recording various data effectively. Fig. 3.6 shows the “Project Setup” menu in the HEC-GeoHMS extension tool.

Fig 3.6: Project Setup menu in HEC-GeoHMS

3.6.3 Basin Processing:

This tool was utilized for updating and revising the delineation of the basin and also for merging the smaller sub basins and rivers. The “Basin Processing” tool consists of the following menu (Figure 3.7).

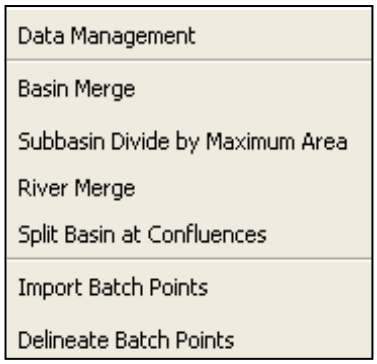

Fig. 3.7: Basin processing menu in HEC-GeoHMS

3.6.4 Characteristic:

The “Characteristics” tool was used in computing various topographic features of sub basins which was utilized in assessing hydrological parameters. The different qualities of the stream and sub basin are saved in the attribute tables which was further exported for using along with different projects. This tool also helps us in generating the ‘River Length’, ‘River Slope’, ‘Basin slope’, ‘Longest Flowpath’, ‘Basin Centroid’, ‘Centroidal Elevation’ and ‘Centroidal Longest Flowpath’. The “Characteristics” menu on the HEC-GeoHMS toolbar for topographic characteristics extraction of streams and sub basins is shown in figure 3.8.

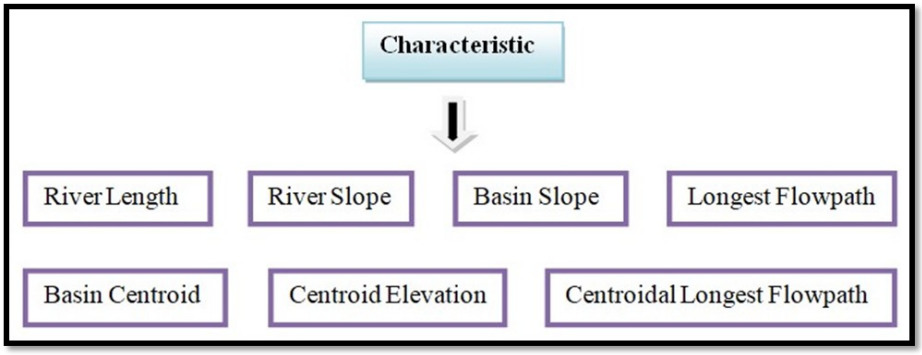

Fig. 3.8: Characteristics menu in HEC-GeoHMS

3.6.5 Parameters:

After the physical attributes of streams and sub basins have been computed, several hydrological parameters were evaluated. Parameters can be assessed as grid-based values and as average values for the sub basin utilizing both soil map and land use map. Under the ‘Select HEC-HMS’ menu the loss and transform method chosen for sub basin was “SCS method”, base flow method as “Recession” and routing method as “Muskingum - Cunge” method. The ‘Parameter’ menu was used for computing the ‘TR55 Flow Path Segments’, ‘TR55 Flow Segment Parameters’, ‘ Muskingum-Cunge and Kinematic wave parameters’ and CN Lag time. It was also use for auto naming the river and basin name.

3.6.6 Utility:

The Utility menu was used to generate various parameters needed for the project. For

utilizing this tool, the land use and soil map polygons were prepared as merging of both the polygons was needed to generate the CN grid. A column containing the names 'Landuse' and a "Lookup table" which relates both the landuse and HSG to a curve number is also needed to generate the CN grid.

Merging of both land use map and soil map polygons was done by using the "Merge" menu under the "Geoprocessing" tool in the ArcMap window. Then, the merged polygons were assigned a unique Hydro ID. The 'Utility' menu was used for assigning the Hydro ID, generating the Curve Number and for averaging the precipitation over the basin for which the Theissen polygon map was generated. For generating the Theissen polygon map, five rainfall gauging stations were selected namely: Thunacadavu, Peruvaripallam, Chalakudy, Kerala Sholayar Dam (KSD) and Parambikulam.

3.6.7 HMS:

The "HMS" menu was helpful in generating various hydrologic inputs for the HEC-HMS project. The HMS program was used in checking whether any error in data has occurred while carrying out the necessary steps. HMS unit was mapped using 'Map to HMS' menu. The "HMS schematic" menu was used for creating the schematic hydrologic elements such as junction, reaches, sub basin, sink, reservoir and diversions. For the toggle legend the "HEC-HMS legend" was selected and the X and Y co-ordinate system was added through the "Add co-ordinate" menu. The background shape file and the basin model file were also added and the grid cell file was generated using the "Grid Cell File" menu. For the met model file, the specified hydrograph and the gage weight procedure were also carried out.

Once all the procedures were completed the data was prepared for model export and the HEC-HMS project was finally created using the "Create HEC-HMS Project" menu. The data created for the project was exported by creating a specific folder. The created HEC-HMS Project was ready to be imported to the HEC-HMS software. Figure 3.9 depicts an outline of the processes involved in HMS tool.

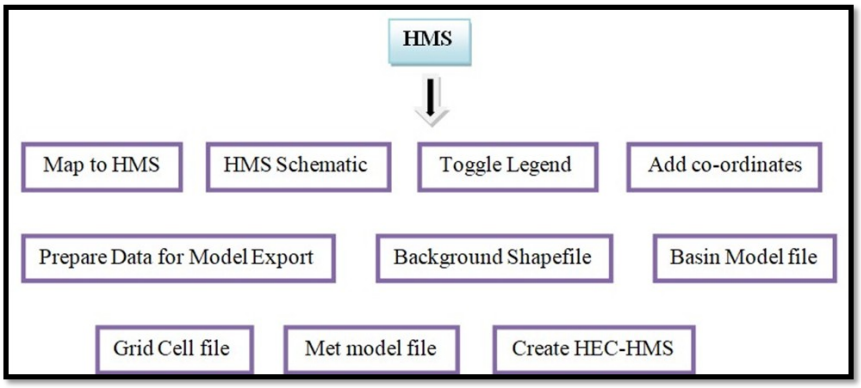

Fig. 3.9: HMS menu in HEC-GeoHMS

3.7 PROCESSES INVOLVED IN RUNNING HEC-HMS:

After completing all the processes involved in HEC-GeoHMS, the supporting data created by using the extension tool were exported to the HEC-HMS. Before starting the project in HEC-HMS the background shape files such as river and basin shape files were added using the "View" menu option in the HEC-HMS window. Once the created project file is connected to the HEC-HMS model, the basin model view can be seen which shows the legend for sub-watersheds indicated by 'W' assigned with different number codes for each sub watershed, reach as 'R' and junction as 'J'. After this, all the necessary procedures were carried out in HEC-HMS to run the project. The procedures involved are mentioned below in detail.

3.7.1 Components

The watershed explorer is mainly partitioned into four sections: Components, Parameters, Compute and Results. The "component" tab available in the HEC-HMS is shown in the figure 3.10. The "Basin Model", "Meteorologic Model", "Control Specification", "Time-Series Data", "Paired Data and Grid Data" managers are accessible through the "components" menu. Other parameters like precipitation, relative humidity, maximum and minimum temperature, wind speed and sunshine hours were added by using the "Time-series Data Manager".

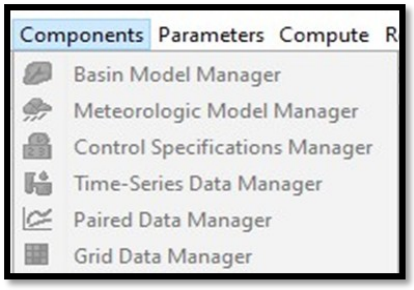

Fig 3.10: Components menu in HEC-HMS

***Basin Model Manager*:**

The representation of a basin is accomplished with the help of a basin model which is one of the main components in a project. The basin map is the primary element for portraying all the hydrologic elements like the junction, reaches, source, sink, sub basin etc. that are included in the basin model manager for displaying the watershed. Its main aim is to transform the hydrologic data into stream flow at a particular location within the basin. It also helps in understanding the physical characteristics of the basin and the stream network topology. Hydrologic components are associated in a dendritic system for runoff simulation.

The "Basin Model Manager" was used for selecting the modeling components such as the canopy method, surface storage method, loss method and transform method. "Simple canopy" and "Simple surface" was selected for the canopy and surface method while for baseflow, the "Recession" method was selected. "SCS CN" method and "SCS Unit Hydrograph" were selected for the loss and transform method. The calculation continues from upper stream components to a lower stream component. There are eleven techniques inbuilt in the software for converting excess rainfall into surface overflow i.e., "Deficit and Constant Loss", "Exponential Loss", "Green and Ampt Loss", "Gridded Deficit Constant Loss", "Gridded Green and Ampt Loss", "Gridded SCS Curve Number Loss", "Gridded Soil Moisture Accounting", "Initial and Constant Loss", "SCS Curve Number Loss", "Smith Parlange Loss" and "Soil Moisture Accounting Loss". Some methods are meant mainly for event based simulation while some methods are meant for long period continuous simulation. Nonetheless, all the methods are based on mass conservation. For the present study the "SCS Curve Number Loss" method was selected because the parameters needed for

the SCS CN method was available. This method executes the CN for incremental losses (NRCS, 2007). The SCS CN method editor is shown in fig. 3.11.

The equation for runoff computation by SCS Curve Number method is given by,

$$Q = \frac{(P-0.2S)^2}{(P+0.8S)} \quad \text{For } P > I_a$$

$$Q = 0 \quad \text{For } P < I_a$$

$$S = \left(\frac{25400}{CN}\right) - 254$$

Where, Q = Volume of runoff (mm)

P = Rainfall volume (mm)

I_a = Initial abstraction (mm)

S = Maximum potential retention (mm)

CN = Curve number

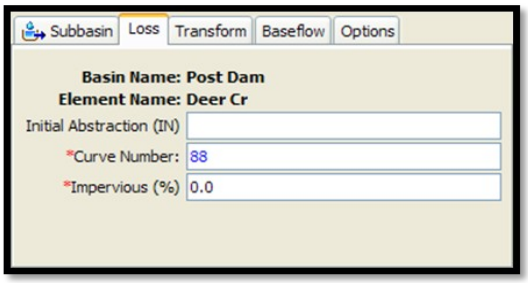

Fig. 3.11: SCS CN method editor.

For the transform method there are seven methods available i.e., “Clark Unit Hydrograph Transform”, “Kinematic Wave Transform”, “Mod Clark Transform”, “SCS Unit Hydrograph Transform”, “Snyder Unit Hydrograph Transform”, “User-Specified S-Graph Transform” and “User-Specified Unit Hydrograph Transform”, out of which the “SCS Unit Hydrograph” method was selected for the transform method. Fig. 3.12 shows the “SCS Unit Hydrograph” editor. For “SCS Unit Hydrograph” the input parameter required was ‘Lag time’. On a theoretical basis the “Lag time” is directly related to “T_c” (time of concentration) which is represented by the formula

Lag time = 0.6 * T_c

Where, $T_c = 0.01947 * \left(\frac{L^{0.77}}{S^{-0.385}}\right)$

T_c = Time of concentration (minutes)

L = Maximum length of travel of water (m)

S = Slope of the catchment = ΔH/L

ΔH = Difference in elevation between the most remotest point on the catchment and the outlet (m)

(K. Subramanya, 2016)

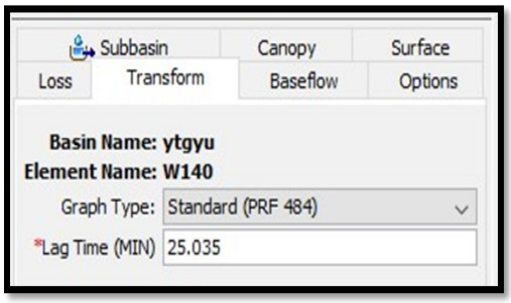

Fig. 3.12: "SCS Unit Hydrograph" editor

The HEC-HMS model has six hydrologic routing techniques namely: "Kinematic wave", "Lag", "Modified Puls", "Muskingum", "Muskimgum-Cunge" and "Straddle stagger". "Muskingum" method was selected for the routing and for the loss/gain option, the "Constant" method was selected. The "K" value in the editor box represents the time of travel to pass through the reach and the value inputted in the editor box was a calibrated value. The "X" value represents the weighting factor and its value usually ranges from 0.0 to 0.5. When "X" value equals to '0', it represents maximum attenuation while a maximum of 0.5 shows no attenuation. Since the number of sub reaches within the basin was three, the number of sub reaches selected for this study was three. Fig. 3.13 shows the Muskingum routing editor.

The Muskingum routing equation is given by:

$$S = KQ + K X (1 - Q)$$

Where S = KQ (Prism storage in the reach)

K = proportionality coefficient

KX (I − Q) = Volume of the wedge storage

X = Weighting factor, $0 \leq X \leq 0.5$.

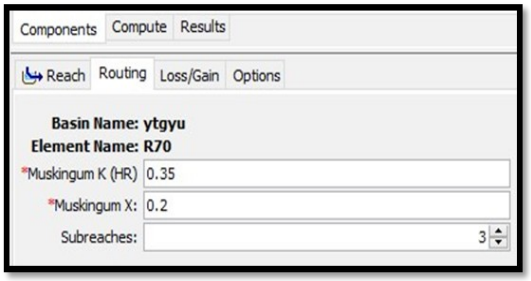

Fig. 3.13: Muskingum routing editor

Meteorologic Basin Model:

The second menu in the "Component" tab is the **"**Meteorologic Basin Model. In the "Meteorologic Basin Model" manager, precipitation, evapo-transpiration, and unit system were incorporated. Since all these segments are not mandatory for runoff simulations, the short wave and long wave radiations along with snowmelt parameters were omitted due to non-availability of data. Seven techniques are available for analyzing historical precipitation which are "Frequency Storm", "Gage Weights", "Gridded Precipitation", "HMR 52 Storm", "Inverse Distance", "Hypothetical Storm", "Specified Hyetograph" and "Standard Project Storm", out of which the Specified Hydrograph technique was selected. Another seven methods are available for computing evapotranspiration which are "Annual Evapotranspiration", "Gridded Penman Monteith", "Gridded Priestley Taylor", "Hamon", "Hargreaves", "Monthly Average", "Specified Evapotranspiration", "Penman Monteith" and "Priestley Taylor" out of which the "Penman Monteith" method was selected. Under the specified hydrograph the gauging stations were assigned to each sub basin and for the unit system, the metric unit was selected. View of Penman Monteith window is shown in Fig. 3.14

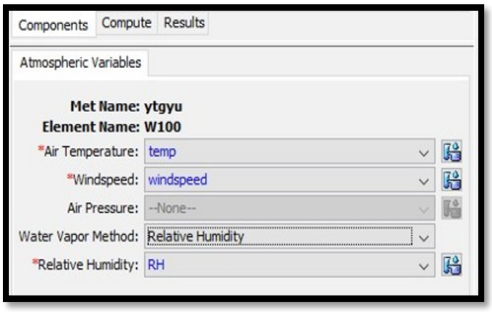

Fig 3.14: View of Penman Monteith window

Penman Monteith equation:

The formula derived by Penman is purely a semi-empirical formula which combines both the concept of mass transfer and energy budget equation. To compute the evapotranspiration using this equation, several parameters are needed which includes the maximum and minimum temperature, solar radiation, wind speed and relative humidity etc., The formula and the steps involved in calculating the evapotranspiration are mentioned below.

'H_n' is computed by the following formula:

$$H_n = H_a(1 - r)(a + b\frac{n}{N}) - \sigma T_a^4(0.56 - 0.092\sqrt{e_a})(0.10 + 0.90\frac{n}{N})$$

Where, H_a = Incident solar radiation (mm of evaporable water/day).

a = Constant depending upon the latitude 'ϕ' (a=0.29 cosϕ)

b = Constant (b = 0.52)

n = Duration of sunshine (Hours)

N = Maximum possible sunshine hours.

r = Reflection coefficient (albedo).

Values of 'r' for different surface covers is given in table 3.2

'e_s' is computed by the formula represented below:

$$e_s = 4.584 * \exp\left(\frac{17.27\,t}{237.3 + t}\right) \text{ mm of Hg}$$

Where, t = Temperature (^{o}C)

'e_a' is computed by the formula given below:

$$E_a = 0.35 * (1 + \frac{u}{160}) * (e_s - e_a)$$

Where, e_a = Mean of actual vapour pressure (mm of Hg)

e_s = Saturated vapour pressure (mm of Hg)

u = wind speed (km/day)

Potential evapotranspiration is computed by the following formula

$$PET = \frac{AH_n + E_a\gamma}{E + \gamma}$$

Where, PET = Daily potential evapotranspiration (mm/day)

A = Temperature curve at mean air temperature Vs Saturated vapour pressure slope (mm of Hg/^oC)

H_n = Net solar radiation (mm of evaporable water/day)

γ = Psychometric constant (0.49 mm of Hg/ ^oC)

E_a = Parameters including wind velocity and saturated deficit

Table 3.2: Reflection coefficient (r) values for different surface cover

Surface	Range of 'r' values
Close Ground Crops	0.15-0.25
Bare Lands	0.05-0.45
Water Surface	0.05
Snow	0.45-0.95

(Gupta *et al.*, (2016)

Control Specifications Manager:

The "Control Specifications Manager" was used for adding the time of run for the model i.e. the time duration and time interval. The starting date as well as the ending date has to be mentioned before running the model. Since, the model was calibrated for five years, the starting date mentioned was 1st January 2003 and ending date as 31st December 2007 as shown in fig. 3.15. The time interval chosen was one day.

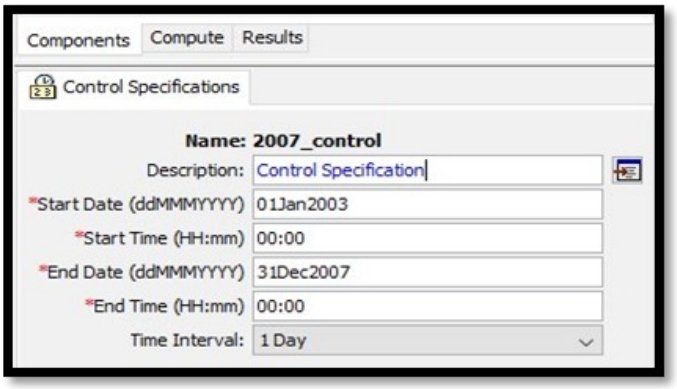

Fig 3.15: View of control specification window.

***Time Series Manager*:**

Under the time series menu, each precipitation gauging station was selected and under the time series gage menu the data source, unit and time interval were entered manually as incremental millimetres and one day respectively. The starting and ending date were mentioned in the time window menu. Five precipitation gauging stations were added automatically under the "Time-Series Manager" as the "Theissen polygon" method for averaging the precipitation was already performed in the HEC-GeoHMS extension tool before creating the HEC-HMS project. The precipitation data were entered manually as per the starting and ending date mentioned in the time series menu. A discharge gauge was added under the time series data which can be done by clicking the "Component menu → Time series data manager →Choose the discharge gage under the drop down menu of data type". Similarly, for the discharge gauging station the unit was selected, the starting and ending date were mentioned. Then, the discharge values for the mentioned period were entered manually. The above procedure was followed to add the other meteorological parameters such as the relative humidity, wind speed, temperature and sunshine hours. Fig. 3.16 shows the Time-Series data window.

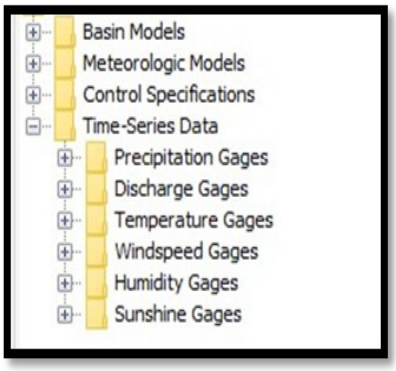

Fig. 3.16: View of Time-Series data window

3.7.2 Parameters:

Sub basin Area, Canopy, Surface, Loss, Transform, Base flow, Routing etc., are the submenu available in the "Parameters" tab. A view of the parameter menu is shown below in fig. 3.17

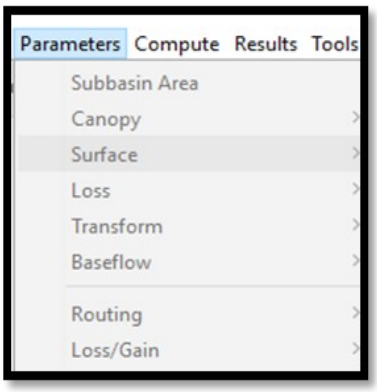

Fig 3.17: Parameters menu in HEC-HMS

Sub basin

A sub basin is a component that typically has just a single outlet. It is mainly for representing a basin and producing a hydrograph of discharge at the outlet of a sub basin. The discharge hydrograph at the outlet is generated from meteorological information by subtracting the losses from the precipitation data. Then, the excess precipitation is used for computing the runoff at the basin outlet by transforming it with the help of UH method which will be finally added to the base flow of the basin. The areas and the methods for each sub basin are selected in the “Basin Model Manager”.

Canopy

There are three methods available for the canopy parameters. They are simple canopy, gridded canopy and dynamic. The simple method was chosen for the present study and the input parameters required were initial storage and maximum storage.

Surface

For the surface parameter there are two methods available i.e. gridded simple and simple. The simple surface method was selected and the input parameters required were initial storage and maximum storage.

Loss rates

The software has eleven methods for computing the losses. A variety of strategies are accessible for computing the losses. “Initial loss”, “SCS curve number”, “exponential”, “Green Ampt” and “Smith Parlange” are used for event simulation while “one-layer deficit constant method” can be used for simple continuous simulation. “Three-layer soil moisture accounting method” can be used for complex infiltration and evapotranspiration situations. Gridded techniques are accessible for the “Deficient constant”, “Soil moisture accounting method”, “Green Ampt” and “SCS curve number methods”. The SCS curve method was chosen for this study and the input parameters needed for it were initial abstractions, curve number and percent impervious.

Transform method

Actual surface runoff calculations are performed by a transform method contained within the sub basin. Seven strategies are incorporated for converting the excess rainfall into runoff. UH strategies incorporate the “SCS”, “Clark”, User-Specified” and “Snyder” procedures. The “modified Clark” is a linear quasi-distributed UH strategy which can be utilized with gridded rainfall information. An execution of the “kinematic wave” strategy is likewise available for the transform method. For the present study the “SCS” method was chosen for which the lag time was needed as an

input parameter. The lag time parameter was generated in the HEC-GeoHMS tool itself.

Base flow

Five techniques are present in the software for computing the base flow to sub basin outlet. The recession method was selected for the present study. The input parameters required were “Initial Flow Rate or Initial Flow Rate per Area”, “Recession Constant” and “Threshold Ratio or Threshold Flow Rate”. This method is designed typically for approximating the observed flow in the basin when channel flow declines exponentially after an event.

Routing

HEC-HMS offers a number of options for the reaches and routing of flood hydrographs. The “Muskingum” method used for this study uses a simple technique of mass conservation for routing the flow through the stream reach but the water level was not assumed.

3.7.3 Compute: Both the simulation model run and the optimization of various parameters were done with the help of the “Compute” menu which is shown in fig. 3.18.

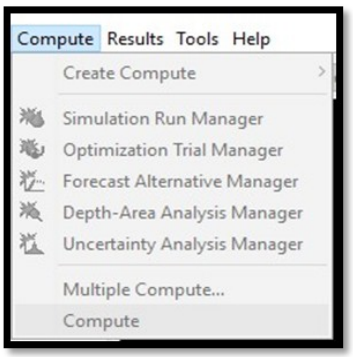

Fig. 3.18: View of compute menu in HEC-HMS.

Simulation Run Manager

To run the model the HEC-HMS software was opened and the project created in the HEC-GeoHMS was browsed and opened in HEC-HMS using the browse ( ) menu. The simulation run menu was used for running the model after adding all the required parameters. Every simulation run consisted of basin model, meteorologic model, control specifications and time-series data. The final results generated were obtained in the form of "element graphs", "element summary tables" and "element time-series tables". In addition to selecting the meteorologic, basin, and control components, advanced features for controlling the run are also included. Before running the model under the control specification, the start and end date were entered as per the calibration period and the time interval "1 day" was chosen. Finally, for running the project, select the Compute menu →Simulation run manager →New →Next →Finish →Select compute →Compute Run →Press OK. View of simulation run manager window is shown in fig. 3.19

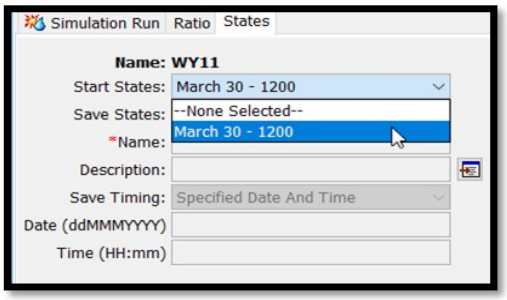

Fig. 3.19: View of simulation run window

Optimization Trial Manager

After running the model, the parameters were optimized using the optimization trial manager menu. There are two different methods inbuilt in the software itself to optimize the parameters: Nelder Mead and Univariate gradient. For optimization, the basin model and the meteorologic model were selected; the starting and the ending time were also added in the optimization model window. For optimizing the parameters the compute menu was selected →Optimization trail manager →New →Next →Finish. Select compute and click the Trial menu →Right click and Select Add parameter, and all the parameters were added which were to be

optimized. Fig. 3.20 shows the view of optimization trial window

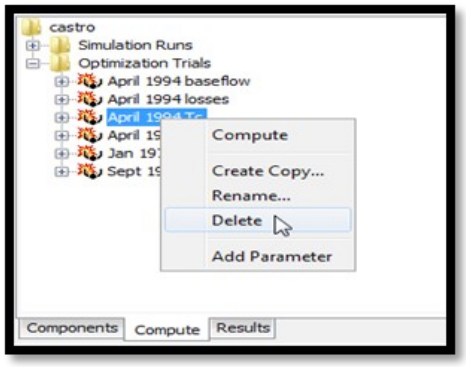

Fig. 3.20: View of optimization trial window

3.8 OPTIMIZATION OF THE MODEL

This process involves the utilization of observed flow for optimizing the performance of the model automatically by parameters estimation. Several objective functions are given at the end of the model to study the “goodness of fit” between the simulated and observed flow. One can adjust the parameters manually or by using the automatic optimization menu inbuilt in the software itself. Each optimization trial consists of a “Basin model”, “Meteorologic model” and Time series information. The time interval chosen was “1 Day”, tolerance limit as 0.01 and maximum iterations as 150. The starting date and time as well as the ending date and time were mentioned in the trial watershed explorer window. The parameters to be optimized were added under the trial menu which was done by right clicking the “Trial” menu and choosing the “Add parameters” menu. For optimizing the parameters, the elements *viz* reach and subbasins were chosen and the parameters of each element which are to be optimized were selected specifically, its initial as well as the minimum and maximum values were mentioned in the window explorer. Once the optimization run is completed the results can be viewed in the form of an objective function summary. This shows the volume and the peak flow values with percentage difference, comparison between the observed and simulated flow hydrograph, optimized parameter tables showing the units of each parameter, its initial values and the final optimized values.

3.9 CALIBRATION OF THE MODEL

In the calibration procedure all the parameters involved were balanced in order to match the observed values with the simulated values obtained for the basin. It was mainly done to minimize the contrasts between the observed and obtained values from the model and to get the best set of parameters in calibrating and validating the model. The main aim of calibration is the model approval which is really an alignment procedure. This is to make sure that the calibration procedure appropriately surveys every factor which can probably influence the outcomes of the model. Once the execution of the model was done by doing the adjustments of the parameters, the approval of the model is assessed through the quantitative and qualitative testing, including some graphs obtained between the observed and simulated values and statistical analysis such as "Nash-Sutcliffe efficiency" and "Correlation-coefficient". Calibration of the model consists of a "Basin model" which includes the methods for each sub basin, "Meteorological model" where the meteorological data are entered and "Control specifications" which includes the starting and ending date and time. After the calibration run was done, the result shows a summary table consisting of the hydrologic elements, drainage area, peak discharge, time of peak and volume. The calibration of the model was done by using the compute menu in the HEC-HMS model. This was done for five years i.e. 2003-2007.

3.9.1 Evaluation of model performance

The model performance was evaluated using the parameters Correlation coefficient, Relative root mean square error, Percentage error peak flow and Percentage error in volume. The formulae involved are as follows:-

Correlation co-efficient

The correlation co-efficient was calculated by using the following formula.

$$R = \frac{\sum_{t=1}^{N} (O_t - \overline{O}) \times (S_t - \overline{S})}{\sqrt{\sum_{t=1}^{N} (O_t - \overline{O})^2 \times (S_t - \overline{S})^2}}$$

Where, O_t = Observed flow at time "t" (m^3/s)

$\overline{O}$ = Average observed flow at time "t" (m^3/s)

S_t = Simulated flow at time "t" (m^3/s)

$\bar{S}$= Average simulated flow at time "t" (m^3/s)

Relative root mean square error (RRMSE)

The RRMSE was calculated by the following formula given below:

$$RRMSE = 100 \times \sqrt{\frac{1}{N}\sum_{t=1}^{N}\left(\frac{S_t - O_t}{S_t}\right)^2}$$

Where, N = Ordinate number of the stream flow

O_t = Observed flow at time "t" (m^3/s)

S_t = Simulated flow at time "t" (m^3/s)

Percent error peak flow (PEPF)

For computing the PEPF, the total volume and the time of occurrence of peak flow are not considered except for the magnitude of the flow. The percent error peak flow is computed by the following formula,

$$PEPF = \left|\frac{Q_0(peak) - Q_S(peak)}{Q_Q(peak)}\right| * 100$$

Where, Qs = Observed peak flow (m^3/s)

Qo = Simulated peak flow (m^3/s)

Percent error in volume (PEV):

The percentage error in volume is computed by applying the formula given below. For computation of PEV the magnitude or the timing of the peak flow volume are not considered except for the computed volume.

$$PEV = \left|\frac{V_0 - V_S}{V_S}\right| * 100$$

Where, Vs = Simulated volume (mm)

Vo = Observed volume (mm)

3.10 VALIDATION OF THE MODEL:

Once the parameters were optimized the validation of the model was done. All the optimized parameters obtained during the calibration period were used as the input

parameters for the validation period. The validation of the model was done for three years from 2015-2017. The same procedure as that of the calibration was followed for validating the model. Validation of the model consists of a “Basin model”, “Meteorologic model” and “Control specifications”. All the results were obtained in the form of graphs, summary table and statistical analysis. The obtained NSE and correlation coefficient value shows the acceptable performance of the model.

3.11 IMPACT OF LAND USE LAND COVER CHANGES ON RUNOFF PROCESSES OF CHALAKUDY RIVER BASIN

To study the impact of LULC changes on runoff processes of Chalakudy basin several analysis were done which includes comparison of maps for LULC changes of three years. LULC maps were compared to trace the changes of different classes that took place over the past two decades. A correlation analysis was done between the average rainfall and LULC classes from 1997 to 2017. Alongside the simulation run of the model was done for three separate years as well. All the analyses done are explained below in detail.

3.11.1 LULC change detection analysis

An analysis of LULC changes was done for a period of two consecutive decades. After preparing the LULC map, the area calculation, percentage area coverage and decadal percentage change of each class was done and the annual rate change of area for each class was also calculated for two different decades i.e., 1997-2007 and 2007-2017. A table was made to represent all the classified seven classes and its percentage area change over the time span of two decades. Comparison of the classified map for various LULC classes over the most recent two decades showed specific transformations that are disturbing.

The procedure developed by Puyravad *et al*., (2003) Teferi *et al.,* (2013) and Batar *et al.,* (2017) was used for the calculating the annual rate change. The formula used is given below

$$r = \left(\frac{1}{T_2 - T_1}\right) * ln\left(\frac{A_2}{A_1}\right)$$

Where, ‘r’ is the annual rate change of area (%)

A_1 and A_2 are the areas of the classes (km^2) at time 1 and time 2

(T_2 - T_1) is the time interval (in years) between the two periods

LULC transition change analysis involves the technique of distinguishing the differences that had occurred to various LULC classes of a basin. It shows and measures the contrasts between pictures of similar scene at various time frames. The significant part of transition change analysis is to distinguish and consequently highlight the land-use classes where the changes have occurred i.e., a specific class that has transformed into another class over some undefined time frame. For analyzing the change detection of different LULC classes, a transition change matrix was prepared for 1997-2007 and 2007-2017. The matrix was prepared with the help of Arc GIS and MS excel worksheet. The land use map polygons of 1997 and 2007 were merged using the geo processing tool in ArcGIS and the area was calculated using the raster calculator. The attribute table of the merged land use polygons was then exported to the excel sheet and using the pivot table option available in excel the change detection matrix table was prepared. Following the similar procedure the change detection matrix table for 2007 to 2017 was prepared as well. The general format for transition change matrix is shown in table 3.3. The diagonal bold letters shows the amount of area that remains constant from time T_1 to time T_2.The total gain and loss for each class was calculated from 1997-2007 and 2007-2017, the results obtained were then finally plotted in a graph.

Table 3.3 General format for transition change matrix

LULC	**1**	**2**	**3**	**4**	**5**	**6**	**7**	**TIME T_1**	**LOSS**
1	$\mathbf{A_{11}}$	A_{12}	A_{13}	A_{14}	A_{15}	A_{16}	A_{17}	A_{1+}	A_{1+}-A_{11}
2	A_{21}	$\mathbf{A_{22}}$	A_{23}	A_{24}	A_{25}	A_{26}	A_{27}	A_{2+}	A_{2+}-A_{22}
3	A_{31}	A_{32}	$\mathbf{A_{33}}$	A_{34}	A_{35}	A_{36}	A_{37}	A_{3+}	A_{3+}-A_{33}
4	A_{41}	A_{42}	A_{43}	$\mathbf{A_{44}}$	A_{45}	A_{46}	A_{47}	A_{4+}	A_{4+}-A_{44}

5	A_{51}	A_{52}	A_{53}	A_{54}	$\mathbf{A_{55}}$	A_{56}	A_{57}	A_{5+}	A_{5+}-A_{55}
6	A_{61}	A_{62}	A_{63}	A_{64}	A_{65}	$\mathbf{A_{66}}$	A_{67}	A_{6+}	A_{6+}-A_{66}
7	A_{71}	A_{72}	A_{73}	A_{74}	A_{75}	A_{76}	$\mathbf{A_{77}}$	A_{7+}	A_{7+}-A_{77}
TIME T_2	A_{+1}	A_{+2}	A_{+3}	A_{+4}	A_{+5}	A_{+6}	A_{+7}	1	
GAIN	A_{+1} -A_{11}	A_{+2} -A_{22}	A_{+3}-A_{33}	A_{+4} -A_{44}	A_{+5} -A_{55}	A_{+6} -A_{66}	A_{+7} -A_{77}		

3.11.2 Simulation runs of the model:

After the calibration and validation, the model simulation runs were done for three separate years i.e., 1997, 2007 and 2017. The three years simulation run output flow hydrographs were compared with the corresponding year LULC maps so as to analyze how the changes in the LULC map with the passage of time have influenced the runoff of the Chalakudy basin. The output of the model run shows the graph between the simulated and the observed flow which helped in analyzing the effect of changes of one class to another on the flow of the basin and its peak runoff. The results obtained from the simulation runs are given in chapter 4.

3.11.3 Impact of land use changes on runoff.

To analyze the impact of LULC changes on the runoff processes of the Chalakudy basin, analysis of the relationship between the simulated average flow with respect to the LULC classes was done. In addition, the changes of different classes like the vegetation, paddy, palm etc., and its impact on the flow of the basin have also been discussed in the results section as well. The plotted graph shows the simulated average flow of the basin in the years 1997, 2007 and 2017. It also shows the area coverage of each LULC classes for the years 1997, 2007 and 2017. The results show how the changes of LULC classes from one to another influences the overall runoff of the basin. The correlation among various land use and land cover indicated either a reduction or increment in the area of certain classes. The results obtained indicated the

effect of land use and cover changes on the runoff of the basin. The final results are given in chapter 4.

Results & Discussion

CHAPTER IV

RESULTS AND DISCUSSION

The study related to the impact of LULC changes on the runoff processes of Chalakudy basin has been done by incorporating Remote Sensing and GIS and HEC-HMS model. LULC maps were prepared for three different years i.e. 1997, 2007 and 2017 to study the impact of land use changes on runoff. The results obtained from the study are presented below in different sections.

4.1 INPUT DATA COLLECTED

4.1.1 Digital Elevation Model (DEM)

DEM downloaded from the USGS earth explorer is shown below in fig. 4.1.

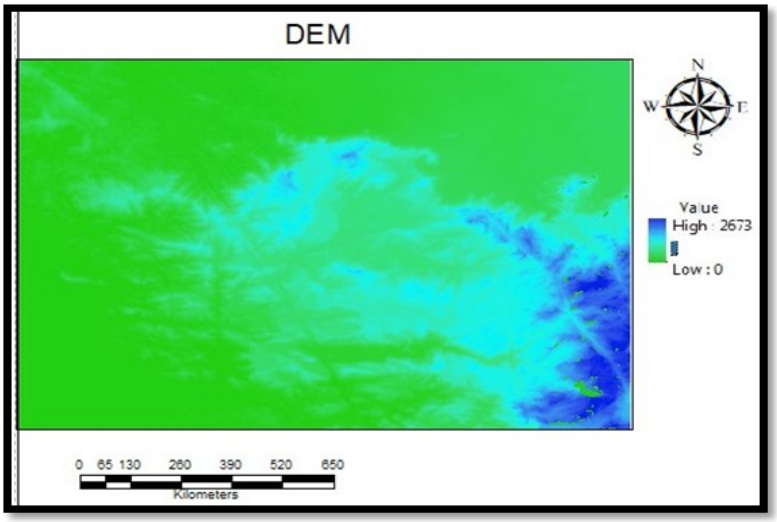

Fig. 4.1 DEM

4.1.2 Rainfall data:

The average monthly rainfall data calculated from daily data collected (ARS, Chalakudy and IMD, Pune) is shown below in table 4.1.

Table 4.1 Average monthly rainfall (mm) at different gauge locations for the period 1997-2017

Month	Thunacadavu	Chalakudy	Peruvaripallam	Parambikulam	KSD
Jan	1	5.00	1.57	0.90	2.69
Feb	11.71	14.86	11.86	11.03	17.76
March	41.29	26.53	46.48	75.45	64.00
April	72.81	87.24	78.90	139.87	114.05
May	97.43	233.69	101.62	157.89	219.49
June	285.33	661.4	295.48	501.13	788.13
July	384.33	629.24	391.90	643.81	909.40
August	274.24	444.89	289.90	428.62	660.83
Sept	213.67	386.18	227.67	324.14	488.00
Oct	216.48	348.98	232.38	325.15	370.75
Nov	125.29	178.07	144.52	121.62	122.35
Dec	33.57	29.51	39.09	30.13	18.56

The rainfall values in the upstream catchments like Parambikulam and Kerala Sholayar are higher in almost all months compared to the other downstream areas of the basin. Rainfall is highest during the South-West monsoon months from June to September with a maximum average value of 909.40 mm followed by the North-East monsoon season from October-November with a maximum of 370.75 mm.

4.1.3 Stream flow data:

The average yearly stream flow data calculated from the daily data collected (flow data at Arangali from CWC, Bangalore) is shown below in table 4.2.

Table 4.2 Average Stream flow recorded at Arangali gauging station for the period1997-2017.

Year	Average flow (Cumec)	Year	Average flow (Cumec)
1997	45.7	2008	42.53
1998	78.27	2009	55.91
1999	67.86	2010	51.94
2000	36.84	2011	64.94
2001	43.63	2012	29.47
2002	42.86	2013	82.39
2003	48.33	2014	65.83
2004	60.09	2015	49.92
2005	64.66	2016	31.62
2006	54.36	2017	42.94
2007	101.85		

The highest average stream flow (101.85 cumecs) at the outlet was recorded in the year 2007 followed by the year 2013 (82.39 cumecs) while the least was found to be in the year 2012 (29.47 cumecs).

4.2 PREPARATION OF LAND USE LAND COVER MAPS

Land use changes in the Chalakudy basin were mapped for the years 1997, 2007 and 2017 and the information collected was predominantly based on the cloud free satellite image and ground truthing. The land use map relating to the years 1997, 2007 and 2017 are given in figures 4.2, 4.3 and 4.4. The LULC map was classified into seven classes as shown in the figures. The identified classes were water body, vegetation, barren land, tea, paddy and urban area. In the present study comparison of the classified map for various LULC classes over the most recent two decades were done. The results showed decline in vegetated area and increase in urban land which aggravated the terrain conditions of Chalakudy basin leading to recurring floods over the past two decades in the basin. The details of areal extent and percentage change of area of each class are explained under the section 4.9.

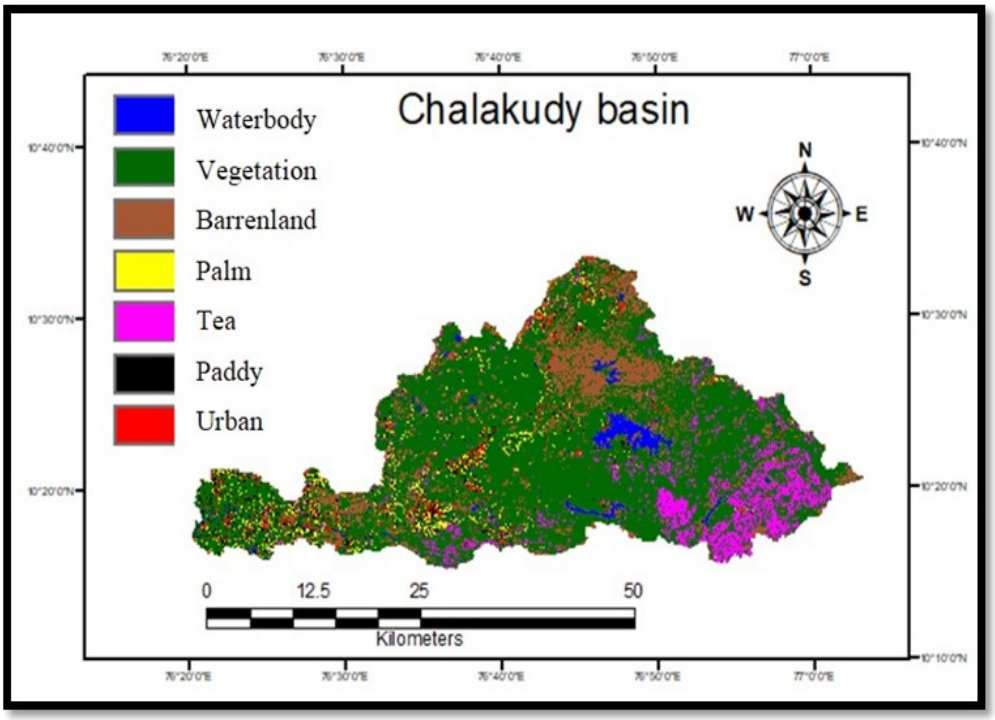

Fig. 4.2: LULC map of Chalakudy basin for the year 1997

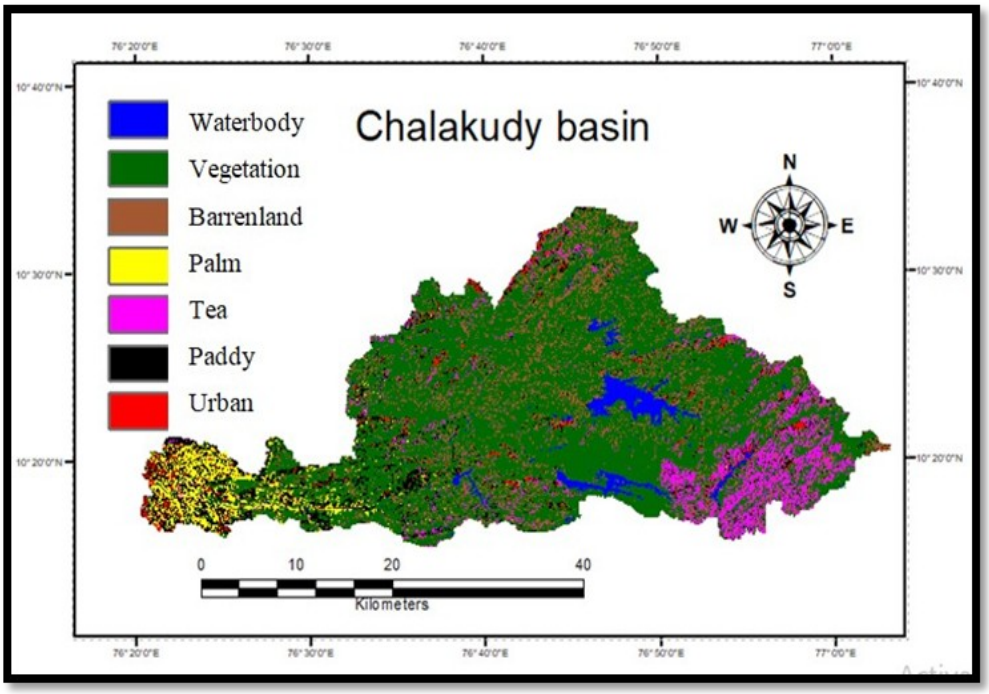

Fig. 4.3: LULC map of Chalakudy basin for the year 2007

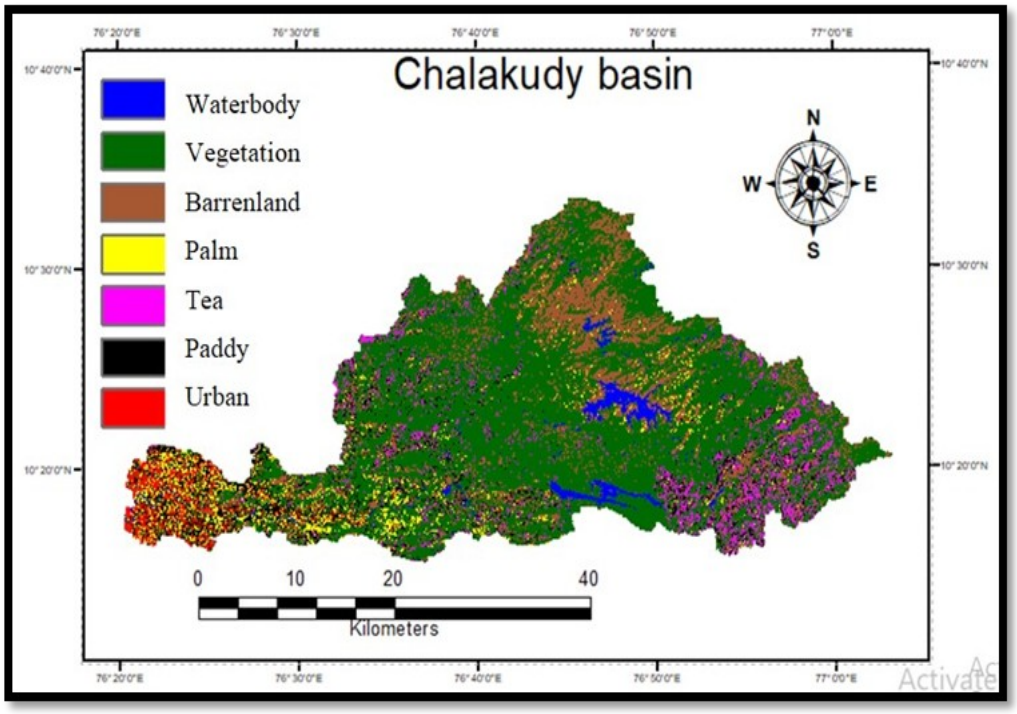

Fig. 4.4: LULC map of Chalakudy basin for the year 2017

4.3 RELATIONSHIP BETWEEN AVEARGE ANNUAL RAINFALL AND STREAM FLOW

Relationship between the average annual rainfall and average annual stream flow for the years 1997-2007 and 2007-2017 is shown in figures 4.5 and fig 4.6. Fig. 4.5 shows highest average rainfall and average flow for the year 2007 and the least for the year 2000. The obvious reason for the year 2007 experiencing highest flow is the increased rainfall received by the basin during this year and the lowest flow for the year 2000. Another reason behind the increment of flow in 2007 might be because of the reduction in vegetation area including forest and an increment in urban zone. In view of advancement and urbanization, the infiltration capacity of the soil decreased which led to percentage increment in the flow as well. After a decade the average flow was seen as the least for the year 2012 as appeared in fig. 4.6. During the decade 2007-2017 a further decline in the water body was seen, the possible explanation might be the diminishing rainfall towards the decade's end and in light of which a decline in the average flow was seen towards the end of the decade.

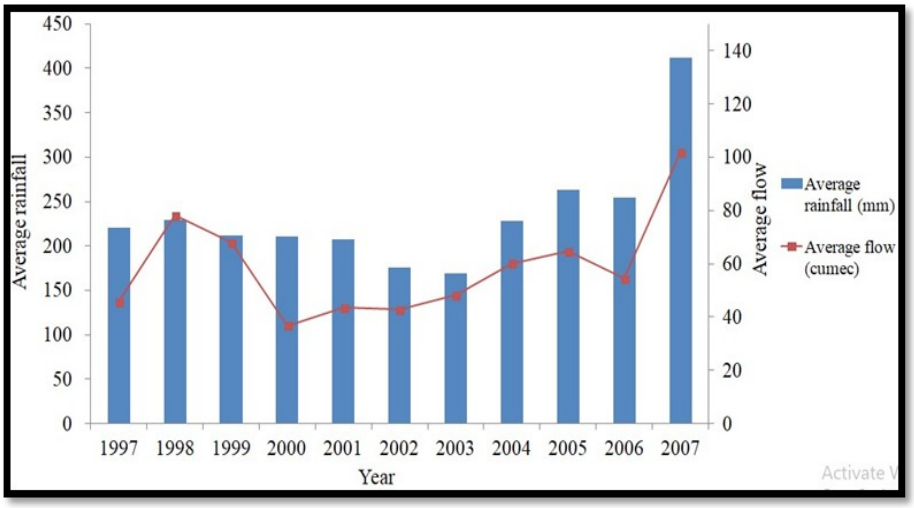

Fig. 4.5: Variation of average rainfall and average flow for the years 1997 to 2007

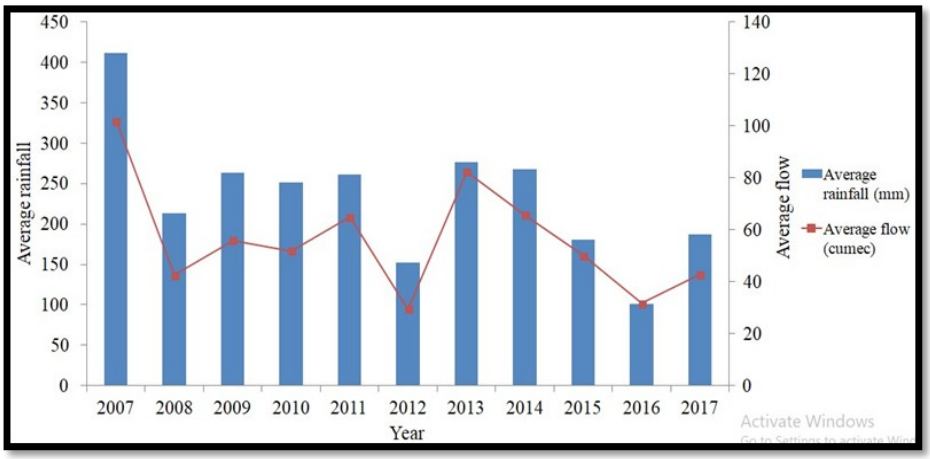

Fig. 4.6: Variation of average rainfall and average flow for the years 2007 to 2017

The variation of stream flow with variation in rainfall was seen more consistent in the decade 2007-2017. Correlation analysis was done between the average rainfall and the average flow for two different decades which is depicted in figures 4.7 and 4.8. An R^2 value of 0.79 was obtained for the linear regression analysis plotted between the average rainfall and average flow for the years 1997-2007 while an R^2 value of 0.86 was obtained for the years 2007-2017. From the R^2 value obtained

for the two decades, it shows that the flow of the basin is dependent on the rainfall and is also influenced by other factors like the changes in the LULC over a stretch of time. Consequently, it is also inferred that the increase in peak flow and the diminishing stream flow are the after effects of land use land cover changes.

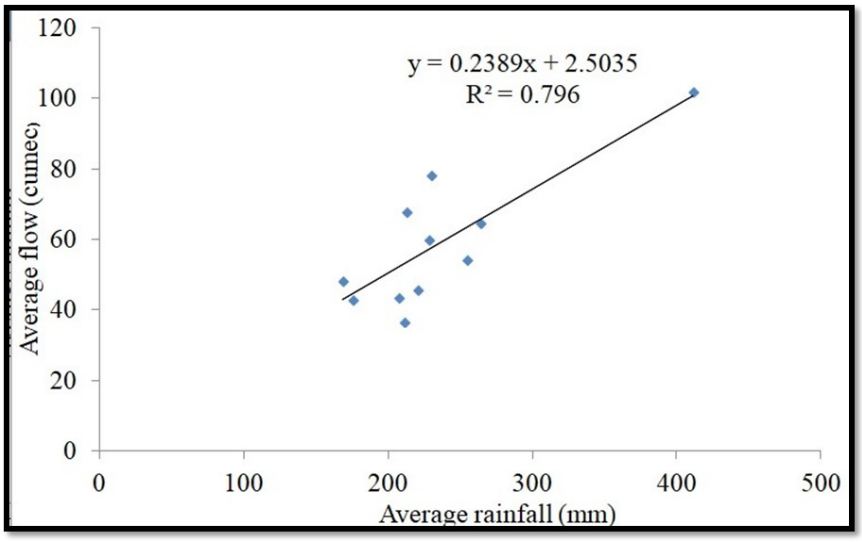

Fig. 4.7: Correlation analysis between average rainfall and flow (1997 to 2007)

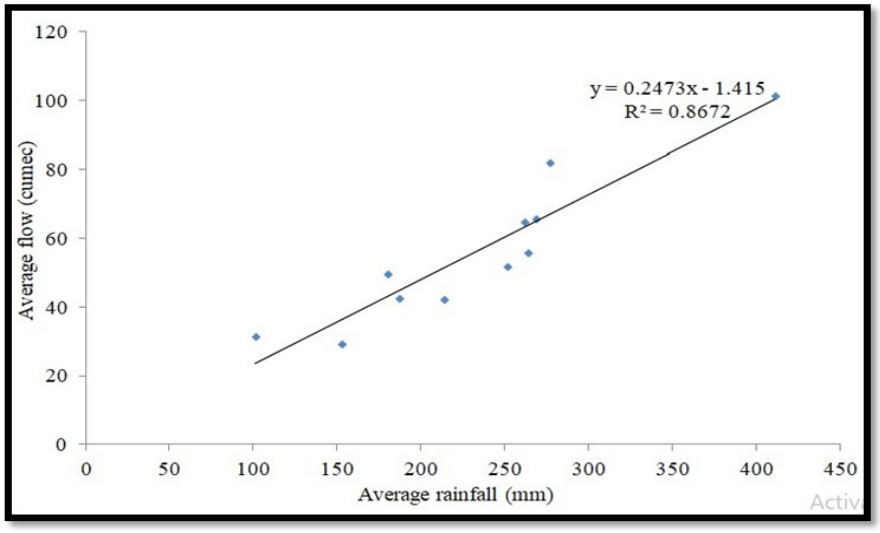

Fig. 4.8: Correlation analysis between average rainfall and flow (2007 to 2017)

4.4 SOIL MAP

Depending on the soil characteristics, the study area was divided into four hydrological soil mapping units namely HSG A, HSG B, HSG C and HSG D (USDA, soil texture class). The code HSG 'O' was assigned for the areas like water body and habitation. Different shades of colour in the soil map depict different HSG's. The HSG A is the soil having low runoff potential and high infiltration rate, example can be the gravelly sands while HSG B has moderate infiltration rate with moderately fine to coarse texture and HSG C with moderately fine to fine texture. The HSG D has high runoff potential with poor infiltration rate, and typical example for this group is the clayey soil. Koneti *et al.,* 2018 have made a similar study to analyze the impact of LULC map on the runoff processes of Godavari river basin for which they have prepared a soil map based on the soil type, the classified soil classes taken were clayey, clayey-skeletal, loamy, loamy-skeletal and rock-outcrops. Pampaniya *et al.,* 2015 made a study on hydrologic modelling of Hadaf river using the HEC-HMS model. They have prepared a soil map as an input for their studies and the soil map prepared was categorized into three classes based on the soil type i.e., clayey soil, loamy soil and fine sand. Similarly, Singhal *et al.,* 2018 estimated the surface runoff by SCS-CN method using ArcGIS, the soil map of the study area i.e., Modikuntavagu watershed was divided into two classes i.e., clayey and loamy soil. Likewise the soil map for Chalakudy basin was prepared for the present study based on the soil type. The map showing the different units and spatial distribution of each soil type in the basin is depicted in figure 4.9.

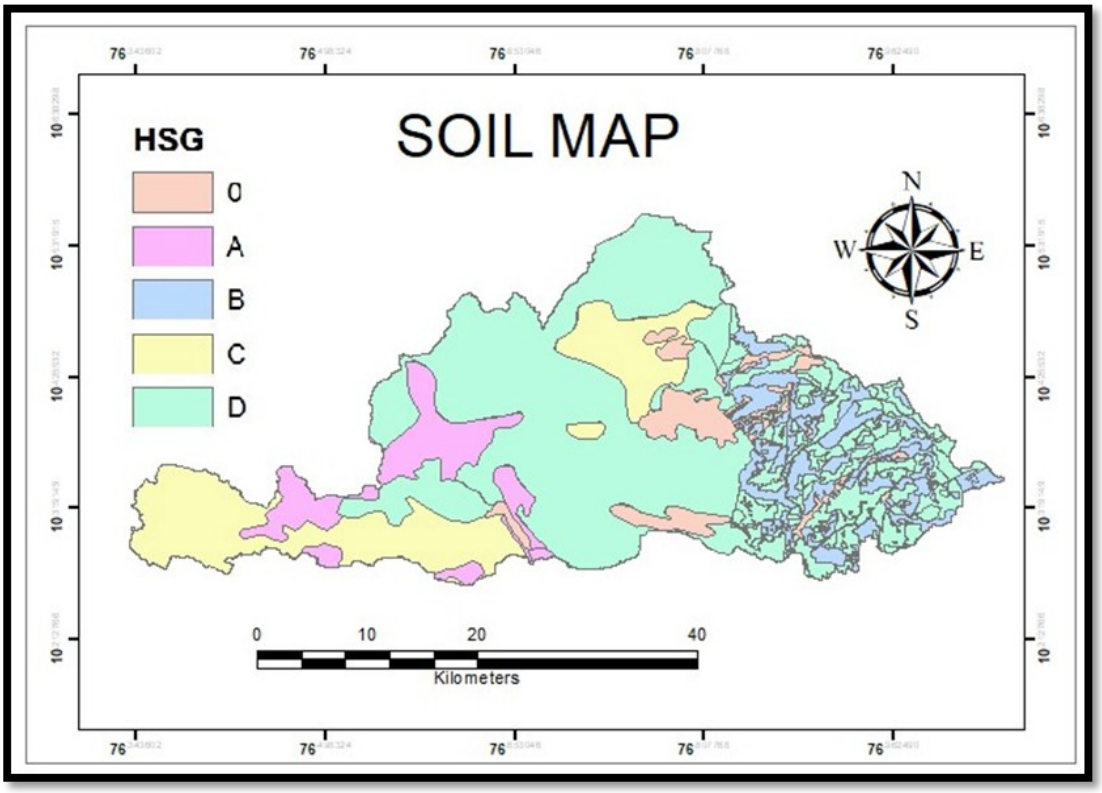

Fig 4.9: Soil map of Chalakudy river basin

4.5 MODELLING WITH HEC-GEOHMS:

4.5.1 Pre-processing:

The initial phase in building up HEC-GeoHMS project is terrain preprocessing. Before starting the hydrologic modeling in the HEC-HMS software, the preprocessing tool was used to derive eight datasets for stream and sub basin delineation. For carrying out the delineation procedure the HEC-GeoHMS extension tool in the ArcMap was used. All the output derived from the HEC-GeoHMS toolbar is depicted in the figure 4.10 (a-h) below:

The datasets derived under pre processing menu are:

a. Flow direction
b. Flow accumulation
c. Stream definition
d. Stream segmentation
e. Catchment grid delineation
f. Catchment polygon processing
g. Drainage line processing
h. Adjoint catchment processing

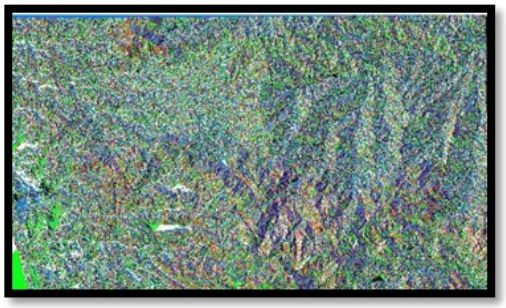

a. Flow direction output

b. Flow accumulation output

c. Stream Definition output

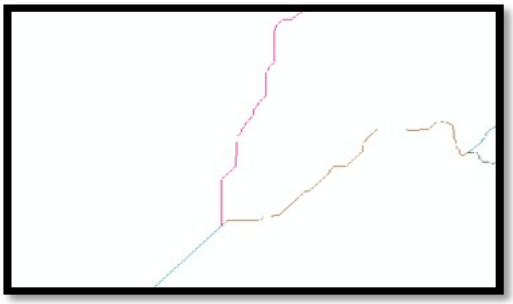

d. Stream Segmentation output

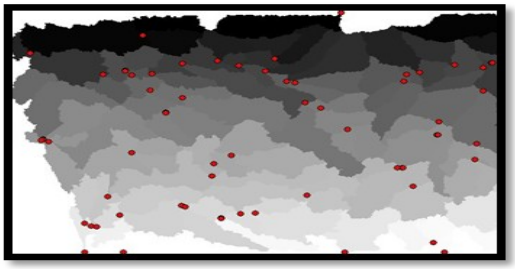

e. Catchment Grid Delineation

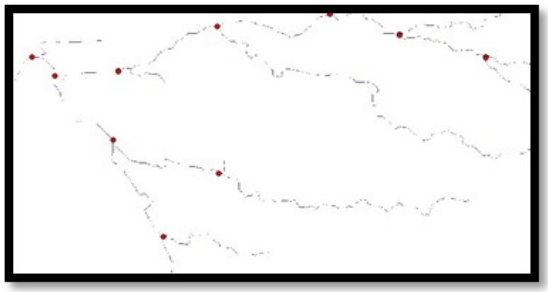

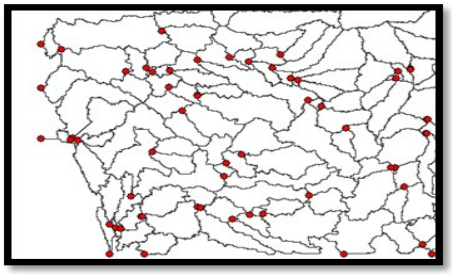

f. Catchment Polygon processing

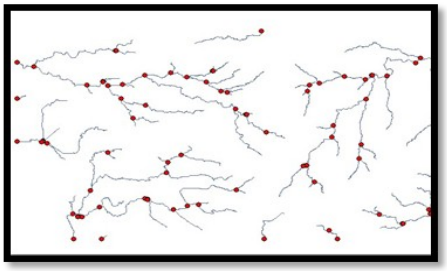

g. Drainage Line Processing

Fig 4.10: View of the results obtained from Pre-processing menu

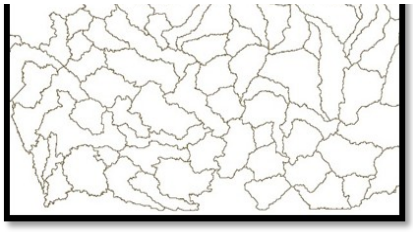

h. Adjoint Catchment

4.5.2 Project Setup

The delineated area finally portrays the boundary for the working of HEC-HMS project. Once the delineation procedure was carried out, the outlet for the watershed was specified at the downstream section. The delineated basin along with the specified outlet is shown in fig. 4.11.

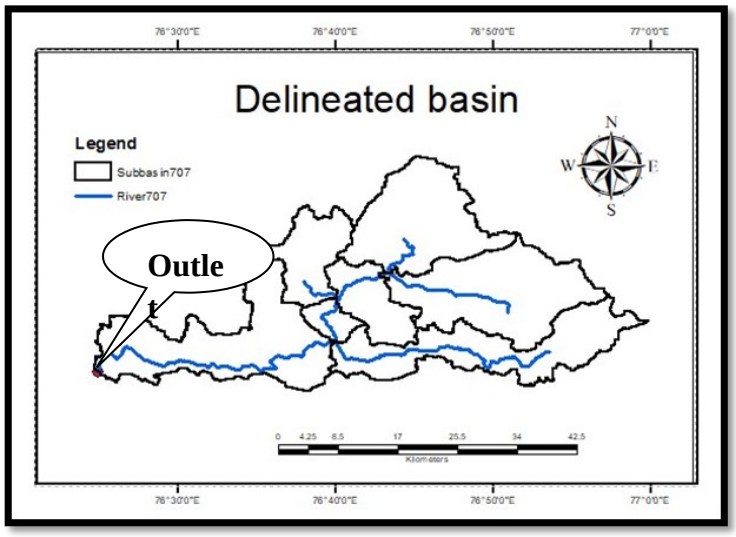

Fig. 4.11: Delineated shape file

4.5.3 Characteristics

This tool was used in generating the river length and slope, basin slope and centroid, longest flow path and centroid elevation. The generated output shape files are shown in the figures below (fig. 4.12, a-e):

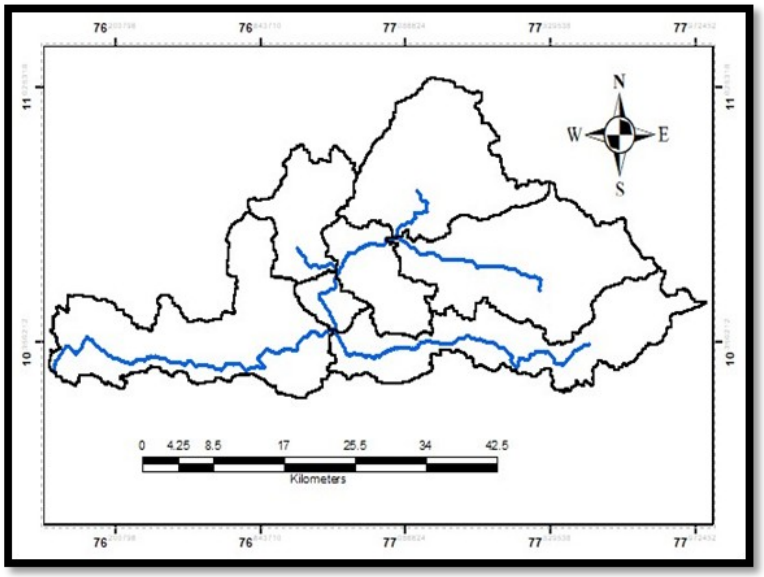

a. River length characteristics

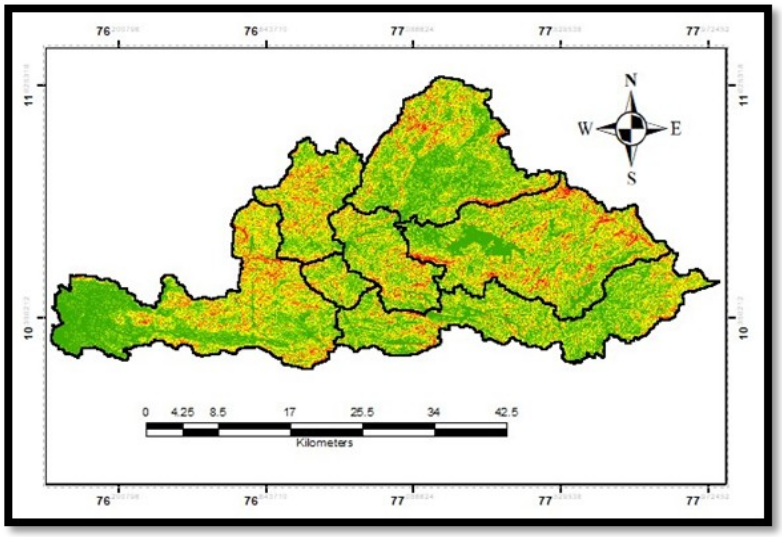

b. River and basin slope

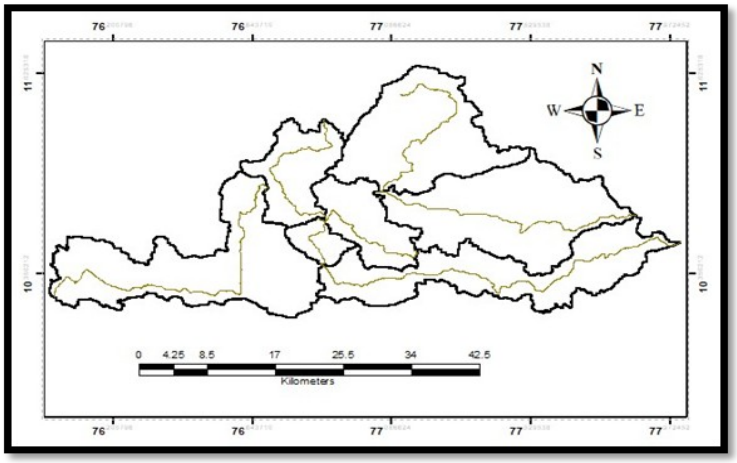

c. Longest flow path

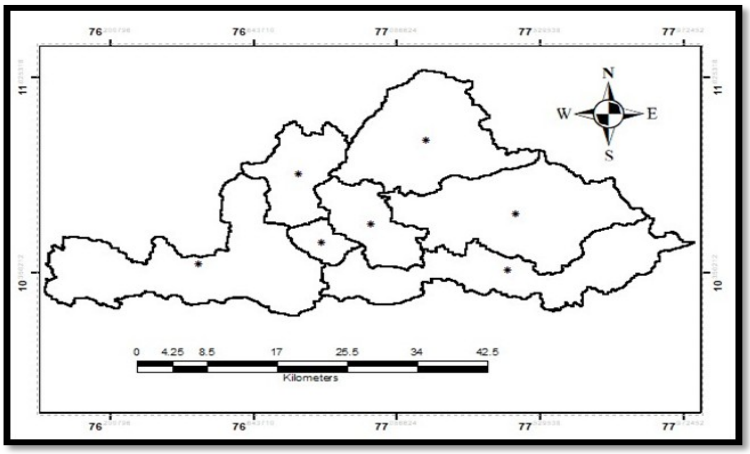

d. Basin centroid

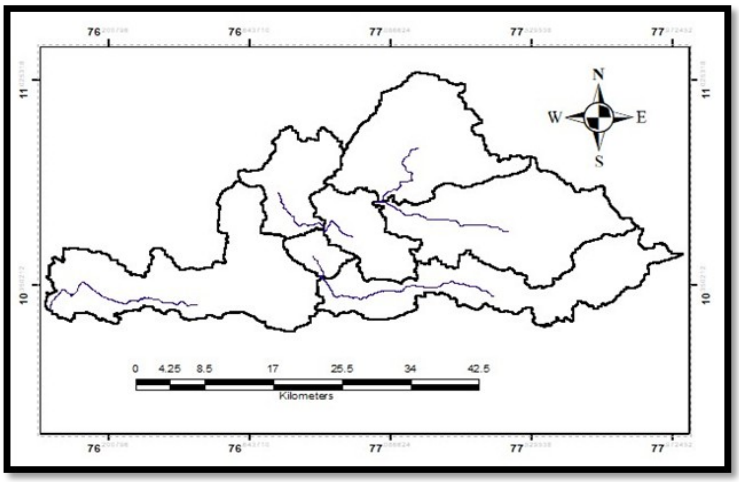

e. Centroidal longest flow path

Fig. 4.12: View of the results obtained from Characteristics menu

4.5.4 HMS:

The HMS schematic obtained from the HMS menu is shown below (fig. 4.13)

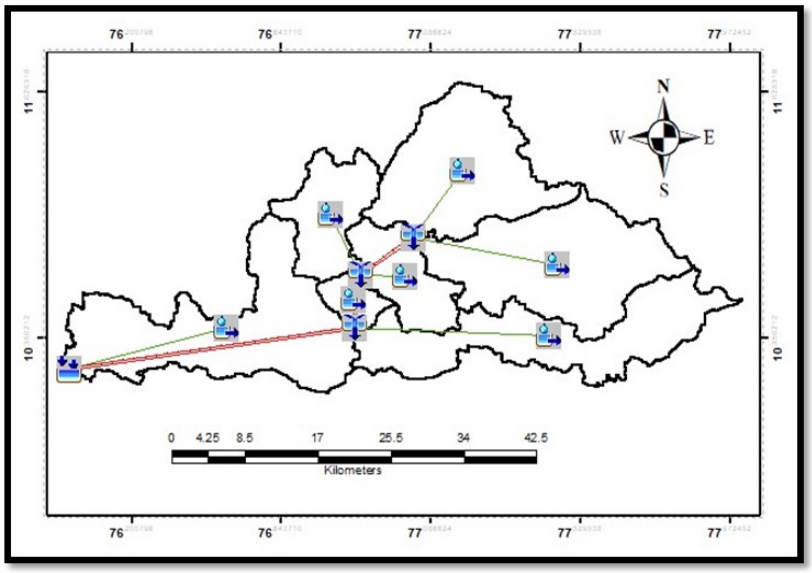

Fig. 4.13: HMS schematic view

4.5.5 Utility

The 'Utility' menu was used for generating the Theissen polygon map and the CN Grid map. The results obtained from the generated map are discussed below.

Theissen polygon map

The generated Theissen polygon map along with the five rainfall gauging stations are shown in fig. 4.14. The influential area of each of the gauging stations are shown in different variant coloured polygons. To compute the average rainfall over the entire basin the Theissen polygon map was created by the use of HEC-GeoHMS extension tool. The rainfall data for the gauging stations were collected from ARS Chalakudy and IMD, Pune for the years 1997-2017.

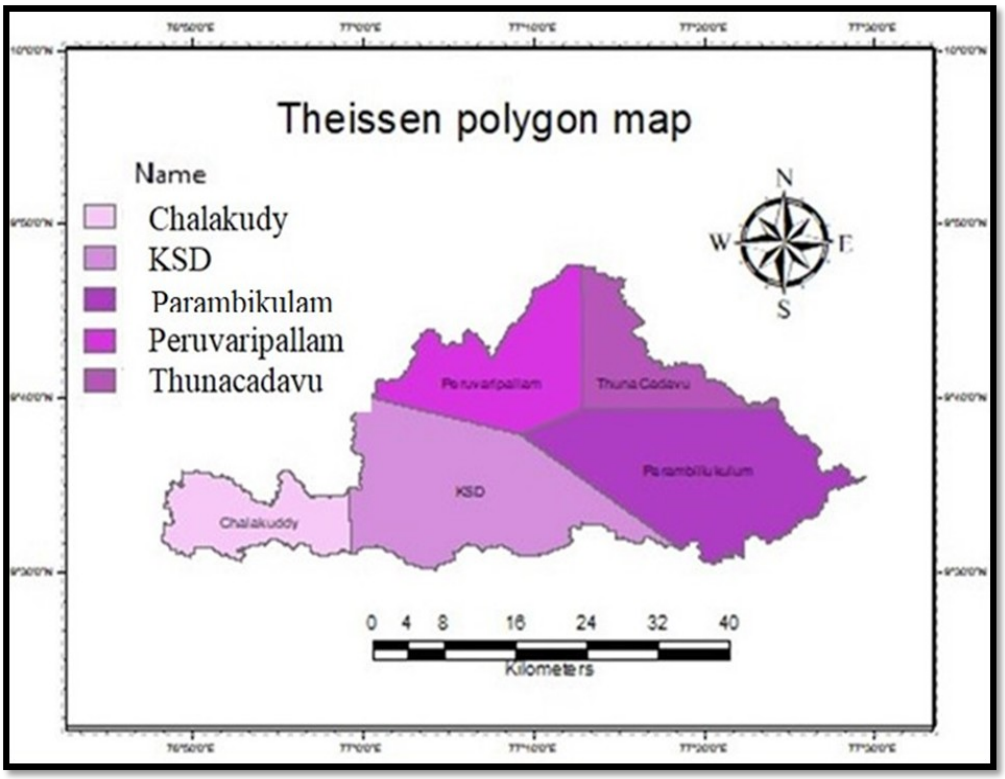

Fig 4.14: Theissen polygon map

It is evident from the above figure that all the five gauging stations are within the basin and each of the station has an influence on the basin with different extent of influential area and weights which is shown in table 4.3. The highest extent of area influencing the average rainfall of the basin is got for the point rainfall data of gauging station at KSD with an area of 385 km^2 and a weight of 0.302 while the least areal extent is of Thunacadavu with an area of 137 km^2 and a weight of 0.107 respectively. The influential area of each station is placed in the increasing order in table 4.3. Table 4.4 shows the total monthly average rainfall of the basin computed by Theissen polygon method. To prepare the Theissen polygon map Singhal *et al.*, 2018 have taken three rain gauge stations (Venkatapuram, Bhopalapatnam and Bizapur) for the total catchment area of 193.91 km^2. The percentage area of influence for each of the gauging stations was found to be 65%, 31% and 4% for Venkatapuram, Bhopalapatnam and Bizapur respectively. Moitrayee Das, 2018 made a study on the use of Theissen polygon method to analyze the monsoon rainfall in Jalpaiguri district

of West Bengal having an area of 6227 km^2. Eight gauging stations were selected for preparing the Theissen polygon map and his results concluded an acceptability of applying the method for estimating the depth, volume and area rainfall probability.

Table 4.3 Gauging station influential area along with their weights

Sl. No.	Gauging station	Area (km^2)	Weights
1	Thunacadavu	137	0.107
2	Chalakudy	144	0.113
3	Peruvaripallam	230	0.18
4	Parambikulam	380	0.298
5	KSD	385	0.302

Month	Thuna-cadavu	Chalakudy	Peruva-ripallam	Parambi-kulam	KSD	Average rainfall
Jan	1	5.00	1.57	0.90	2.69	2.03
Feb	11.71	14.86	11.86	11.03	17.76	13.72
March	41.29	26.53	46.48	75.45	64.00	57.58
April	72.81	87.24	78.90	139.87	114.05	107.95
May	97.43	233.69	101.62	157.89	219.49	168.40
June	285.33	661.4	295.48	501.13	788.13	545.57
July	384.33	629.24	391.90	643.81	909.40	649.03
August	274.24	444.89	289.90	428.62	660.83	458.94
Sept	213.67	386.18	227.67	324.14	488.00	351.33
Oct	216.48	348.98	232.38	325.15	370.75	313.21
Nov	125.29	178.07	144.52	121.62	122.35	132.73
Dec	33.57	29.51	39.09	30.13	18.56	28.55

Table 4.4 Monthly average rainfall (mm) computed by Theissen polygon method (1997- 2017**)**

The highest monthly average rainfall was recorded in the month of July (649.03mm) followed by June (545.57mm). The lowest rainfall was recorded during the month of January (2.03mm).

CN grid map

The CN grid map was prepared by merging the polygons of both the soil map and LULC map. Since, three land use maps were prepared, utilizing the three LULC maps three different CN grid maps were prepared as well. Since, the SCS loss method was selected, the CN grid map was mainly prepared to generate the curve number for each sub basin as the curve number is a must parameter for running the model. Fig. 4.15, 4.16 and 4.17 shows the CN grid map for the years 1997, 2007 and 2017 respectively. Table 4.5 shows an overview of the 'CN Lookup table' whereas the CN and area of each sub basin is shown in table 4.6. For an easy comprehension of the specific curve number assigned to each sub basin, an overview of basin model is shown in fig. 4.18 to represent the entire sub basin along with the code of hydrologic element.

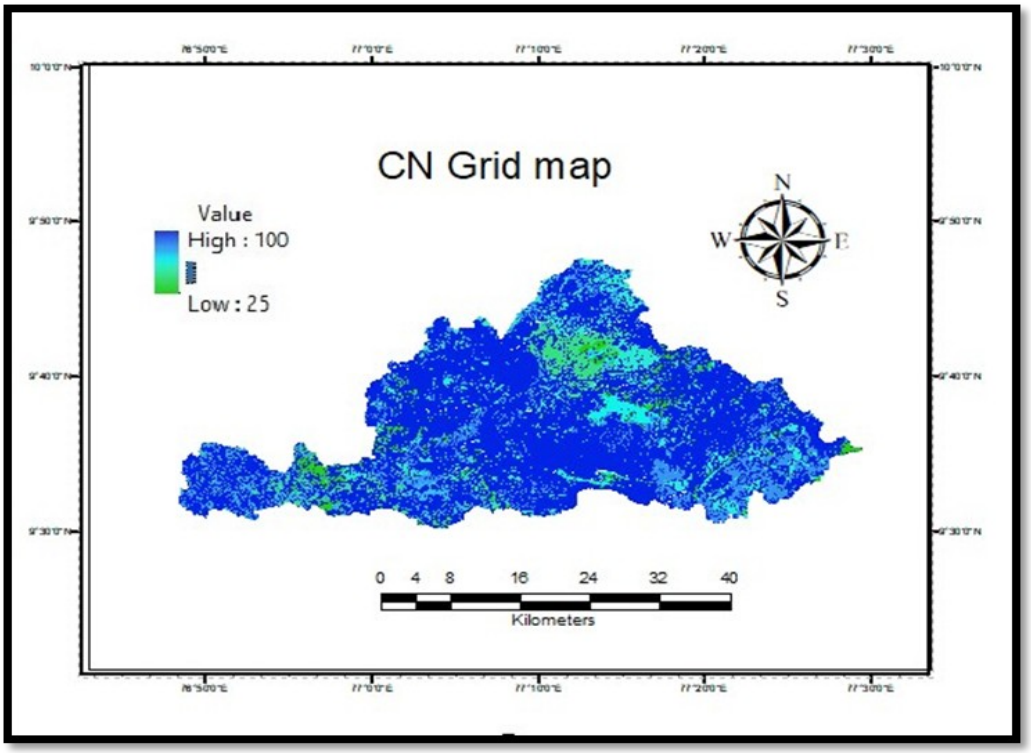

Fig. 4.15: CN grid map 1997

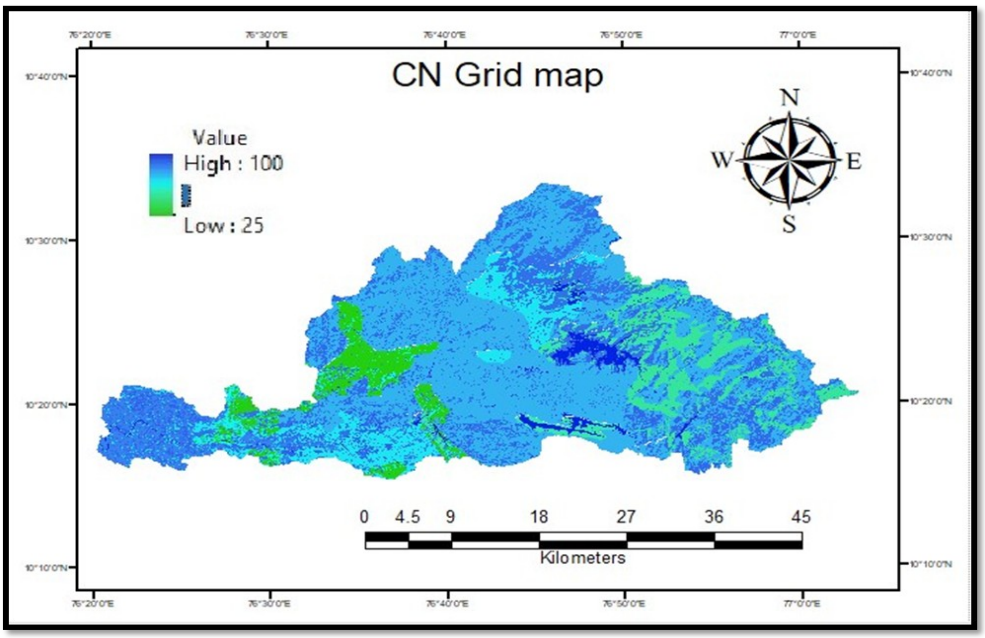

Fig. 4.16: CN grid map 2007

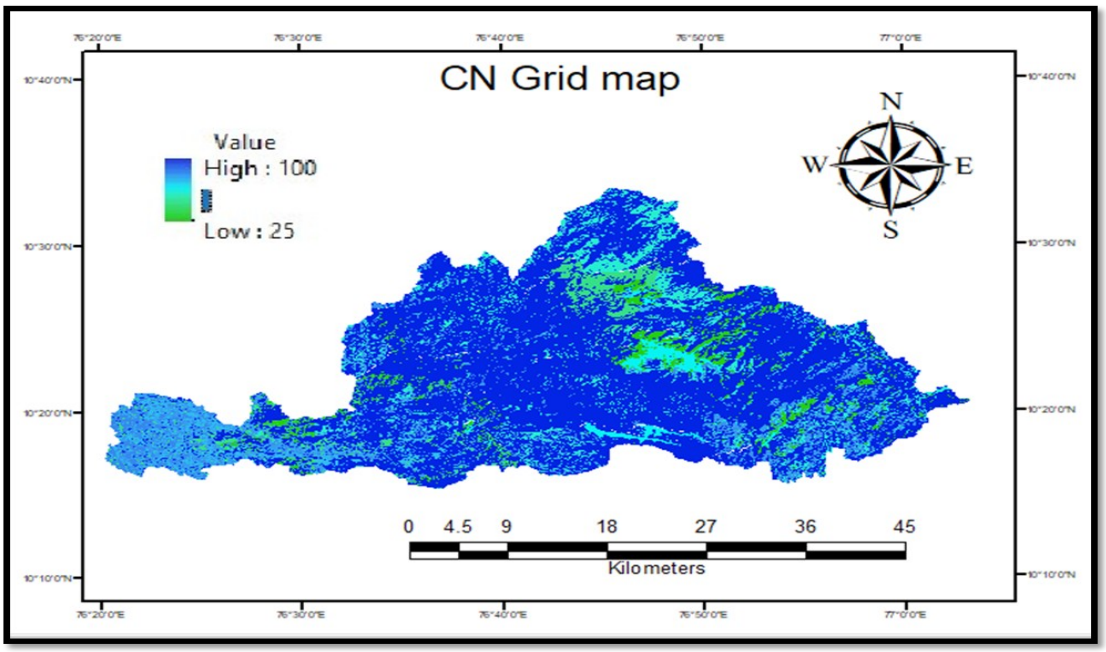

Fig. 4.17: CN grid map 2017

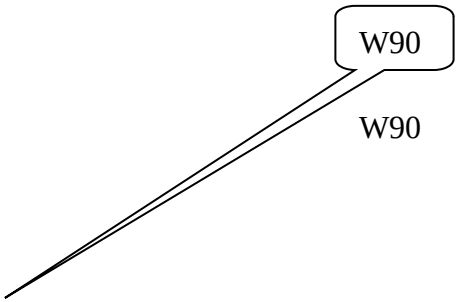
W90
W90

Fig. 4.18: View of the basin model

Table 4.5 An overview of CN Lookup table for different classes

LU value	Description	A	B	C	D
1	Paddy	67	78	85	89
2	Waterbody	100	100	100	100
3	Vegetation	25	55	70	77
4	Barren land	71	80	85	88
5	Tea	67	78	85	89
6	Urban area	77	85	90	92
7	Palm	67	78	85	89

Table 4.6 Overview of CN and area of each sub-basin

Hydrologic element	Curve Number (1997)	Curve Number (2007)	Curve Number (2017)	Area (km^2)
W140	84.17	87.53	88.59	237.21
W130	85.10	84.09	85.93	299.69
W120	84.85	89.27	90.75	31.438
W110	86.75	92.49	92.71	104.57
W100	85.21	89.68	88.29	277.14
W90	87.89	93.86	94.33	93.49
W80	89.47	84.47	86.96	230.99

There are seven sub watersheds, out of which the highest area was found to be of W130 (299.69 km^2) and the least for W120 (31.438 km^2). The CN value greater than 90 is generally considered to be a highly impervious surface. The higher the CN value, the more impervious the surface is, this is evident from the table 4.6. The vegetation area which includes the forest carries the lesser CN value while the water body has a CN value of 100. The sub watershed W90 has CN value almost higher than the rest of the sub watersheds, the reason for this can be inferred from the figs. 4.2, 4.3 and 4.4 of LULC maps which shows that the larger portion of the water body lies around W90. The notation ‘W’, ‘J’ and ‘R’ in figure 4.18 denotes a sub watershed, junction and a reach.

4.6 PARAMETER SENSITIVITY ANALYSIS

The sensitivity analysis is needed to find out which parameter has the highest influence on the model output. It is mainly done to adjust the parameters in a way that the adjusted parameter improves the model output or increases the efficiency of the model. The sensitivity analyses of the parameters were carried out after running the HEC-HMS model. The sensitivity analysis shows an increase or decrease of certain parameters. The most sensitive parameter for the present study was found to be the 'Curve Number' followed by Initial abstraction and Lag time. The least sensitive parameter was the 'Simple Canopy'. The remaining sensitive parameters are placed in the decreasing sequential manner as represented in table 4.7. Looking at the table of the optimized value it is evident that the increased parameters after optimization were Recession - Recession constant, Muskingum 'X' and 'K' value, Recession – Initial Discharge and the parameters which decreased were SCS Curve Number – Curve Number, Initial abstraction, Lag time, Simple Surface – Maximum Storage, Simple Canopy – Maximum Storage, Simple Surface – Initial Storage, and Simple Canopy – Initial Storage. Choudari *et al.,* 2014 simulated the rainfall-runoff in Balijore nala watershed using the HEC-HMS model and got a similar result, the most sensitive parameters obtained were initial abstraction, curve number and lag time. Pampaniya *et al.,* 2015 have likewise used SCS-CN, SCS unit hydrograph and Muskingum approaches as loss, transform and routing methods and the most sensitive parameters identified in their studies were curve number and initial abstractions. Sarminingsih *et al.,* 2019 simulated the rainfall-runoff in Garang watershed using the HEC-HMS model. The methods used were User Hyetograph, SCS UH, Exponential Recession and Lag as the Precipitation, Transformation, Baseflow and Routing methods and the most sensitive hydrological parameters found were SCS-CN, groundwater content (S), and Initial abstraction.

Table 4.7 Optimized parameters for the watershed

Sl. No.	Parameters	Units	Initial	Optimized
1	SCS Curve Number – Curve Number		88.77	82.35
2	SCS Curve Number – Initial abstraction	mm	17.25	13.15
3	Lag time	Min.	18.51	16.97
4	Simple Surface – Maximum Storage,	mm	4.4	2.91
5	Simple Canopy – Maximum Storage	mm	4.2	2.85
6	Recession – Recession Constant		0.4	0.75
7	Muskingum - X		0.2	0.5
8	Recession – Initial Discharge	m^3/s	5	5.07
9	Simple Surface – Initial Storage	%	0.1	0.04
11	Muskingum - K	hr	0.35	0.36
12	Simple Canopy– Initial Storage	%	0.1	0.09

4.7 CALIBRATION OF THE MODEL

Calibration is an iterative technique of assessment for all the parameters involved and attempts in refining the parameters on the basis of comparison between simulated and observed values. Calibration for the present study was carried out to produce the best agreement between simulated and observed values all throughout the calibration time frame. Since, calibration depends on quite a long year of simulation; the parameters were assessed under an assortment of climate, soil moisture, and water flow conditions. Therefore, for the present study five years (2003- 2007) were chosen to calibrate and discover the best sets of parameters for the HEC-HMS model. With the auto-calibration technique i.e., ‘Univariate gradient’ accessible in HEC-HMS model the calibration was done to derive the best parameters set for each event. Once the auto-calibration step was carried out, the ranges of calibrated parameters were found to either decrease or increase. It also made the trial and-error process much more easy and quick to come up with the best set of parameters for all the five events chosen for calibration. A comparison between the observed and simulated flow was done for both the calibration and validation period. The graphs between the observed flow hydrograph and the simulated flow hydrograph before and after the calibration are

shown in figure 4.19 and after the calibration in fig. 4.20 respectively. The NSE value for the calibration period was found to increase from 0.726 to 0.766 and R^2 i.e., correlation coefficient value from 0.80 to 0.83 (Fig 4.21 and 4.22) after the optimization was done which was found to be in the acceptable range. The percentage difference between the computed peak flow and observed peak flow was found to be 8.9% (1060.4 m^3/s and 973.1 m^3/s) and the volume difference between the two was 15 % for the calibration period. The RMSE was found to be 1.9 which shows a good performance of the model. Ismael *et al.,* 2017 have used HEC-HMS model to simulate the runoff in Ruiru basin and the peak flow difference during the calibration period was found to be 27.2%. Reshma *et al.,* 2013 for their studies have taken four date events for the calibration period and the percentage peak flow difference was found to vary from a negative value to 8. Roy *et al.,* 2013 calibrated and validated the model for Subarnarekha basin for studying the hydrological response and the net difference of peak flow for the calibration period was found to be 19%. The comparison of the percentage difference of peak flow with other studies showed similar results in acceptable ranges for the present study. Summary of results for the entire hydrologic elements for the calibration period is shown in table 4.8.

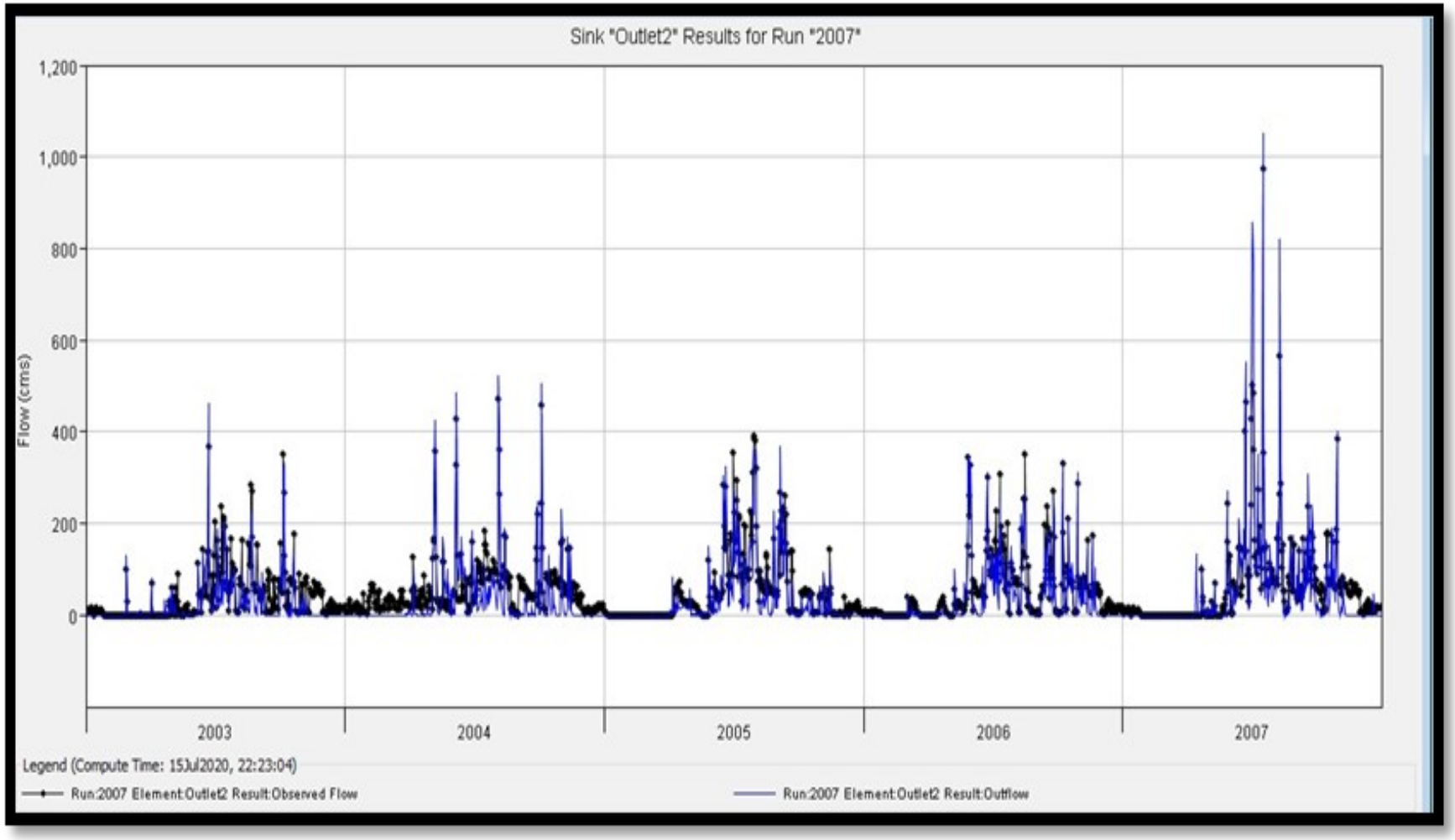

Fig 4.19: Observed and simulated flow hydrographs before calibration (2003-2007)

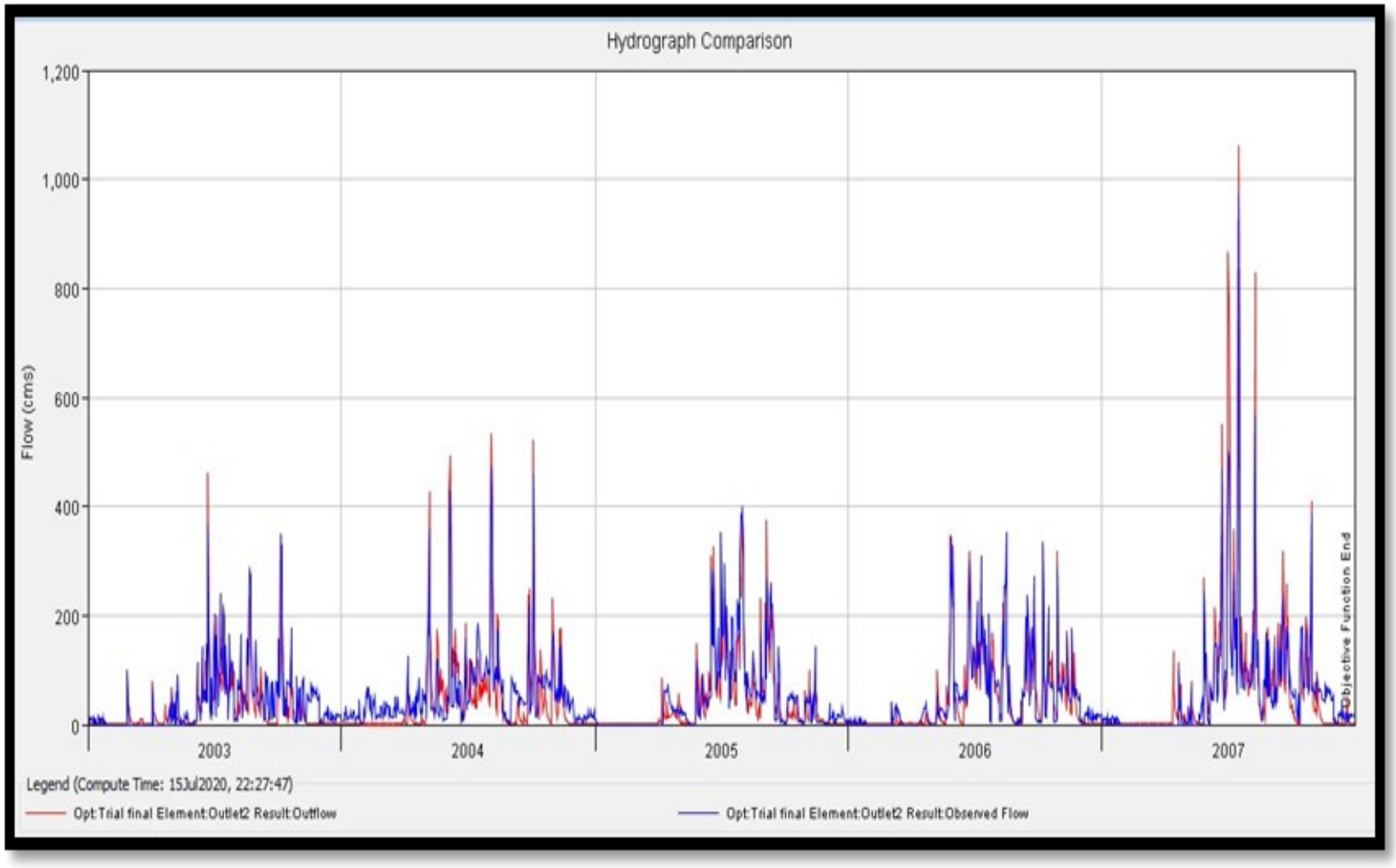

Fig 4.20: Observed and simulated flow hydrograph after calibration (2003-2007)

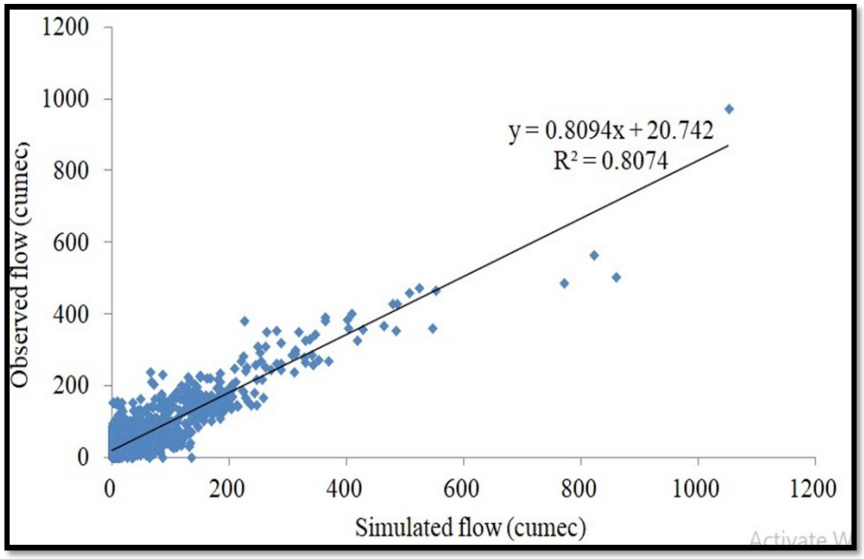

Fig 4.21: Correlation coefficient before calibration (2003-2007)

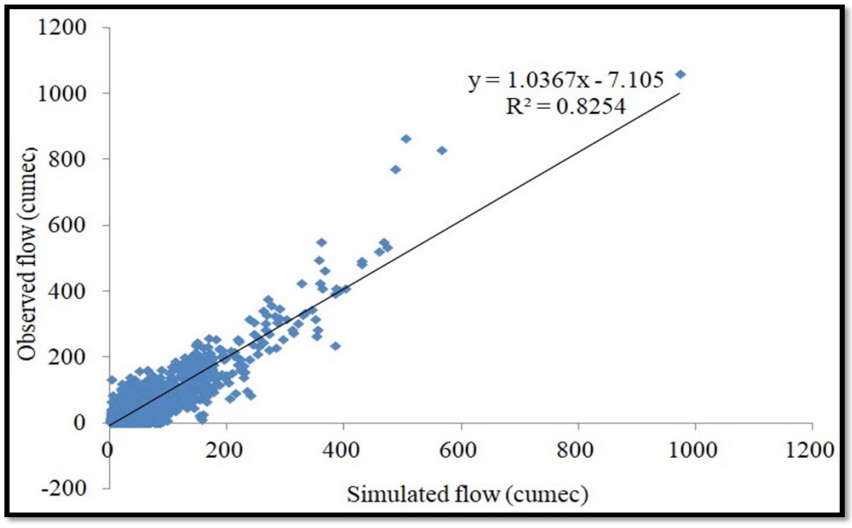

Fig 4.22: Correlation coefficient after calibration (2003-2007)

Table 4.8 Summary table of the watershed for the calibration period 2003-2007

Hydrologic element	**Peak discharge (m^3/s)**	**Time of peak**	**Volume (Million m^3)**
W140	790.4	17 Jul2007	3715.79
W130	493.6	04 Oct2004	4669.38
W120	64.9	16 Jul2007	605.53
W110	165.7	02 Nov2004,	1048.51
W100	923.4	17 Jul2007	4225.73
W90	311.5	6 Aug2007	1458.24
W80	289.1	11 Sep2005	2034.09
Outlet	1049.6	04 Aug2004	5673.11
J96	1677.7	17 Jul2007	8403.76
J103	1488.8	17 Jul2007	8270.92
J106	1128.5	17 Jul2007	6259.82
R30	1089.7	17 Jul2007	5702.91
R50	866	17 Jul2007	4037.09
R70	764.8	17 Jul2007	962.36

The peak discharge value was found highest for ‘J96’ (1677.7 m^3/s**)** followed by J103 (1488.8 m^3/s) and the least for ‘W120’ (64.9 m^3/s). Similarly, the volume was also found to be the highest for ‘‘J96’ (8403.76 Million m^3) followed by J103 (8270.92 Million m^3) and the least for ‘W120’ (605.527 Million m^3). At the outlet the peak discharge value was computed to be 1049.6m^3/s with a volume of 5673.11 Million m^3.

4.8 VALIDATION OF THE MODEL:

A validated model is the one in which the accuracy as well as its forecasting ability in the validation time set proves to be lying within an acceptable range. For the current examination the approval of the model is done by utilizing the optimized parameters for comparing the observed and simulated flows for a different time step. A few

statistical measures were used to assess if the calibrated parameters can imitate the hydrographs appropriate with the observed one. Utilizing the parameter sets acquired from the calibration period, HEC-HMS model was validated for the period 2015-2017. The parameters optimized during the calibration period were taken as input values for the validation period. The simulated and observed hydrograph for the validation period is shown in fig. 4.23. Summary table for validation period is shown in table 4.9. For the validation period the NSE value was found to be 0.810 and correlation coefficient as 0.85 (Fig 4.24). The contrast between the observed peak flow and simulated peak flow was found to be 1.9% (552.7 m^3/s and 563.2 m^3/s) and the volume difference between the two was found to be 10.5%. The RMSE for the validation period was found to be 1.4 % which is in the acceptable range. Ismael *et al.,* 2017 validated the HEC-HMS model for one year and the difference of peak flow between the observed and simulated value was found to be 9.5%. Reshma *et al.,* 2013 have taken three date of rainfall events for the validation period, the difference between the peak flow values obtained by them varied from a negative value to 16.21% while the study done by Roy *et al.,* 2013 obtained a value of 1.9% for the validation period. Since, the values obtained were similar to several earlier studies, the results obtained in the present study were considered to be in the acceptable range. The increase in the model efficiency itself proves that the parameters that were calibrated are compatible and prognostic which can be helpful in runoff estimation from the acquired rainfall data of Chalakudy basin.

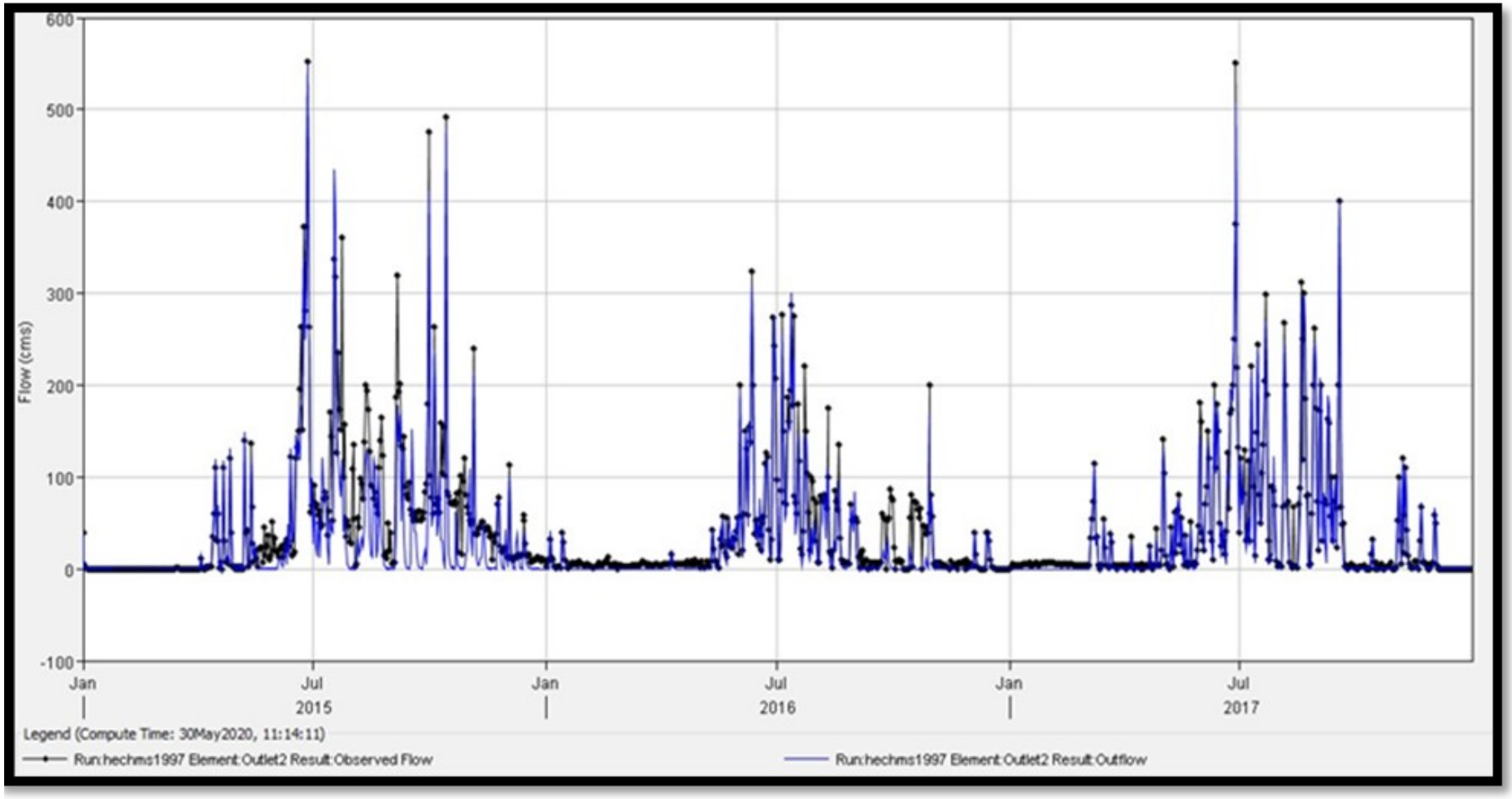

Fig 4.23: Observed and simulated hydrograph after validation (2015-2017)

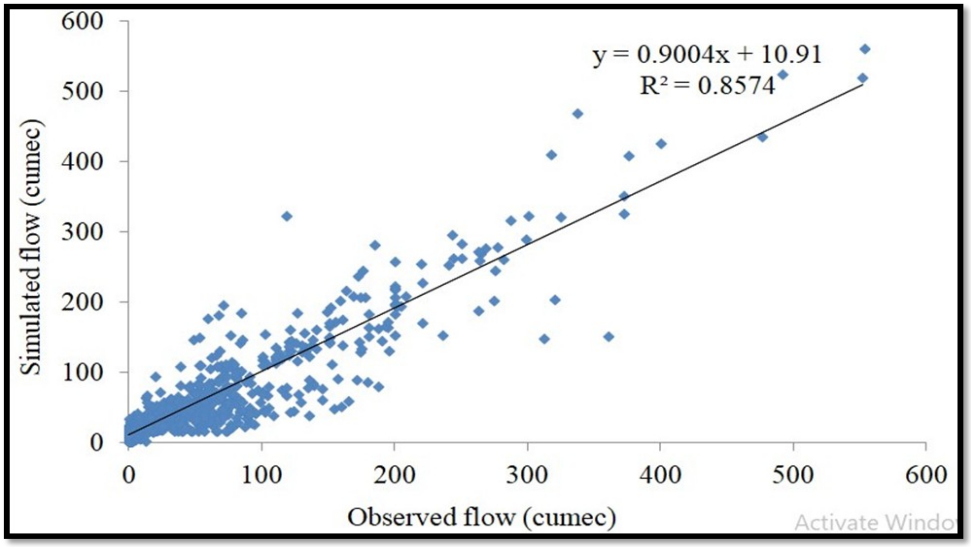

Fig. 4.24: Correlation coefficient after validation (2015-2017)

Table 4.9 Summary of the watershed for validation

Hydrologic element	**Peak discharge(m^3/s)**	**Time of peak**	**Volume (Million m^3)**
W140	310.2	18 Sep2017	1166.21
W130	326.5	01 Oct2015	1863.12
W120	44.3	17 Sep2017	218.04
W110	158.1	28 Jun2017	349.75
W100	362.4	18 Sep2017	1282.65
W90	122.3	18 Sep2017	431.36
W80	183.4	27 Jun2015	598.64
Outlet	549.4	27 Jun2015	2993.34
J96	848.7	28 Jun2017	3223.09
J103	671.2	28 Jun2017	2286.93
J106	523.0	18 Sep2017	1881.29
R30	422.0	18 Sep2017	1830.2
R50	547.2	28Jun2017	1494.43
R70	403.0	28Jun2017	1118.82

For the validation period the peak discharge value was found highest for 'J96' (848.7m^3/s**)** followed by J103 (671.2m^3/s) and the least for 'W120' (44.3m^3/s).

Similarly, the volume was also found to be the highest for ‘‘J96’ (3223.09Million m^3) followed by the outlet (2993.34 Million m^3) and the least for ‘W120’ (44.3Million m^3). At the outlet the peak discharge value was computed to be 549.4m^3/s.

Table 4.10 Performance assessment of HEC-HMS model

	Calibration period (2003-2007)		**Validation period (2015-2017)**
Metric	**Before optimization**	**After optimization**	
NSE	0.726	0.766	0.81
R^2	0.80	0.83	0.85
RMSE		1.9%	1.4%

As the value of NSE and R^2 value for the calibration period was found to increase after the optimization of the parameters were done and the NSE value for the validation period was found to be in the acceptable range, therefore the results concluded a good performance of the HEC-HMS model for computing the peak flow and runoff volume with the SCS CN loss method. Tassew *et al.,* 2019 obtained an NSE value of 0.746 and correlation coefficient of 0.842 for the calibration period while an NSE value of 0.884 and correlation coefficient of 0.925 for the validation period. Similarly Roy *et al*., 2013 in their studies obtained an NSE value of 0.72 to 0.84 and correlation coefficient as 0.70 to 0.85 before and after calibration. Likewise Ismael *et al.,* 2017 obtained an NSE value of 0.74 and 0.72 for the validation and calibration period respectively. From the obtained NSE and R^2 value (Table 4.10) it can be concluded that the calibrated and validated value is acceptable and the HEC-HMS model is effective in modelling the hydrology of Chalakudy river basin as it considers the different parameters which have an influence on the runoff and peak flow of the basin.

4.9 IMPACT OF LULC CHANGES ON THE RUNOFF PROCESSES OF CHALAKUDY BASIN:

In order to understand the impacts of LULC changes on runoff characteristics of Chalakudy basin, the simulation runs of the validated model was done for three separate years, i.e., 1997, 2007 and 2017 using the land use maps of respective years as input along with other data files and its results were analyzed. The final output of the model was compared to the corresponding years of LULC map changes. For the change detection analysis the area of each class, percentage coverage and decadal percentage change were calculated which is shown in tables 4.11, 4.12 and 4.13 respectively. Contrasts in the observed and simulated flow hydrographs and the related changes in model parameters were consequently connected with changes in the LULC. The procedure followed is explained below.

4.9.1 LULC Change Detection Analysis

Table 4.11 Areal extent of various LULC classes during the period 1997- 2017

Year	**1997**	**2007**	**2017**
LULC category	**Area (km^2)**	**Area (km^2)**	**Area (km^2)**
Waterbody	27.84	40.10	29.32
Vegetation	886.21	833.68	803.09
Barren land	163.91	144.37	179.16
Palm	30.88	42.9	49.48
Tea	97.57	85.97	77.91
Paddy	36.35	90.74	93.64
Urban	31.74	36.76	41.93

Table 4.12 Percentage area of various LULC classes during 1997 – 2017

Year	1997	2007	2017
LULC category	**Area (%)**	**Area (%)**	**Area (%)**
Waterbody	2.18	3.15	2.3
Vegetation	69.53	65.41	63.01
Barren land	12.86	11.33	14.06
Palm	2.42	3.37	3.88
Tea	7.66	6.75	6.11
Paddy	2.85	7.12	7.35
Urban	2.49	2.88	3.29

Table 4.13 Decadal percentage change in area of various LULC classes

	1997-2007	2007-2017	(1997-2017)
LULC category	**Percent change (%)**	**Percent change (%)**	**Percent change (%)**
Waterbody	0.97	-0.85	0.12
Vegetation	-4.12	-2.4	-6.52
Barren land	-1.53	2.73	1.2
Palm	0.95	0.51	1.46
Tea	-0.91	-0.64	-1.55
Paddy	4.27	0.23	4.5
Urban	0.39	0.41	0.8

Table 4.14 Annual change rate of LULC classes (%)

Annual change rate (%)

LULC category	**1997-2007**	**2007-2017**	**(1997-2017)**
Water body	3.64	-3.13	1.04
Vegetation	-0.61	-0.37	-1.97
Barren land	-1.27	2.16	1.78
Palm	3.29	1.43	9.43
Tea	-1.27	-0.98	-4.5
Paddy	9.15	0.31	18.93
Urban	1.47	1.32	5.57

Area coverage of 27.84 km^2, 40.10 km^2 and 29.32 km^2 of urban area was noticed and the highest area coverage found was for the vegetation class which are 886.21 km^2 to 833.68 km^2 and 803.09 km^2 respectively for the years 1997, 2007 and 2017 (Table 4.11). The comparison of results for various decades reveals that the vegetation zone, barren land and tea plantation showed reduction of area by 4.12%, 1.53% and 0.91% respectively from 1997-2007. An increase of water body, palm, paddy area and urban area by 0.97%, 0.95%, 4.27% and 0.39% was also found after comparing the LULC maps of 1997 and 2007 (Table 4.13). A lessening in the water body class by 0.85% and abatement in the territory of vegetated area and tea by 2.4% and 0.64% respectively were further observed in the subsequent decade. Expansion in the territory of barren land, palm, paddy and urban area by 2.73%, 0.51%, 0.23% and 0.41% was noticed. The highest decadal percentage increment from 1997-2017 was found to be of paddy i.e., 4.5% (Table 4.13). The Kerala state planning board 2019 economic review also stated that there is an increasing trend of paddy area since 2016 due to the intervention of Haritha Kerela mission (Kerala state planning board, 2019). These changes were noticed after evaluating the LULC changes that took place between 2007 and 2017 (Table 4.13).

The reduction in the vegetation area might be a result of populace increment. The highest decrease in percentage area was found to be for vegetation class which was found to decrease consistently in between the two decades from 69.53% to 65.41% and 63.01% respectively (Table 4.12). The results obtained from

LULC change study for the period from 1997 to 2017 revealed that there was a consistent decrease in the area of vegetated land and tea whereas a critical increment in the region of barren land, palm, urban area and paddy. Examination of LULC maps of 1997, 2007 and 2017 (Figs. 4.2, 4.3 and 4.4) revealed that the basin right now shows a fluctuating pattern for each decade with respect to different classes. Figures 4.2, 4.3 and 4.4 demonstrate the general changes over the time span examined. Munthali *et al.,* 2019 analyzed the change of LULC for Dedza district of Malawi. The LULC map was prepared for three years i.e., 1991, 2001 and 2015. For preparing the LULC map they have done a hybrid supervision algorithm for which first the Unsupervised classification was done followed by Supervised classification as the separation of barren land and built-up areas from agricultural areas was difficult due to spectral reflectance confusion. In the studies done by Mayaja *et al.,* 2017 on the LULC changes impact on Pampa river basin, they have used ERDAS Imagine. Supervised classification was used for preparing the LULC map by classifying them into six classes *viz* forest land, agriculture land, built up area, wasteland, grass land and water bodies. Lydia *et al.,* 2018 made a study to evaluate the LULC changes in Coimbatore cooperation using RS and GIS, the LULC map was prepared by classifying the area into seven classes *viz,* built up, agriculture, barren land, forest, industries, water bodies and scrubland. For the map preparation initially they have used unsupervised classification process which was refined by comparing it to a referenced image, later on a hybrid supervised classification was used.

The annual change rate of LULC classes for 1997-2007 (Table 4.14) was found to be the highest for paddy with 9.15% and least for vegetation with -0.61% while for 2007-2017 the highest declination of annual rate change was for the water body (-3.13%) and the highest increment was for barren land (2.16%). From 1997-2017, there was a drastic percentage change for paddy and palm with 18.93% and 9.43%.

Quantifying the shifting of different LULC classes from one to another is an important part in LULC studies therefore for the present study the change detection matrix was obtained for the years 1997-2007 and 2007-2017 for the LULC change analysis. Munthali *et al.,* 2019 have made similar studies to analyze the LULC map on Dedza district, Africa. For their studies they have prepared three change detection

matrix based on the area of different classes, the change detection matrix prepared for different LULC maps were for the years 1991 to 2001, 2001 to 2015 and 1991 to 2015 so as to get an idea about the transition of one class to another over a period of time. Koneti *et al.,* 2018 have also made a study to assess the impact of LULC changes on the Godavari basin, they have likewise made three detection error matrix for the years 1985 to 1995, 1995 to 2005 and 2005 to 2014, later on a confusion error matrix was also prepared using the reference and classified data to get an idea about the classification accuracy.

The change detection matrix was prepared by merging the LULC maps of 1997 and 2007, 2007 and 2017 with the help of Geoprocessing menu available in the ArcGIS. The matrix obtained for the year 1997-2007 and 2007-2017 are shown in tables 4.15 and 4.16 respectively.

Table 4.15 Land use area change detection matrix for the period 1997-2007 (km^2)

Class name	**Water body**	**Veget-ation**	**Barren land**	**Palm**	**Tea**	**Paddy**	**Urban**	**1997 Total**
Water body	**24.39**	3.06	0.2	0.06	0.03	0.09	0.01	**27.84**
Veget-ation	10.06	**662.36**	95.24	33.45	31.93	43.76	9.4	**886.2**
Barren land	5.08	95.73	**23.7**	1.08	3.09	22.74	12.49	**163.91**
Palm	0.1	10.72	6.17	**3.04**	1.16	7.71	1.98	**30.88**
Tea	0.07	35.16	12.79	0.71	**45.85**	2.81	0.18	**97.57**
Paddy	0.38	10.18	2.49	0.94	1.99	**8.1**	12.27	**36.35**
Urban	0.01	16.45	3.78	3.62	1.9	5.53	**3.45**	**31.74**
2007 Total	**40.1**	**833.68**	**144.37**	**42.9**	**85.97**	**90.74**	**36.76**	**1274.52**

Table 4.16 Land use area change detection matrix for the period 2007-2017 (km^2)

Class name	Water body	Veget-ation	Barren land	Palm	Tea	Paddy	Urban	2007 Total
Water body	**27.04**	6.5	6.17	0.05	0.02	0.26	0.07	**40.11**
Vegetation	2.18	**655.09**	95.53	21.13	26.6	25.57	7.58	**833.68**
Barren land	0.02	90.61	**25.79**	3.87	10.14	8.62	5.3	**144.35**
Palm	0.01	5.16	1.49	**15.35**	1.44	12.3	8.15	**43.9**
Tea	0.01	22.36	15.93	0.03	**30.36**	15.52	1.07	**85.28**
Paddy	0.03	21.51	25.7	6.4	4.23	**20.27**	12.36	**90.5**
Urban	0.03	1.86	8.55	2.64	5.12	11.11	**7.36**	**36.67**
2017 Total	**29.32**	**803.09**	**179.16**	**49.48**	**77.91**	**93.64**	**41.93**	**1274.53**

Table 4.17 (Gain-Loss) area (km^2) for each LULC class

LULC Classes	Area Gain		Area Loss	
	1997-2007	**2007-2017**	**1997-2007**	**2007-2017**
Water body	15.71	2.28	3.45	13.07
Vegetation	171.32	148	223.84	178.59
Barren land	120.67	153.37	140.21	118.56
Palm	39.86	34.13	27.84	28.55
Tea	40.12	47.55	51.72	54.92
Paddy	82.64	73.37	28.25	70.23
Urban	36.31	34.57	31.29	29.31

Table 4.18 Net (Gain-Loss) area (km^2) for each LULC class

LULC Classes	Net gain area (km^2) 1997-2007	Net loss area (km^2) 2007-2017
Water body	12.26	-10.79
Vegetation	-52.52	-30.59
Barren land	-19.54	34.81
Palm	12.02	5.58
Tea	-11.6	-7.37
Paddy	54.39	3.14
Urban	5.02	5.26

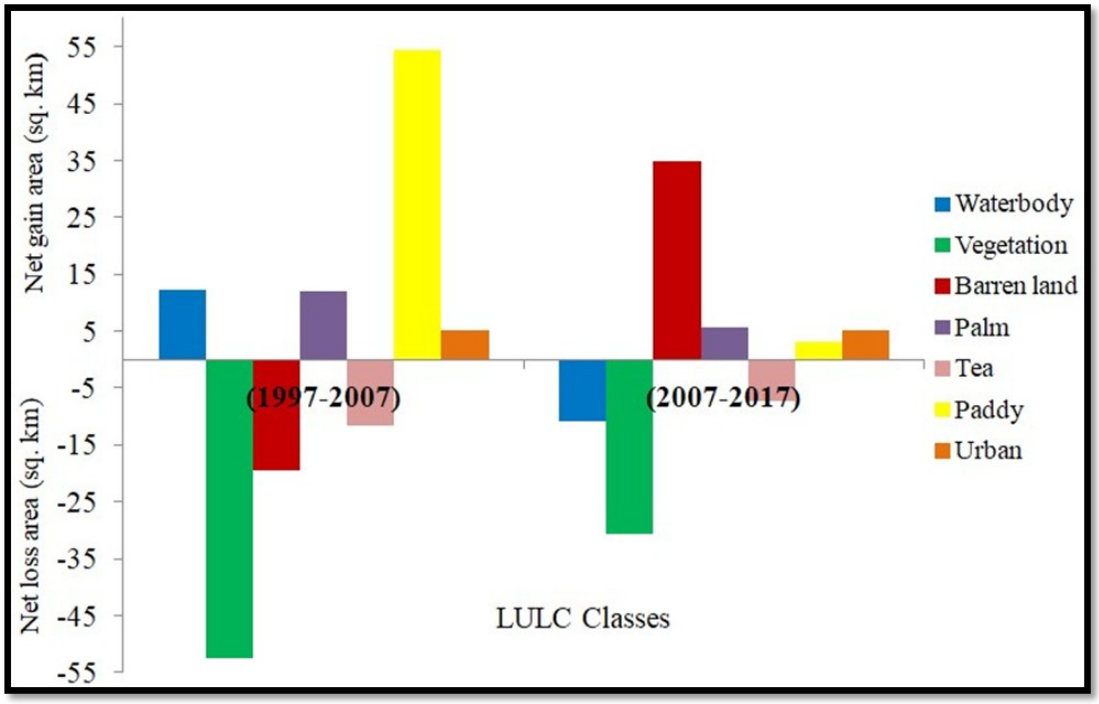

Fig 4.25: Net gain and losses for different LULC classes.

The table 4.15 and 4.16 shows the spatial distribution of each class for three different years (1997, 2007 and 2017). It also shows the shifting of one class to another over a period of time. The LULC transition change matrix results obtained for the year 1997 to 2017 showed an exceptional change in the vegetation and paddy area as compared to the rest of the other classes.

Table 4.15 shows that 24.39 km^2 of water body area remains the same from 1997 to 2007 while a water body area of 27.04 km^2 remains constant from 2007 to 2017 (Table 4.16). Table 4.15 shows that a water body area of 3.06 km^2, 0.2 km^2, 0.06 km^2, 0.03 km^2, 0.09 km^2 and 0.01 km^2 shifts to vegetation, barren land, palm, tea, paddy and urban respectively from 1997 to 2007. Maximum area to remain constant from 1997 to 2007 is of the vegetation area i.e., 662.36 km^2, the same was observed for the year 2007 to 2017 which is 655.09 km^2. Table 4.15 and 4.16 shows the area shifting mostly towards the urban area is paddy which are 12.27 km^2 and 12.36 km^2 respectively for 1997 to 2007 and 2007 to 2017.The tea area decreased from 97.57 km^2 to 77.91 km^2 over the two decades. The paddy, urban and palm area increased from 36.35 km^2 to 93.64 km^2, 31.74 km^2 to 41.93 km^2 and 30.88 km^2 to 49.48.

From the area gain-loss calculation (Table 4.17) it was observed that the highest area gain from 1997-2007 was of vegetation with 171.32 km^2 and for 2007-2017 it was of barren land with 153.37 km^2 while the least gain was of water body for both the decades with an area of 15.71 km^2 and 2.28 km^2 respectively. The highest area loss was of vegetation for both the decades with an area of 223.84 km^2 and 178.59 km^2 (Table 4.17) and the least area loss was of water body with an area of 3.45 km^2 and 13.07 km^2 respectively.

Table 4.18 and fig 4.25 shows that the highest loss from 1997-2007 was found to be of vegetation (-52.52 km^2) and the highest gain was of Paddy (54.39 km^2). In between 2007-2017 the highest loss was noticed for vegetation (-30.59 km^2) while the highest gain was for barren land (34.81 km^2).

4.9.2 Model Simulation Runs

Figure 4.26, 4.28 and 4.30 shows the final output flow hydrograph for the years 1997, 2007 and 2017 for the basin while figure 4.27, 4.29 and 4.31 shows the R^2 value obtained between observed and simulated hydrograph for 1997, 2007 and 2017 respectively.

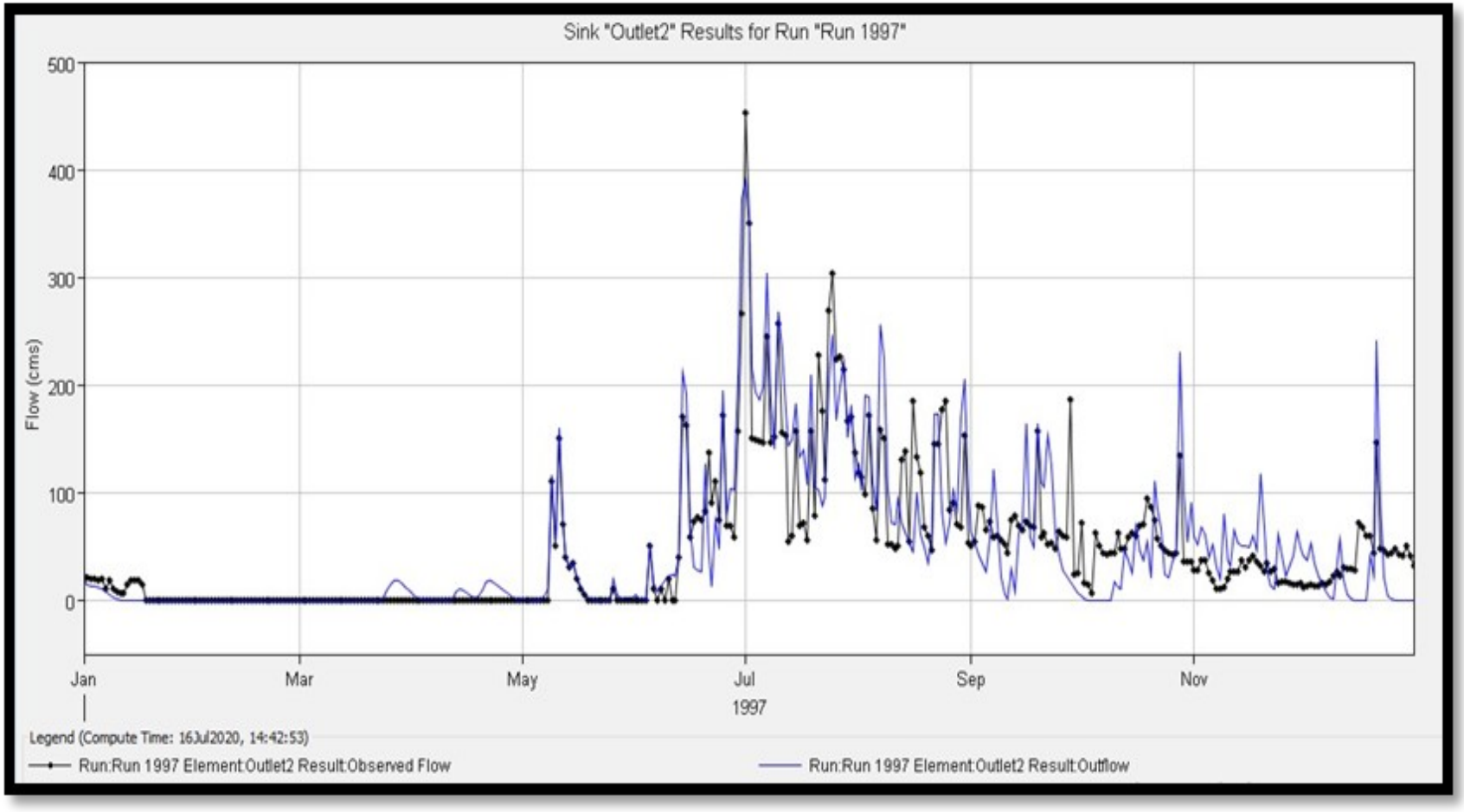

Fig 4.26: Observed and simulated hydrograph for the year 1997

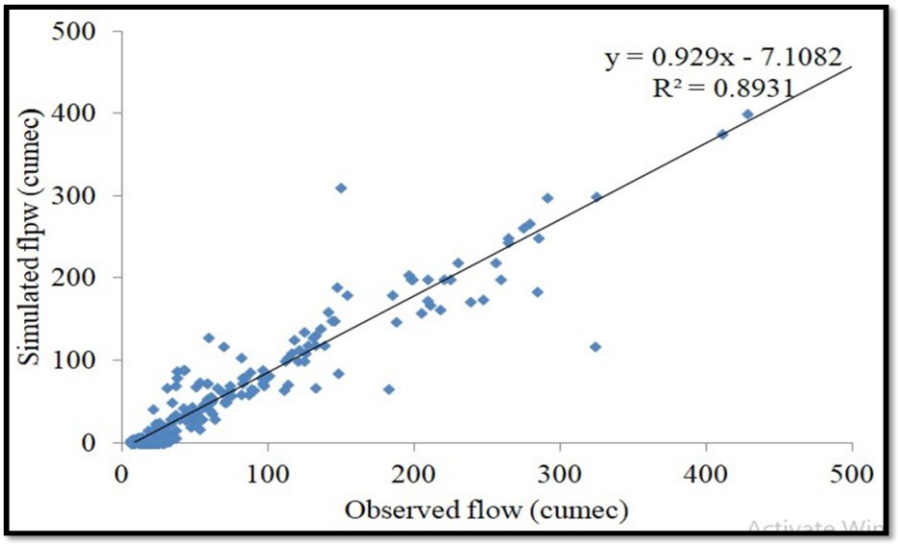

Fig 4.27: Correlation between observed and simulated flow for the year 1997

As validation of the model was done, the simulation runs done for all the three years showed a high value of R^2 value obtained between the observed and simulated flow which indicated a good performance of the model. For the simulation run done for 1997, the R^2 value obtained was 0.89. The total volume of flow computed was 1513.81 million m^3 which happened to be the lowest total volume as compared to 2007 and 2017. The NSE value obtained was 0.72 which was in the acceptable range.

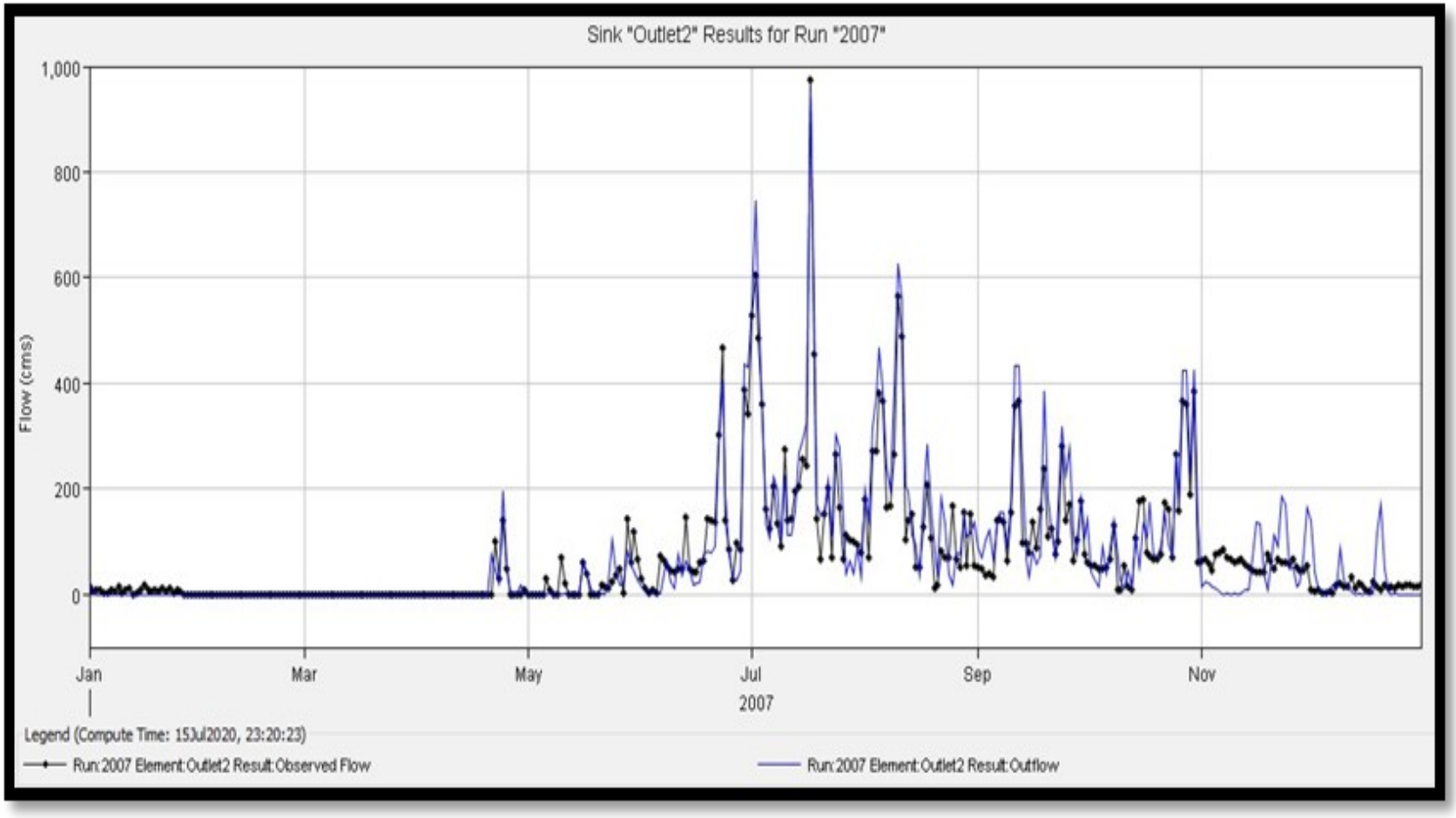

Fig 4.28: Observed and simulated hydrograph for the year 2007

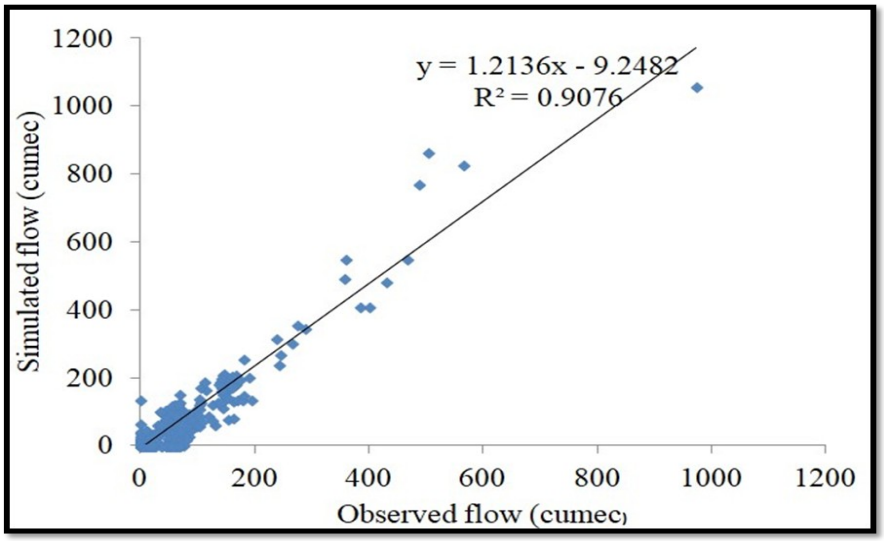

Fig 4.29: Correlation between observed and simulated flow for the year 2007

The R^2 value obtained for the year 2007 is 0.91 as shown in fig 4.29 and the NSE value obtained was 0.76 which showed a good performance of the model. The total volume computed for the year 2007 was 2481.98 million m^3. From the results obtained it was noticed that the total volume of flow was found to be the highest for the year 2007 which can also be one of the reasons why, the water body area was found to be the highest for the year 2007.

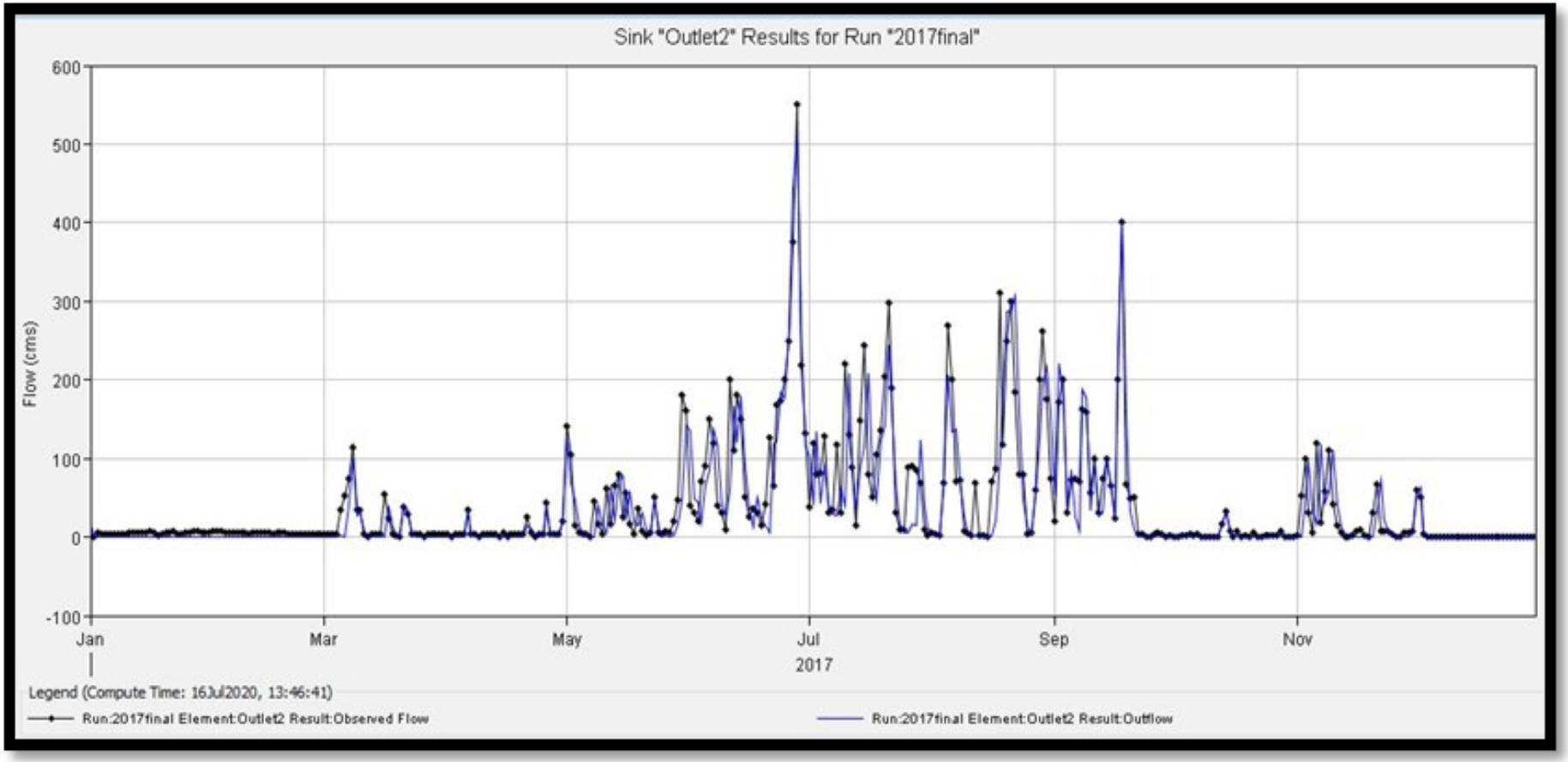

Fig 4.30: Observed and simulated hydrograph for the year 2017

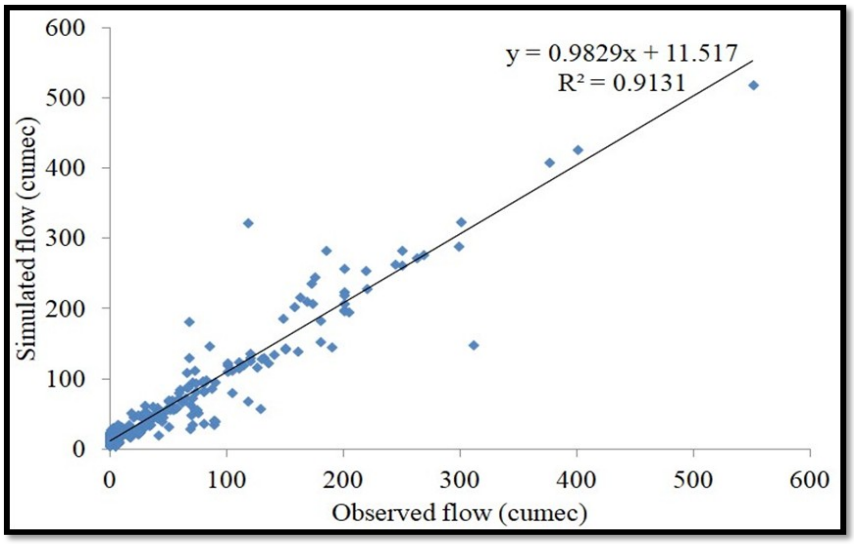

Fig 4.31: Correlation between observed and simulated flow for the year 2017

Fig 4.31 showed that the R^2 value obtained for the year 2017 was 0.91 and NSE value obtained was 0.81. Total computed volume of flow for the year 2017 was 1528.44 million m^3.

The peak discharge value of 1997, 2007 and 2017 along with the date when the peak flow occurred for each year are shown in table 4.19

Table 4.19 Peak discharge and total volume simulated for 1997, 2007 and 2017

Year	Peak discharge (m^3/s)	Date	Volume (Million m^3)
1997	403.7	1thJuly	1513.81
2007	954.1	16thAugust	2481.98
2017	483.5	28thJune	1528.44

The annual flow during 1997 was seen significantly lesser than 2007 and 2017. The peak discharge for 1997, 2007 and 2017 was observed to be on 1thJuly, 16th August and 28thJune with a discharge of 403.7m^3/s, 954.1m^3/s and 483.5m^3/s respectively.

4.9.3 Impact of land use land cover changes on runoff of the basin

Graph plotted between simulated average flow in relation to the LULC classes for the years 1997, 2007 and 2017 are shown in fig 4.32 and fig. 4.33.

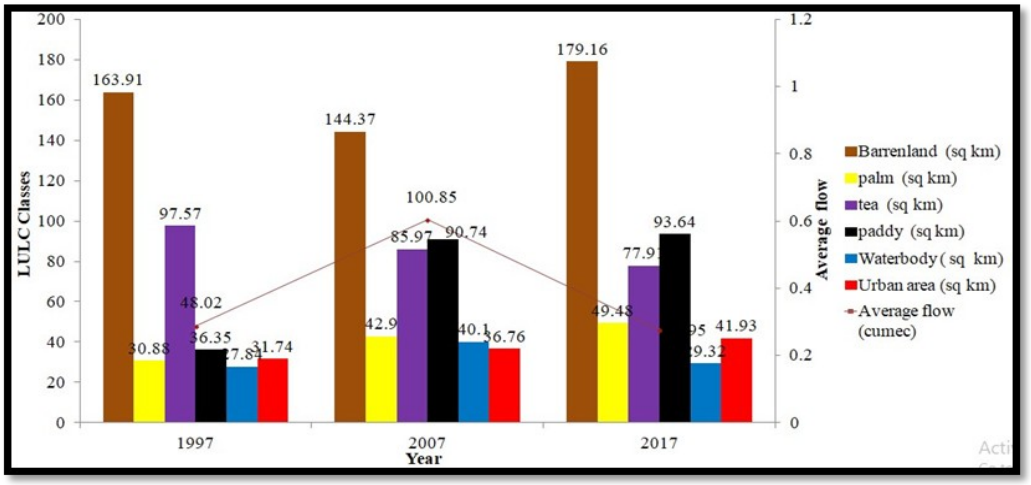

Fig. 4.32: Average flow Vs LULC for the years 1997, 2007 and 2017

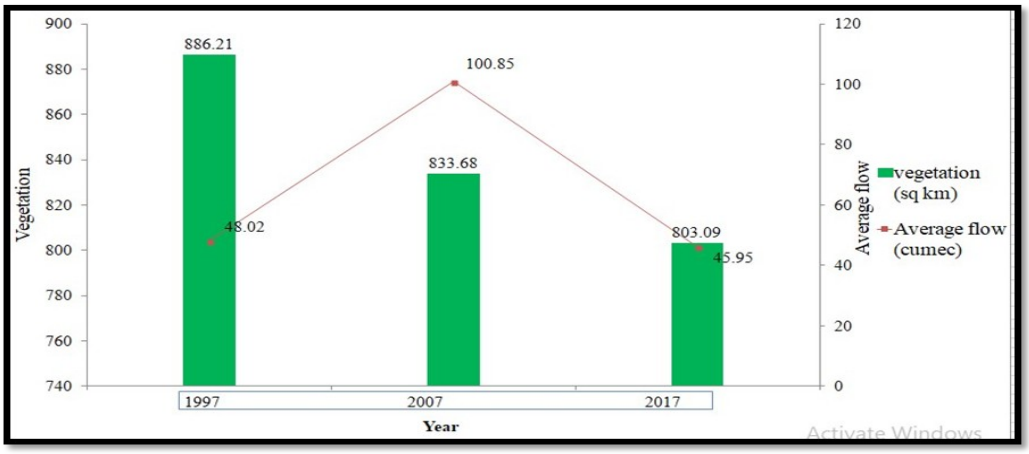

Fig. 4.33: Average flow Vs vegetation area for the years 1997, 2007 and 2017

The graph shows a consistent increase in the urban area, paddy and palm over the two decades. Due to an increase in urban development and changing cultivation practices, the soil particles are loosened, prompting soil disintegration, lessening the surface roughness and thereby eventually increasing the surface overflow. Urbanization likewise in general decreases the infiltration of water through the soil and increases the degree of impenetrable surfaces. The reason behind the decrease in the vegetation area may be because of the increase in the urban settlement over a stretch of time.

The increase in the urban area from 1997 to 2017 by a percentage of 0.8% and and 1.2% respectively and decline of vegetation area by 6.52% (1997-2017) seem

to increase the flow of the basin. The simulated average observed flow was found to be the highest for the year 2007 (100.85 cumec). It was observed that although the changes in the LULC map influences the flow of the basin, the LULC changes alone doesn’t cause an increment in the flow of the basin but it also depends on the amount of rainfall the basin receives. In 2017 there was a further decline in the flow of the basin, the obvious reason may be the decrease in the amount of rainfall the basin received in the year 2017. It may also be because of the changing trend in the use of land. As the vegetation area was found to decrease subsequently from 1997-2017 (Fig. 4.33), the surface runoff increment is due to the decline in the infiltration capacity of the soil and groundwater recharge processes. The frequent experience of high intensity rainfall by the basin in saturated and heavy clay soil also led to higher surface runoff rates and subsequently higher discharge.

The use of HEC-HMS model along with remote sensing and GIS was seen as supportive for the present study for investigating the quantitative changes in the precipitation excess flow of the basin that has occurred because of the LULC changes. Hydrological analysis done for the present study has drawn out significant effect of LULC changes on runoff at the basin scale, showing the model's capacity to effectively translate the entirety of the ecological and scene factors. The study demonstrates that deforestation and urban development prompts decrease in the general evapotranspiration (ET) and infiltration rate, with an expansion in overflow of the basin. Therefore, in conclusion we can say that the runoff of the Chalakudy basin is influenced by the increase in the area of urbanization and barren land along with the decline in the vegetated area with the passage of time which created a negative impact on the runoff flows of the basin. The results of the investigation showed that the incorporation of remote sensing and GIS along with HEC-HMS model can effectively model the hydrological issues in a watershed. The HEC-HMS model is exceptionally useful for examining the runoff flows in response to land-use change scenarios and the suggestion of this model for hydrological studies at basin level will be highly valuable for future studies.

Summary & Conclusion

CHAPTER V

SUMMARY AND CONCLUSION

The base of runoff estimation in any basin is to incorporate the processes of the hydrological parameters and to establish a relationship between the precipitation in the basin and the geography, existing land use and soil type. The runoff processes in Chalakudy basin also changes with LULC, soil status and precipitation amount. Studies likewise reasoned that the transformation of agriculture land and forests to human settlements reduces the conservation of moisture in the soil and enhances the runoff amount. The present study was conducted in the Chalakudy river basin of Kerala to analyze the effect of land use land cover changes on the runoff processes of this basin using Arc GIS, ERDAS Imagine and HEC-HMS softwares. For the present study the LULC maps were prepared for three different years i.e., 1997, 2007 and 2017. The soil map was prepared based on the soil type and grouped into different Hydrologic soil groups. A correlation analysis was also carried out between the average rainfall and average flow for two decades (1997-2007 and 2007-2017). After calibrating (2003-2007) and validating (2015-2017) the HEC-HMS model, simulation runs were carried out for three years (1997, 2007 and 2017) separately.

By the analysis of different LULC maps it can be concluded that the runoff is influenced not only because of LULC changes but also by an increase in the amount of rainfall the watershed receives. Another reason behind the runoff experienced by the watershed is a consistent decrease in the amount of vegetation area and an increase in barren land over the past two decades which created a negative impact on the infiltration capacity of the soil as well. Area coverage of 27.84 km^2, 40.10 km^2 and 29.32 km^2 for urban area class was noticed and the highest area coverage was for the vegetation class which was 886.21 km^2, 833.68 km^2 and 803.09 km^2 respectively for the years 1997, 2007 and 2017.The percentage area covered by urban area class varied from 2.49% to 2.88% and 3.29% and the highest area coverage was found for the vegetation class which was 69.53%, 65.41% and 63.01% respectively for the years 1997, 2007 and 2017. The annual rate change for 1997-2007 was found to be the highest for paddy with 9.15% and least for vegetation with -0.61% while from 2007-2017 the highest decline of annual rate change was for the

water body (-3.13%) and least for paddy (0.31%). An R^2 value of 0.79 was obtained for the linear regression analysis plotted between the average rainfall and average flow for the years 1997-2007 while an R^2 value of 0.86 was obtained for the years 2007-2017. From the R^2 value obtained, it is understood that the flow of the basin is not only dependent on the rainfall but is also influenced by other factors like the changes in the LULC over a stretch of time.

The present study also portrays the capability of HEC-HMS model for modelling the hydrology of Chalakudy basin. The model depends on the hydrological attributes like climatic characteristics, soil type and land use of the study area. The HEC-HMS model has been applied for modelling the runoff for two decades. The rainfall-runoff computation was carried out utilizing precipitation values and the results demonstrated visible contrast between the simulated and observed peak flows and rainfall volumes in the basin. Consequently, the calibration of the model was carried out for optimizing the parameters. Model calibration was done for five years (2003-2007) and validated for another three set of years (2015-2017). For knowing the most sensitive parameter influencing the output of the model the sensitivity analysis was done. From the results of sensitivity analysis, it was found that curve number was the most sensitive parameter for simulating the runoff. The curve number was found to change from 88.77 to 82.35 after the optimization of parameters were carried out. The model gives detailed information about the rest of sensitive parameters as well. The performance of the calibrated and validated model for Chalakudy basin was analyzed utilizing statistical parameters such as Nash Sutcliffe- model efficiency (NSE), correlation co-efficient, RMSE and the percentage difference between simulated and observed peak flow and volume. The NSE for the calibration period was found to be 0.726 before the calibration and increased up to 0.766 after the calibration likewise the value of R^2 i.e., correlation co-efficient also increased from 0.80 to 0.83 after the calibration was done, showing an acceptable performance of the model. Similarly for the validation period the NSE value was found to be 0.810 and correlation coefficient was found to be 0.85. The values obtained for the validation period demonstrated good performance of the HEC-HMS model for simulating the runoff of the Chalakudy basin.

The peak discharge for 1997, 2007 and 2017 were observed to be on 1st July, 16th August and 28th June respectively. The volume of flow was found to be highest for 2007 (2481.98 Million m^3). In order to analyse how the changes of LULC from one class to another affects the flow of the basin, a transition change matrix was prepared for the years 1997-2007 and 2007-2017. Transition change matrix shows that the area shifting mostly towards the urban class is paddy area which is 12.27 km^2 and 12.36 km^2 respectively for 1997 to 2007 and 2007 to 2017. The highest loss from 1997-2007 was found to be for vegetation (-52.52 km^2) and the highest gain was for Paddy (54.39 km^2). In between 2007-2017 the highest loss was noticed to be for vegetation (-30.59 km^2) while the highest gain was for barren land (54.39 km^2).

The extreme variability in the land use pattern of Chalakudy basin reflected negative changes influencing the basin nature and resulting in flood and dry season circumstances in the basin. As the basin has been portrayed by urbanization in the course of the most recent decade and may keep on encountering broad scene changes later on, the potential for increased runoff and urban flooding is plausible. The data obtained from this study will be valuable in anticipating crisis like urban floods and to suggest mitigation measures. Such investigations can provide guidelines for future land use and flood studies which will help us in executing designs so as to ensure and decrease the harm to human beings, flora and fauna. This study will also provide an insight to the government authorities as well to come up with some effective steps to prevent further degradation of basin in the near future. A policy oriented approach to control deforestation and conversion of vegetated areas to urban livelihoods is the only solution to prevent or at least reduce the occurrence of natural hazards.

References

CHAPTER VI

REFERENCES

Abdulkareem, J. H., Pradhan, B., Sulaiman, W. N. A. and Jamil, N. R. 2017. Prediction of spatial soil loss impacted by long term landuse/landcover change in a tropical watershed. *Geoscience Frontiers.* 10 (2019) 389-403.

Arekhi, S. 2012. Runoff modelling by HEC-HMS model (Case study: Kan watershed, Iran). *Int. J. agric. crop sci.* 4(23): 1807-1811.

Asadi, A., Sedghi, H., Porhemmat, J., Babazadeh, H. (2012). Calibration, verification and sensitivity analysis of the HEC-HMS hydrologie model (study area: Kabkian basin and Delibajak subbasin), Iran. *Ecol. Environ. and Conserv*. 18:805-812.

Askar, M. K. 2014. Rainfall-runoff model using the SCS-CN method and geographic information systems: a case study of Gomal River watershed. www.witpress.com 178: 1743-3541.

Balasubramanian, A. 2017. Digital elevation model (DEM) in GIS. https://www.researchgate.net/publication/319454004.

Batar, A. K., Watanabe, T., and Kumar, A. 2017. Assessment of Land-Use/Land-cover change and forest fragmentation in the Garhwal Himalayan region of India. *Environ.* 4:34.

Butt, A., Shabbir, R., Ahmad, S. S., Aziz, N. 2015. Land use change mapping and analysis using Remote Sensing and GIS: A case study of Simly watershed, Islamabad, Pakistan. *The Egyptian J. of Remote Sensing and Space Sci.* 18(2): 251–259.

Chen, Q., Chen, H., Wang, J., Zhao, Y., Chen, J., Xu, C. 2019. Impacts of climate change and land-use change on hydrological extremes in the Jinsha river basin. *Water.* 11(7): 1398.

Choudhari, K., Panigrahi, B., Pau, J. C. 2014. Simulation of rainfall-runoff process

using HEC-HMS model for Balijore Nala watershed, Odisha, India. *Int. J. of Geomatics and Geosciences*. 5:2.

Coskon, H. G., Alganci, U., Eris, E., Agiralioglu, N., Cigizoglu, H. K., Yilmaz, L. 2010. Remote Sensing and GIS innovation with hydrologic modelling for Hydroelectric Power Plant (HPP) in poorly gauged basins. *Water Resour. Manag.* 24(14):3757–3772.

Das, M,, 2018. Assessment of Theissen polygon method to analyze monsoon rain in Ernstwhile Jalpaiguri district, West Bengal, India. *J. of Climatol. and weather forecasting.*6(4):241.

Donigian, A. S. 2002. Watershed model calibration and validation: the HSPF experience. *Proc. of the Water Environ. Fed*. 8:44-73

Elwell, H.A., 1978. Modeling soil losses in Southern Africa. *J. of Agric. Eng. Researc.* 23:117-127.

Esa, E., Assen, M. and Legass, A. 2018. Implications of land use/cover dynamics on soil erosion potential of agricultural watershed, northwestern highlands of Ethiopia. *Environ. Syst. Res.* 7:21.

Ezemonye, M., N. and Emeribe, C., N. 2011. Flood characteristics and management adaptations in parts of the Imo river system. *Ethiopian J. of Environ. Stud. and Manag.* 4(3).

Fleming, M. J., and Doan, J. D. 2013. HEC-GeoHMS geospatial hydrologic modeling extension version 10.1. User's manual. 10.1.

Francesca, F., Gabriele, B., Emanuele, M., Diofantos, G. H., Athos, A. 2016. Satellite remote sensing and GIS-based multi-criteria analysis for flood hazard mapping. *Nat. Hazards.* 83(1).

Gangodagamage, C. 2001. Hydrological modeling using remote sensing and GIS. *Asian Conf. Remote Sensing* . 5-9.

Gupta, A., Sarangi, A., Singh, D., K. and Parihar, S., S. 2016. Evaluation of methods for estimation of reference evapotranspiration. *Indian J. of hill farming.* 29(1): 79-86)

Haberlandt, U. and Radtke I. 2014. Hydrological model calibration for derived flood frequency analysis using stochastic rainfall and probability distributions of peak flows. *Hydrol. Earth Syst. Sci*. 18: 353–365.

Han, F., Ren, L., Zhang, X., and Li, Z., 2016. The WEPP model application in a small watershed in loess plateau. *PLoS ONE*. 11(3):1-11.

Halwatura, D., Najim, M. M. M .2013. Application of the HEC-HMS model for runoff simulation in a tropical catchment. *Environ. modelling software***. 46**: 155-162.

Hilbert, A., A. 2015. Rainfall runoff simulation using modified SCS-CN and HEC-HMS model in Kuantan watershed. B.Eng (Civil) thesis, Universiti Malaysia Pahang, 82p.

Islam, R. 2015.A review on watershed delineation using GIS tools. https://www.researchgate.net/publication/240626931.

Ismael, O., Joseph, K. S., Patrick, G. P. 2017. HEC-HMS model for runoff simulation in Ruiru reservoir watershed. *American J. of Eng. Res.* 6(4):1-7.

Jin, X., Jin, Y., and Mao, X. 2019. Land use/cover change effects on river basin hydrological processes based on a modified soil and water assessment tool: a case study of the Heihe river basin in northwest China's Arid Region. *Sustainability.* 11:1072.

Jitender, S. 2017. Soil erosion: causes, extent and management in India. *Int. J. of Creative Res. Thoughts.* 5(4): 2320-2882.

Kabiri, R. 2014. Simulation of runoff using modified SCS-CN method using GIS system, Case Study: Klang watershed in Malaysia. *Res. J. Of Environ. Sci.* 8:178-192.

Kamali, B. and Mousavi, S. J. 2014. Automatic calibration of HEC-HMS model using multi-objective fuzzy optimal models. *Civil Eng. Infrastructures J.* 47(1):1–12.

Khatami, S., and Khazaei, B., 2014. Benefits of GIS application in hydrological modelling: A brief summary. *J. of Water Manag. and Res.* 70:41–49.

Koneti, S., Sunkara, S. L., and Roy, P. S. 2018. Hydrological modelling with respect to impact of land-use and land-cover change on the runoff dynamics in Godavari river basin using the HEC-HMS model. *Int. J. for Geo-Inf.* 7,206.

Kaul, H. A., and Sopan. I. 2012. Land use land cover classification and change detection using high resolution temporal satellite data. *J. of Environ*. 1(4):146-152.

Laflen, J.M., and Flanagan, D.C. 2013. The development of U.S soil erosion prediction and modelling. *Int. Soil and Water Conserv. Res.* 1(2):1-11.

Letha, J., Thulasidharan, B. N. and Chand, B. A. 2011. Effect of land use/land cover changes on runoff in a river basin: a case study. *Water Resour. Manag.* VI. 145:1743-3541.

Li, Z. 2014. Watershed modeling using arc hydro based on DEMs: a case study in Jackpine watershed. *Environ. Syst. Res.* 1(3):11

Long III, W., Srihann. S. 2004. Land cover classification of SSC image: Unsupervised and Supervised classification using ERDAS Imagine. *Proceedings. IEEE International Geoscience and Remote Sensing Symposium.* Volume 4.

Lydia, A., Selvam , S., Sivasubramanian, P., Murugan, D. 2018. Evaluation of land use/land cover changes in the Coimbatore Corporation of Tamil Nadu using remote sensing and GIS. *J. of Emerging Technol. and Innovative Res.* 5(12).

Majidi, A., and Vagharfard, H. 2013. Surface runoff simulation with two methods using HEC-HMS model. *Curr. Adv. in Environ. Sci*. 1(1): 7-11.

Maya, K., 2005. Studies on the nature and chemistry of sediments and water of periyar and chalakudy rivers, Kerala, India. PhD. (Marine geology) thesis, The Cochin University of Science and Technology. 129p

Mayaja, N. A., and Srinivasa, C. V. 2017. Land use and land cover changes and their impacts in Pampa river basin in Kerala: A remote sensing based analysis . *J. of Geomatics.* 11(1).

Merrritt, W.S., Letcher, R.A., and Jakeman, A. J. 2003. A Review of erosion and sediment transport model. *Environ. Modelling and Software*. 18:761-799.

Mousavi, S. M., Roostaei, S., & Rostamzadeh, H. 2019. Estimation of flood land use/land cover mapping by regional modelling of flood hazard at sub-basin level case study: Marand basin. *Geomatics Natural Hazards and Risk.* 10(1):1155–1175

Munthali, M., Botai, O. J., and Davis, N. 2019. Multi-temporal analysis of land use and land cover change detection for Dedza district of Malawi using geospatial techniques. *Int. J. of Appl. Eng. Res.* 14(5):1151-1162.

Muthusi, N. N., Dulo,S. O. (2020). Runoff estimation for an urban area using SCS-CN method, remote sensing and geographic information systems approach: A Case Study of Mavoko Municipality, Kenya. *Int. J. of Eng. Res. & Technol. 9:4.*

Giang, T. N., Phuong, T. A. 2010. Calibration and verification of a hydrological model using event data. *VNU J. of Sci., Earth Sciences.* 26:64-74.

Niravkumar, K. P., Mukesh, K. Tiwari., M. L. Gaur. 2015. Hydrological modeling of an agricultural watershed using HEC-HMS hydrological model, remote sensing and geographical information system. *16th Esri India User Conf.*

Nouri, A., Saffari, A. and Karami, J. 2018. Assessment of land use and land cover changes on soil erosion potential based on RS and GIS, Case Study: Gharesou, Iran. *J. Geogr. Nat. Disast*. 8: 222.

Pampaniya, N. K., Tiwari, M. K., Gaur, M. L. 2015 Hydrological modeling of an agricultural watershed using HEC-HMS hydrological model, remote sensing and geographical information system. *16th Esri India User Conf.*

Patel, M. M., Gandhi, H.M., Shrimali, N. J. 2014. Literature study on application of HEC-HMS for event and continuous based hydrological modeling. *Int. J. for Sci. Res. & Dev*. 1(11): 2321-0613.

Pathan, H., Joshi, G. S. 2019. Estimation of runoff using SCS-CN method and ArcGIS for Karjan reservoir basin. *Int. J. of Appl. Eng. Res.* 14(12):2945-2951.

Paudel, R. C., Basnet, K., Sherchan, B. 2019. Application of HEC-HMS model for runoff simulation: A case study of Marshyangdi river basin in Nepal. *Proceedings of IOE Graduate Conf., 2019-Winter.*

Pechlivanidis, I. G., Jackson, B. M., Mcintyre, N. R., Wheater, H. S. 2011. Catchment scale hydrological modelling: a review of model types, calibration approaches and uncertainty analysis methods in the context of recent developments in technology and applications. *Global NEST Int. J.* 13(3):193-214.

Prakash, C.R., Sreedevi, B., 2017. Land-use land-cover change and its impact on surface runoff using remote sensing and GIS. *Int. J. of Advanced Remote Sensing and GIS*. 6 (1): 2103-2113.

Puyravaud, J. P., 2003.Standardizing the calculation of the annual rate of deforestation. *For. Ecol. and Manag*. 177:593-596.

Rajkumar, R., Viji, R. 2019. Runoff depth estimation using RS & GIS - NRCS-CN method. *Int. J. of Eng. Res. & Technol.* 7:2.

Rathod, P., Kalpesh, B., Vivek, M. 2015. Simulation of rainfall-runoff process using HEC-HMS. *20th Int. Conf. on Hydraulics, Water Resour. and River Eng.*

Rawat, J. S., Kumar, M. 20.15. Monitoring land use/cover change using remote sensing and GIS techniques: A case study of Hawalbagh block, district Almora, Uttarakhand, India. ***The Egyptian J. of Remote Sensing and Space Sci***. **18(1)**: 77-84

Reshma, T., Venkata, R. K., Deva, P. 2013. Simulation of event based runoff using HEC-HMS model for an Experimental Watershed. *Int. J. of Hydraulic Eng.* 2(2):28-33.

Roy, D., Begam, S., Ghosh, G., and Jana, S. 2013. Calibration and validation of HEC-HMS model for a river basin in eastern India. *ARPN J. of Eng. and Appl. Sci.* 8:1

Sai, H. L., Amin, M. S. M., Puong, L. L., and Yau, S. M. 2008. Applications of GIS and remote sensing in the hydrological study of the upper Bernam river basin, Malaysia. *The Inst. of Eng., Malaysia*. 69(1).

Sarminingsih, A., Rezagama, A., and Ridwan. 2019. Simulation of Rainfall-runoff process using HEC-HMS model for Garang Watershed, Semarang, Indonesia. *J. Of Phys.: Conf. Ser. 1217 (012134).*

Scharffenberg, W.A 2013 US army corps of the engineers. Hydrological engineering centre Hydrologic modelling system (HEC-HMS): user manual 4.0.

Sharma, A., Bhadoria, B. P. S., and Tiwari, K. N., 2010. Effect of land use land cover change on soil erosion potential in an agricultural watershed. *Environ. Monit. Assess*. 173:789–801.

Sheak, H., Bhar, K. K. 2019. Delineation of catchment area of Kangsabati reservoir using ArcGIS for hydrological applications. *I-Manager's J. on Civil Eng*. *9(3): 28-34.*

Shougang, Z., Na, L., and Ruishe, Q. 2014. The application and study of GIS in soil erosion model. *Adv. in Sci. and Eng*. 6(2):31-34.

Singhal, R., Kumar, S. 2018. Surface runoff estimation by SCS-Curve number method using ArcGIS for Modikuntavagu watershed, Khammam district, Telangana state. *19th Esri India User Conf.*

Sopan, T., Ingle., 2012. Land use land cover classification and change detection using high resolution temporal satellite data. *J. of Environ.* 1(04):146-152.

Su, Z., Neumann, P., Schumann F.A., and Schultz G.A. 1992. Application of remote sensing and geographic information system in hydrological modeling. *Earsel. Adv. Remote sensing. 1: 3-7.*

Sudheer, K. P., Thomas, J., Bhallamudi, M., and Bindhu, V. M. 2019. Role of dams on the floods of August 2018 in Periyar river basin, Kerala. *Curr. sci. 116(5):* 780-794.

Sunita, S. 2016. Remote sensing applications in soil survey and mapping: A Review. *Int. J. of Geomatics and Geosciences*. 7(2).

Syed, M. Z. Y., Ahmad A. 2018. Quantification of impact of changes in land use-land cover on hydrology in the upper Indus basin, Pakistan. *The Egyptian J. Of Remote Sensing and space sci.* 21: 255-263.

Tandon, P.N., Nimbalkar, P. T. 2014. Rainfall-runoff relationships using curve number method: a case study. *Int. J. of Adv. Eng. Res. and Studies.* IV(I): 73-77.

Tassew, B.G., Belete, M. A., Miegel, K. 2019. Application of HEC-HMS model for flow simulation in the lake Tana basin: The case of Gilgel Abay catchment, upper Blue Nile basin, Ethiopia. *Hydrol. 6*: 21.

Teferi, E., Bewket, W., Uhlenbrook, S., and Wenninger, J. 2013. Understanding recent land use and land cover dynamics in the source region of the Upper Blue Nile, Ethiopia: Spatially explicit statistical modeling of systematic transitions. *Agric. Ecosyst. Environ.* 165: 98–117.

Tsegaye, B. 2019. Effect of land use and land cover changes on soil erosion in Ethiopia. *Int. J. Agric. Sci. Food Technol.* 5(1): 026-034.

Uddin, k., Uddin, M. A. and Maharjan, S. 2018. Assessment of land cover change and its impact on changes in soil erosion risk in Nepal. *Sustainability*. 10(12):4715

Venkatesh, K., Ramesh, H. 2018. Impact of land use land cover change on run off generation in tungabhadra river basin. I*SPRS Ann. of the Photogrammetry, Remote Sensing and Spatial Inf. Sci.* IV-5.

Visweshwaran, R. 2017. Application of the HEC-HMS model for runoff simulation in the Krishna basin. https://www.researchgate.net/publication.

Winsemius, H. C., Van Beek, L., P., H., Jongman, B., Ward, P., J. and Bouwman, A. 2013. A framework for global river flood risk assessments. *Hydrol. and Earth Syst. Sci.* 17:1871–1892.

Yasin, Z., Nabi, G., Randhawa, S. M. 2015. Modeling of hill torrent using HEC Geo-HMS and HEC-HMS models: A case study of Mithawan watershed. *Pakistan J. of Meteorol*. 11(22).

Yener, M.K., Şorman, A.U., Şorman, A.A., Şensoy, A., and Gezgin, T. 2006. Modeling studies with HEC-HMS and runoff scenarios in Yuvacik basin, Turkiye. *Int. Congr. River Basin Manag.* 623-634.

Younis, S. M. Z., Ammar, A. 2018. Quantification of impact of changes in land use-land cover on hydrology in the upper Indus basin, Pakistan. *The Egyptian J. of Remote Sensing and Space Sci.* 21: 255–263.

Zamfir, A., and Simulescu, D. 2011. Automatic delineation of a watershed using a DEM. case study – the Olteţ watershed. *Sci. Ann. of Stefan cel Mare University of Suceava Geogr. Ser.* 20(1).

Appendices

APPENDIX I

Average daily rainfall (mm) over the Chalakudy basin (1997-2017)

Day	Jan	Feb	Mar	Apr	May	Jun	Jul	Aug	Sep	Oct	Nov	Dec
1	0.11	0.3	0	1.39	4.27	5.64	20.21	16.54	12.44	10.96	8.3	2.11
2	0.13	1.3	0.14	1.54	3.15	13.25	24.56	17.12	13.14	8.72	9.83	1.42
3	0.12	0.02	0.91	0.66	2.54	9.42	21.24	14.45	13.02	16.07	4.36	1.26
4	0.23	0.06	2.67	2.51	6.09	8.25	19.96	22.92	7.93	11.7	3.59	0.91
5	0	0.17	0.9	1.45	7.07	11.99	19.13	18.28	8.69	9.11	4.15	0.12
6	0	0.17	1.55	4.58	6.39	15.84	17.03	19.9	11.23	7.89	6.25	0.15
7	0	0.26	2.38	3.19	7.07	17.43	15.75	16.15	11.72	8.08	8.85	0.66
8	0	0.02	0.73	2.72	8.93	16.08	13.81	15.39	10.16	11.38	8.35	1.05
9	0.19	0.12	0.27	2.76	7.46	12.09	15.55	15.99	10.82	6.3	7.27	1.51
10	0.52	0	3.6	2.48	2.05	11.79	22.41	17.09	9.17	5.8	9.92	1.47
11	0.02	0.62	0.48	1.58	3.44	13.71	21.02	15.61	8.94	8.25	3.57	2.36
12	0	0.34	0.71	1.7	1.88	20.28	22.85	13.03	8.36	11.17	3.89	1.12
13	0.08	0.87	2.18	2.48	5.41	20.99	16.26	11.36	6.77	11.28	2.02	1.22
14	0.43	0	2.52	2.78	2.78	18.76	22.01	9.96	9.17	15.77	1.54	1.44
15	0.06	0.56	2.25	2.62	1.61	18.34	19.97	9.42	8.41	13.91	3.23	0.87
16	0	1.07	3.33	1.83	4.38	14.88	26.03	13.51	11.57	11.46	3.17	0.5
17	0.07	0	1.86	4.19	4.87	17.96	29.53	14.56	12.33	8.23	1.91	0.38
18	0	0.17	1.82	3.94	6.22	18.44	27.74	13.49	10.32	8.21	4.93	0.59
19	0	1.47	2.05	3.58	6.85	17.77	18.27	9.35	9.75	8.19	3.42	2.7
20	0.02	0	1.54	3.19	1.84	16.14	15.51	12.97	7.11	10.54	2.48	1.99
21	0	0.01	1.58	6.12	3.05	15.77	14.69	15.57	5.44	8.36	4.15	1.56
22	0.02	0.14	1.42	3.73	2.27	20.54	13.19	14.7	5.82	8.06	6.96	0.29
23	0.05	0.16	1.13	2.85	3.66	23.01	13.07	12.57	8.86	6.14	5.48	0.05
24	0	0.63	0.87	5.69	5.58	22.59	16.03	10.15	9.54	9.39	4.7	0.02
25	0	1.39	0.4	4.73	7.73	17.29	13.34	9.59	8.05	8.81	1.26	0
26	0	1.78	1.54	3.13	6.82	16.81	15.3	9.79	9.77	10.54	3.53	0
27	0	1.95	2.42	5.46	6.81	22.76	16.36	9.3	7.13	9	2.39	0.15
28	0.02	0.5	0.69	3.98	8.11	23.34	19.44	9.56	7.91	12.67	1.08	1.86
29	0.2	0.17	2.75	2.91	7.86	22.87	14.86	11.31	8.25	11.54	1.85	0.72
30	0		3.37	2.4	8.89	25.35	15.15	12.47	9.13	7.94	2.92	0.49
31	0		3.24		7.6		11.85	13.43		8.39		0.19

APPENDIX II

Average daily flow (cumec) of Chalakudy basin (1997-2017)

Day	January	February	March	April	May	June
1	9.27	3.05	2.53	1.57	5.13	35.74
2	8.91	2.71	3.28	1.68	5.17	39.18
3	9.78	3.92	3.44	2	4.75	33.81
4	9.41	3.38	2.17	3.39	4.49	31.68
5	9.11	4.38	2.05	3.55	6.57	53.78
6	8.3	4.84	2.9	3.25	9.63	60.65
7	8.4	5.8	3.08	5.69	9.52	56.01
8	9.08	4.58	2.76	3.4	11.23	61.44
9	6.83	5.49	2.82	4.53	8.44	51.13
10	6.41	5.4	2.1	2.98	7.35	53.41
11	6.19	3.57	2.39	3.74	6.49	55.36
12	7.55	5.07	1.9	3.81	7.41	58.54
13	6.5	3.75	1.88	3.16	6.18	82.47
14	6.77	3.11	1.74	4.1	9.77	83.63
15	6.53	3.05	1.87	2.39	7.74	87.84
16	6.93	4.34	1.96	4.51	7.11	83.11
17	6.32	3.75	2.67	2.53	7.26	88.58
18	6.04	4.73	2.17	2.58	7.75	95.73
19	6.37	2.94	3.35	4.62	11.47	94.53
20	4.95	3.1	1.66	5.05	9.44	94.81
21	4.85	2.87	2.95	3.84	13.02	109.56
22	4.74	2.6	3.47	6.32	12.39	100.61
23	4.4	2.95	2.36	3.88	15.22	121.59
24	4.15	2.78	2.3	3.47	15.52	132.82
25	4.34	2.78	1.87	6.12	17.44	117.2
26	3.99	2.52	2.03	5.4	17.43	89.67
27	6.36	3.41	2.02	5.99	8.96	113.95
28	3.72	3.43	2.1	6.39	15.79	102.21
29	3.72	5.27	2.13	5.52	21.66	102.83
30	3.43		1.99	6.16	22.51	128.27
31	3.17		1.87		21.88	

Average daily flow (cumec) of Chalakudy basin (1997-2017)

Day	July	August	September	October	November	December
1	127.51	233.57	116.49	77.02	61.23	19.66
2	154.67	222.37	111.38	68.49	58.7	16.14
3	151.19	189.49	126.64	86.7	53.58	11.65
4	152.79	223.35	112.59	114.97	51.31	11.94
5	144.97	199.69	121.23	79.36	52.51	14.51
6	130.29	183.89	117.01	74.18	52.66	13.46
7	150.21	167.1	115.51	71.55	56.24	12.42
8	125.27	160.23	103.31	82.96	53.88	13.81
9	122.87	144.15	130.83	68.78	62.7	15.31
10	130.33	171.23	122	60.07	63.19	12.24
11	143.37	163.95	108.81	69.9	68.64	15.01
12	160.8	136.67	117.75	93.96	55.92	12.11
13	151.29	127.68	106.99	98.76	47.05	11.46
14	167.99	116.58	106.45	85.58	44.76	10.78
15	160.07	96.97	93.5	93.08	43.14	10.21
16	158.08	127.47	101.82	83.23	43.13	11.58
17	230.65	154.62	101.4	76.06	42.14	12.19
18	264.82	122.11	88.34	84.32	40.73	12.02
19	218.43	108.55	100.19	77.15	41.42	12.89
20	168.25	87.37	91.36	79.08	40.36	10.63
21	157.26	92	94.11	72.43	40.34	10.51
22	175.76	95.35	82.98	66.72	49.21	11.04
23	149.52	99.64	89.09	60.21	50.61	8.81
24	144.73	122.01	99.25	62.09	46.76	9.98
25	164.81	128.74	86.88	60.19	45.34	9.52
26	157.21	102.79	84.55	66.67	41.81	10.9
27	159.54	95.39	74.38	75.71	38.05	8.43
28	164.1	82.18	79.49	73.08	40.72	10.81
29	165.47	87.78	72.24	65.24	39.14	8.27
30	165.4	104.36	84.26	76.37	37.16	8.32
31	183.98	111.27		61.56		9.59

APPENDIX III

Average daily maximum and minimum temperature (ºC) from 1997-2017

Day	January		February		March		April		May		June	
	Max	**Min**	**Max**	**Min**	**Max**	**Min**	**Max**	**Min**	**Max**	**Min**	**Max**	**Min**
1	32.1	22.5	33.7	22.6	35.6	23.5	35.4	25.2	34.6	24.9	31.6	24.1
2	31.9	22.1	33.2	22.2	35.9	23.4	35.0	24.7	34.0	24.8	31.5	24.2
3	32.1	21.8	33.3	22.4	35.8	23.8	35.2	25.2	34.2	25.2	31.5	24.2
4	32.4	22.0	33.9	22.8	35.5	23.4	34.7	24.6	33.8	24.9	31.7	24.1
5	32.7	22.6	34.1	22.7	35.8	23.4	34.9	25.0	33.7	24.8	31.3	24.0
6	32.5	22.9	34.3	22.7	35.8	24.2	35.1	24.9	33.3	24.9	30.0	23.6
7	32.8	22.8	34.3	22.4	35.4	23.9	34.9	24.7	33.3	25.0	30.7	23.5
8	32.2	22.8	34.2	22.5	35.6	23.9	34.9	24.8	33.5	24.5	30.2	23.5
9	32.7	23.5	34.3	22.4	35.6	23.8	34.8	25.2	33.7	24.9	30.1	23.5
10	32.5	23.4	34.2	22.9	35.5	23.9	35.0	25.2	33.9	25.2	30.4	23.5
11	32.7	23.0	34.4	23.0	35.6	24.1	34.8	25.1	33.8	24.8	29.8	23.6
12	32.7	22.6	33.9	23.1	35.7	24.0	34.3	25.0	33.2	25.0	29.7	23.5
13	32.5	21.9	34.3	22.7	35.7	23.9	34.3	24.9	33.3	24.8	29.3	23.4
14	32.6	21.9	34.9	22.3	35.6	23.7	34.6	24.7	33.4	25.2	29.7	23.3
15	32.5	21.6	34.6	22.5	35.8	24.2	34.5	24.9	33.6	25.1	30.2	23.5
16	32.7	22.1	34.7	22.6	35.6	24.2	34.7	25.1	33.2	24.9	29.8	23.3
17	32.7	22.1	34.8	22.5	35.6	24.2	34.4	25.5	32.5	24.8	29.3	23.3
18	33.2	22.2	35.0	22.8	35.9	24.1	34.6	25.2	32.4	24.8	29.5	23.0
19	33.2	22.3	34.6	22.6	35.5	24.0	34.7	25.0	32.8	24.3	29.9	23.1
20	32.9	21.8	35.1	22.8	35.6	24.5	34.9	25.5	32.5	24.6	29.8	23.2
21	33.3	21.9	35.0	23.4	35.3	24.7	34.6	25.0	32.5	24.6	29.3	23.3
22	33.4	22.4	34.9	23.1	34.9	25.1	34.6	24.6	32.7	24.7	29.5	23.2
23	33.6	22.0	35.3	22.9	35.2	24.5	34.6	25.5	32.9	25.1	29.6	23.1
24	33.7	22.4	35.2	22.7	35.4	24.8	34.4	24.7	33.1	25.1	29.8	23.1
25	33.5	22.6	34.9	23.0	35.1	24.6	34.7	25.1	32.7	24.9	29.6	23.3
26	33.2	22.7	35.2	22.8	35.4	24.5	34.7	25.1	32.5	24.7	29.4	23.0
27	33.0	22.8	35.4	22.8	35.8	24.6	34.3	25.4	31.9	24.3	29.7	22.9
28	33.1	22.8	35.5	23.1	35.3	24.8	34.0	25.4	31.6	24.1	29.2	23.0
29	33.4	22.7	8.3	5.6	35.4	25.0	34.1	25.2	31.7	24.2	29.5	22.9
30	33.7	22.9			35.4	25.1	34.3	25.4	31.3	24.2	29.3	23.1
31	33.3	22.8			35.3	24.9			31.9	24.1		

Average daily maximum and minimum temperature (ºC) from 1997-2017

Day	July		August		September		October		November		December	
	Max	**Min**	**Max**	**Min**	**Max**	**Min**	**Max**	**Min**	**Max**	**Min**	**Max**	**Min**
1	28.9	22.8	29.3	23.0	30.0	23.2	31.1	22.9	31.3	23.2	31.5	22.9
2	29.4	22.6	29.3	23.1	30.5	23.4	30.8	22.8	31.1	23.0	31.5	23.1
3	29.5	23.0	29.3	23.2	30.2	23.2	31.0	23.0	31.9	23.2	32.1	23.1
4	29.2	23.0	29.3	23.1	30.3	23.3	30.7	22.8	31.9	23.4	31.8	23.2
5	29.4	23.1	29.2	23.0	30.4	23.3	30.8	23.3	31.8	23.4	31.8	23.2
6	29.8	23.0	29.2	22.7	30.1	23.2	30.3	23.0	31.5	23.2	31.8	23.0
7	29.4	23.0	29.4	23.0	29.7	23.0	30.9	23.0	31.3	23.0	31.6	22.9
8	29.7	23.0	29.1	23.0	30.3	23.0	31.5	22.8	31.6	23.2	31.7	22.1
9	29.3	32.5	29.5	23.1	29.8	23.1	31.0	22.6	31.9	23.4	31.8	22.8
10	29.2	22.8	29.3	23.1	29.8	22.9	31.2	23.0	31.7	22.6	31.9	22.6
11	29.3	22.9	29.4	23.0	30.5	23.2	31.3	23.2	31.7	23.0	32.0	22.5
12	28.9	22.7	29.4	23.0	30.6	23.1	30.8	23.4	31.6	22.9	31.8	22.6
13	29.1	22.7	29.7	23.3	30.6	23.4	31.3	23.5	31.9	22.8	31.8	23.1
14	29.6	23.0	30.2	23.3	30.1	23.2	31.6	23.3	32.1	23.4	31.2	23.2
15	29.5	23.1	30.0	23.5	30.0	23.2	30.9	23.3	32.1	22.5	31.8	22.9
16	29.0	23.1	29.8	23.3	30.3	23.2	31.5	23.3	31.9	22.1	31.9	23.1
17	29.1	22.7	29.4	23.3	30.2	23.2	31.3	23.4	31.9	22.8	31.8	22.9
18	29.1	22.7	29.7	23.3	30.3	23.2	31.6	23.3	32.0	23.1	31.3	23.2
19	29.0	22.8	30.3	23.0	30.4	23.1	31.2	23.1	31.6	23.5	31.7	23.1
20	29.0	22.8	30.2	23.3	30.6	23.2	31.1	23.1	32.1	23.2	31.7	22.9
21	29.0	23.0	29.8	23.5	30.3	23.2	31.5	23.2	32.0	23.3	31.8	22.9
22	29.2	23.2	29.8	23.1	31.0	23.1	31.2	23.1	31.9	23.8	31.7	22.5
23	29.4	23.0	29.9	23.3	31.0	23.0	31.3	23.2	31.5	23.6	32.0	22.3
24	29.6	22.9	30.1	23.2	31.1	23.1	31.4	23.0	31.5	23.1	32.1	22.5
25	29.2	22.8	29.9	23.1	30.8	23.0	31.2	23.3	31.8	23.3	32.2	21.6
26	29.4	22.9	29.8	23.0	31.5	23.1	31.8	23.3	31.5	22.9	32.3	21.5
27	29.2	23.1	29.8	23.3	31.4	23.2	31.4	23.5	32.1	22.8	32.0	21.7
28	29.3	23.0	29.8	23.2	31.4	23.3	31.3	23.2	32.0	22.5	31.7	22.3
29	29.2	23.1	30.0	23.4	31.3	23.3	31.4	23.1	31.8	23.0	31.9	22.5
30	29.4	23.0	29.5	23.2	30.6	23.2	31.6	23.3	32.0	23.0	32.1	22.3
31	29.7	23.5	29.9	23.3			31.3	23.3			31.7	21.9

APPENDIX IV

Average daily relative humidity (RH, %) from 1997-2017

Day	January		February		March		April		May		June	
	8:00 AM	2:00 PM	8:00 AM	2:00 PM	8:00 AM	2:00 PM	8:00 AM	2:00 PM	8:00 AM	2:00 PM	8:00 AM	2:00 PM
1	43	73	38	71	39	79	55	87	60	87	69	92
2	42	74	36	70	38	78	57	88	56	87	70	93
3	41	74	37	73	38	78	53	88	60	88	70	91
4	41	74	40	71	36	80	56	88	61	87	70	91
5	42	71	39	75	40	81	54	88	63	89	75	93
6	42	74	38	75	40	83	52	87	60	86	79	93
7	41	72	37	78	42	85	53	86	62	87	79	94
8	45	75	40	75	40	84	58	87	63	88	80	94
9	44	72	38	73	42	84	56	89	60	88	76	95
10	43	72	39	77	44	82	54	87	59	87	78	94
11	42	76	37	78	45	84	56	87	60	89	80	94
12	41	73	40	75	40	86	56	88	60	88	80	94
13	39	73	38	74	42	82	58	87	64	91	86	95
14	38	70	35	74	48	87	58	87	59	88	77	94
15	40	69	37	80	43	85	58	88	61	90	73	94
16	39	71	38	78	45	87	56	87	65	88	77	94
17	39	72	39	76	45	86	56	87	62	90	78	94
18	39	72	41	80	43	83	57	86	64	90	77	95
19	41	72	39	74	49	82	55	87	65	91	76	94
20	39	72	39	79	48	86	59	86	67	91	79	94
21	38	75	41	81	49	89	57	87	65	90	77	95
22	36	71	36	82	54	89	58	88	64	91	81	95
23	39	73	38	79	53	88	58	86	63	89	83	96
24	39	73	40	80	49	89	56	87	67	90	77	94
25	40	76	42	82	51	128	57	87	68	91	78	94
26	40	71	37	79	46	87	57	87	68	91	77	95
27	41	72	35	77	51	85	59	86	66	91	79	95
28	42	75	38	80	50	88	60	88	71	92	83	95
29	39	77	12	21	53	87	59	88	71	91	79	94
30	38	75			56	89	58	86	96	92	79	94
31	39	72			51	86			67	92		

Average daily relative humidity (RH, %) from 1997-2017

Day	July		August		September		October		November		December	
	8:00 AM	**2:00 PM**	**8:00 AM**	**2:00 PM**	**8:00 AM**	**2:00 PM**	**8:00 AM**	**2:00 PM**	**8:00 AM**	**2:00 PM**	**8:00 AM**	**2:00 PM**
1	81	95	77	94	71	94	70	93	66	90	58	80
2	77	95	77	95	73	93	70	92	63	88	57	79
3	79	93	79	95	73	93	67	93	63	87	54	79
4	79	94	80	95	70	94	68	92	65	87	52	77
5	79	95	80	95	71	94	69	94	64	87	53	76
6	79	94	76	95	76	94	69	92	63	87	49	76
7	76	95	76	95	71	94	69	92	64	86	47	76
8	77	94	78	95	73	93	68	93	60	87	52	79
9	80	94	73	95	75	93	71	92	62	86	50	79
10	78	95	76	95	72	92	69	92	60	85	51	79
11	81	95	76	94	70	94	68	91	60	86	53	80
12	81	95	76	95	69	94	71	93	60	86	50	80
13	78	94	76	94	73	93	74	92	59	86	57	77
14	76	96	70	94	73	93	72	93	59	84	52	76
15	77	94	73	94	72	94	72	92	53	81	51	75
16	78	95	76	95	73	94	68	91	52	81	47	76
17	79	95	76	96	73	93	71	92	55	80	47	73
18	76	95	75	94	71	94	68	91	58	79	52	74
19	77	95	74	93	69	93	69	93	57	79	50	76
20	78	94	73	94	69	93	72	92	59	81	49	74
21	80	95	74	94	69	93	69	129	57	82	47	74
22	77	95	73	94	68	132	66	89	58	79	46	74
23	77	94	71	93	69	92	69	90	58	81	47	74
24	76	95	72	94	68	92	66	89	61	80	45	74
25	80	95	75	95	72	93	68	89	57	82	45	75
26	76	95	75	94	67	91	65	89	52	79	42	72
27	77	95	74	93	65	93	70	91	55	79	45	74
28	78	95	73	94	68	92	65	90	58	81	47	73
29	79	95	73	93	70	92	66	90	56	79	46	72
30	76	94	76	95	70	92	66	89	56	78	44	77
31	74	94	71	94			68	90			47	76

APPENDIX V

Average daily wind speed (km/h) from 1997-2017

Day	Jan	Feb	Mar	Apr	May	Jun	Jul	Aug	Sep	Oct	Nov	Dec
1	9.47	9.38	6.22	5.55	6.22	5.90	6.61	6.92	5.77	4.97	6.57	8.67
2	9.26	9.00	5.40	5.59	5.72	6.14	6.18	7.19	6.43	4.85	6.78	8.25
3	8.97	8.44	5.31	5.09	5.82	5.77	7.32	5.92	6.30	4.88	5.89	8.71
4	8.70	7.76	5.61	5.84	5.94	5.97	7.07	6.12	6.66	5.40	6.14	9.74
5	8.51	7.50	5.68	5.98	6.26	6.33	6.27	6.47	6.74	5.42	6.85	9.51
6	8.60	7.16	6.01	5.84	6.04	6.02	6.90	5.69	6.66	5.47	6.21	8.74
7	9.28	5.90	5.69	6.30	5.76	6.24	6.25	5.33	6.44	5.22	5.60	8.79
8	9.58	6.29	5.63	5.79	5.50	5.30	6.13	5.25	5.76	5.24	6.37	8.09
9	9.34	5.85	5.78	5.32	5.56	6.17	6.56	6.03	6.90	5.33	6.10	7.57
10	9.20	5.94	6.64	5.90	5.19	6.75	6.33	6.08	6.75	6.00	6.30	8.83
11	9.33	6.36	6.80	5.88	5.57	5.90	6.41	5.80	6.54	5.61	6.24	9.71
12	9.00	5.53	6.56	6.12	5.44	5.68	5.67	6.75	6.23	5.17	7.19	8.98
13	8.45	5.53	6.69	5.98	6.12	6.95	5.44	7.04	6.61	5.90	7.72	8.33
14	7.90	5.31	5.11	6.19	5.51	6.53	5.76	6.40	6.00	5.97	7.34	9.07
15	8.60	7.12	4.50	6.01	5.73	6.29	6.35	5.96	6.13	5.52	7.40	9.58
16	8.60	7.19	4.71	5.83	5.32	6.62	7.16	5.64	5.76	4.77	6.99	8.46
17	7.90	6.98	5.62	5.87	5.54	6.73	7.24	6.02	5.49	5.21	6.91	10.09
18	8.74	7.43	4.67	5.88	5.20	6.89	5.79	5.49	5.42	5.21	7.10	10.81
19	8.60	6.82	4.49	4.96	5.33	6.96	6.14	5.57	5.51	6.35	7.00	10.27
20	7.72	5.51	5.60	7.02	5.13	7.13	7.20	5.41	6.54	6.33	6.66	10.87
21	8.12	7.00	5.40	5.63	5.39	6.82	5.75	5.52	5.88	6.61	8.07	10.58
22	7.91	6.52	5.24	5.34	5.11	6.99	6.48	5.58	5.41	5.86	8.31	9.80
23	7.52	6.36	5.54	5.99	5.26	6.07	6.25	5.89	5.09	6.44	8.88	10.04
24	7.67	6.67	5.49	5.49	5.18	6.67	7.09	5.93	5.46	6.00	8.08	8.63
25	7.82	5.15	5.22	5.71	5.04	6.68	6.89	5.64	4.79	6.61	8.04	8.06
26	8.66	4.75	5.72	5.91	6.17	6.14	6.49	5.51	5.00	6.12	7.25	7.87
27	8.88	4.44	5.50	6.25	5.82	6.31	6.19	5.80	5.43	5.94	7.16	8.27
28	8.96	4.94	5.44	5.77	6.25	6.98	6.86	5.90	5.31	5.66	7.27	8.95
29	9.27	1.22	5.41	5.69	5.55	6.04	6.02	6.27	5.70	5.77	7.58	9.61
30	9.33		5.67	6.30	6.18	6.73	6.89	5.87	4.95	6.49	9.25	8.18
31	10.37		5.42		6.78		7.24	6.03		5.68		7.68

APPENDIX VI

Average daily sunshine hours from 1997-2017

Day	Jan	Feb	Mar	Apr	May	Jun	Jul	Aug	Sep	Oct	Nov	Dec
1	8.7	9.0	9.2	8.2	8.1	5.3	1.5	3.3	4.5	5.8	5.0	6.6
2	9.1	8.6	9.1	6.9	7.7	4.7	3.0	3.3	5.2	5.9	6.7	6.4
3	8.8	8.8	8.7	7.3	6.7	4.8	2.9	2.2	4.2	6.1	6.1	7.6
4	9.2	8.9	8.1	7.3	5.9	5.5	2.6	2.4	4.0	5.5	6.2	7.6
5	9.1	8.9	8.8	7.1	6.5	4.4	2.2	2.4	5.1	5.2	5.0	7.7
6	8.9	8.9	8.9	7.3	6.2	2.4	2.3	3.0	3.6	5.2	4.4	8.0
7	9.1	9.2	8.5	7.0	5.5	3.9	2.2	3.5	3.4	6.0	5.5	7.8
8	7.8	8.4	8.5	7.0	6.5	2.3	3.1	2.2	4.9	6.5	6.7	7.6
9	8.5	8.8	8.0	7.2	7.1	3.3	2.4	4.0	3.8	5.6	6.0	7.3
10	8.5	9.3	8.1	6.9	6.7	3.5	2.0	3.0	4.4	5.7	6.1	7.3
11	9.0	8.9	8.6	7.1	6.4	3.4	2.4	2.9	6.0	6.1	5.9	7.6
12	9.2	8.0	8.6	6.5	6.0	2.8	1.6	3.5	5.1	5.1	6.7	7.1
13	8.9	9.2	9.2	7.2	5.7	1.9	1.8	3.8	5.3	4.3	7.2	7.1
14	9.1	9.5	8.7	6.9	6.4	2.1	2.6	4.2	4.0	4.8	6.9	6.4
15	9.2	9.3	8.4	6.9	6.3	2.9	2.4	3.7	4.8	4.2	6.6	6.9
16	9.0	9.7	7.7	7.7	6.0	2.9	3.1	4.5	5.7	5.1	7.2	7.9
17	9.3	9.5	7.9	7.3	5.3	2.0	2.4	3.5	4.9	5.0	7.5	8.2
18	9.0	9.2	8.6	8.0	5.7	2.5	2.0	3.4	5.3	5.6	7.0	6.6
19	9.1	8.9	8.8	7.7	5.4	3.0	1.8	4.6	4.9	4.9	6.9	7.7
20	8.9	8.9	8.2	7.2	5.9	2.9	2.3	5.2	5.8	4.5	6.3	7.1
21	8.9	8.7	8.1	7.0	5.7	2.5	1.8	4.6	5.0	5.1	5.9	8.5
22	8.8	8.7	7.5	7.2	5.8	2.7	2.5	4.4	6.3	4.9	5.9	8.0
23	9.1	9.1	8.1	7.0	7.0	2.8	2.8	3.9	5.9	5.4	5.1	8.4
24	9.3	9.4	8.0	6.8	5.4	2.2	2.6	5.0	6.2	5.4	6.3	8.6
25	9.0	8.7	8.0	7.4	5.1	2.5	2.3	4.5	5.4	5.1	6.9	8.4
26	8.5	8.5	7.8	7.0	4.6	2.7	2.7	4.4	5.7	6.3	7.6	8.4
27	8.0	8.8	8.5	6.6	4.6	2.9	1.9	4.0	6.4	4.9	6.8	8.1
28	7.8	9.2	7.5	6.4	4.8	1.9	2.2	3.9	6.3	5.3	6.4	7.8
29	8.9	2.1	7.9	6.3	5.1	2.2	2.5	4.4	5.9	5.1	6.8	7.5
30	9.2		7.9	7.0	5.0	2.6	2.9	4.1	4.6	5.6	7.0	8.2
31	9.2		7.5		5.4		2.6	4.3		5.3		7.7

MODELLING THE IMPACT OF LAND USE LAND COVER CHANGES ON THE RUNOFF PROCESSES IN CHALAKUDY BASIN USING HEC-HMS MODEL

by

NCHUMBENI M ODYUO

(2018-18-002)

ABSTRACT OF THESIS

Submitted in partial fulfilment of the requirement for the degree of

MASTER OF TECHNOLOGY

IN

AGRICULTURAL ENGINEERING

(Soil and Water Engineering)

Faculty of Agricultural Engineering and Technology

Kerala Agricultural University

Department of Irrigation and Drainage Engineering

KELAPPAJI COLLEGE OF AGRICULTURAL ENGINEERING AND TECHNOLOGY

TAVANUR—679573, MALAPPURAM

KERALA, INDIA

2020

ABSTRACT

Fast development of urbanization alongside other expanding anthropogenic factors have been distinguished as significant reasons for land use changes and land transformations. This eventually causes several devastations like floods, droughts, water contamination and soil debasement. There is a need for target evaluation and investigation on the land utilization patterns and the mode of operation of water conserving structures in order to take up any preventive and additional healing measures. The state of Kerala in particular is notable for significant level of development as far as socio–monetary components, education, human services and so forth are considered. The broad financial changes have prompted expanded pace of framework, building development and several land use changes in the most recent decade. Evaluating the spatial and temporal changes in land use and land cover (LULC) of a basin is one of the analytic strategies to comprehend the issues continuing in a basin and gives significant understanding of its effect on runoff processes. The Chalakudy river basin in Kerala was one of the worst affected basins during the floods of 2018 and has experienced unaccountable damages to human life, ranches, gardens, domesticated animals, buildings, roads etc.

The present study compares the LULC changes over two different decades 1997- 2007 and 2007-2017 by analysing the LULC maps and the effect of these changes on the runoff processes in Chalakudy river basin. From the LULC maps, the area under each class, the percentage area coverage and decadal percentage change for each class were calculated. The Hydrologic Modelling System HEC-HMS, developed by the US Army Corps of Engineers Hydrologic Engineering Centre (HEC) was used to model the flood flows of the basin. Calibration and validation of the model was done by employing the SCS CN as the loss method. Calibration of the model was done for five years (2003- 2007) to discover the best parameters of HEC-HMS model while validation of the model was done for three years (2015- 2017). The final analysis of the model showed CN to be the most sensitive parameter for simulating the runoff in the basin. The Nash-Sutcliffe model efficiency (E) for the calibration period was found to increase from 0.726 to 0.766 and 0.816 for the validation period. The correlation coefficient (R^2) value was observed to increase from

0.80 to 0.83 before and after the calibration and a value of 0.85 was obtained for the validation period respectively indicating good performance of the model. Simulation runs of the model were done separately for another three years i.e., 1997, 2007 and 2017 in order to analyze the changes in runoff with respect to land use changes.

It was observed that the vegetation area decreased consequently from 886.21 km^2 to 803.09 km^2 while the urban area was found to increase from 31.74 km^2 to 41.93 km^2 (1997-2017). Aside from that the annual rate change for each class was calculated and results showed an increment in the class of paddy, palm, barren land and urban area while a decrease in annual rate change of vegetation class was also observed. LULC transition matrix was also prepared for 1997-2007 and 2007-2017. From the net loss and gain calculation it was observed that the highest loss from 1997-2007 was found to be for vegetation (-52.52 km^2) and the highest gain was of Paddy (54.39 km^2). In between 2007-2017 the highest loss was noticed to be for vegetation (-30.59 km^2) while the highest gain was for barren land (54.39 km^2). The study highlights a disturbing observation in the last two decades and how this change has prompted the occurrence of floods and runoff. After analyzing the decadal land use changes and the simulated runoff values, it was understood how, loss of vegetation cover and increase in urbanization being the most significant reasons for LULC changes have altered the overall basin ecology.